

Comparison of Rainfall-Runoff Models for Flood Forecasting

Part 1: Literature review of models

**Technical Report
W241**

Comparison of Rainfall-Runoff Models for Flood Forecasting

Part 1: Literature review of models

R&D Technical Report W241

R J Moore and VA Bell

Research Contractor:
Institute of Hydrology

Publishing Organisation

Environment Agency, Rio House, Waterside Drive, Aztec West, Almondsbury,
BRISTOL, BS32 4UD.

Tel: 01454 624400 Fax: 01454 624409
Website: www.environment-agency.gov.uk

© Environment Agency 2001

September 2001

ISBN 1 85705 396 6

All rights reserved. No part of this document may be reproduced, stored in a retrieval system, or transmitted, in any form or by any means, electronic, mechanical, photocopying, recording or otherwise without the prior permission of the Environment Agency.

The views expressed in this document are not necessarily those of the Environment Agency. Its officers, servants or agents accept no liability whatsoever for any loss or damage arising from the interpretation or use of the information, or reliance upon views contained herein.

Dissemination Status

Internal: Released to Regions
External: Released to Public Domain

Statement of Use

This report gives an overview of the different types and approaches to rainfall-runoff modelling for the purposes of flood forecasting. It is intended to be used as a general guide to the wide variety of techniques available for hydrological modelling as applied specifically to flood forecasting.

Research Contractor

This document was produced under R&D Project W5-005 by:
Institute of Hydrology, Maclean Building, Crowmarsh Gifford, Wallingford, Oxfordshire,
OX10 8BB

Tel: 01491 838800 Fax: 01491 692424

Environment Agency's Project Manager

The Environment Agency's Project Managers for Project W5-005 were:
Owen Wedgwood, North West Region
Nigel Outhwaite, Thames Region

Further copies of this report are available from:
Environment Agency R&D Dissemination Centre, c/o
WRc, Frankland Road, Swindon, Wilts SN5 8YF



tel: 01793-865000 fax: 01793-514562 e-mail: publications@wrcplc.co.uk

ACKNOWLEDGEMENTS

Particular thanks are due to the following Environment Agency members of the Steering Committee:

Owen Wedgwood (Project Coordinator and Committee Chairman)
Tim Harrison
Mike Knowles
Nigel Outhwaite
Jennifer Soggee

Richard Cross is thanked for providing information on the Midlands Catchment Runoff Model.

The Flood Protection Commission of the Ministry of Agriculture, Fisheries and Food, through its strategic funding of flood forecasting research at the Institute of Hydrology, has provided the foundation for aspects of the work reported here.

CONTENTS

| | Page |
|--|------|
| Acknowledgements | i |
| Contents | ii |
| List of tables and figures | v |
| Executive summary | vii |
| Keywords | viii |
| 1. Introduction | 1 |
| 1.1 Background | 1 |
| 1.2 Forecasting requirements | 1 |
| 1.3 Previous model intercomparisons | 1 |
| 1.4 Purpose and outline of the report | 2 |
| 2. Selection of rainfall-runoff models for review and assessment | 3 |
| 2.1 Introduction | 3 |
| 2.2 Choice of models to review and assess | 3 |
| 2.3 Forecasting methods for review | 5 |
| 3. The Thames Catchment Model | 7 |
| 3.1 Introduction | 7 |
| 3.2 Zone structure | 7 |
| 3.3 Basin runoff and channel flow routing | 11 |
| 3.4 Model parameters | 11 |
| 4. The Midlands Catchment Runoff Model | 13 |
| 4.1 Introduction | 13 |
| 4.2 Model formulation | 13 |
| 4.3 Model parameters | 19 |
| 5. The Probability Distributed Moisture model | 21 |
| 5.1 Introduction | 22 |
| 5.2 Soil moisture store | 22 |
| 5.3 Surface and subsurface storages | 29 |
| 5.4 Groundwater losses | 30 |
| 5.5 Model parameters | 32 |
| 6. Nonlinear storage models: the Isolated Event and ISO function models | 34 |
| 6.1 Introduction | 34 |
| 6.2 The Isolated Event Model | 34 |
| 6.3 ISO-function models | 37 |

| | Page |
|--|------|
| 7. US National Weather Service Sacramento model | 39 |
| 7.1 Introduction | 39 |
| 7.2 Model formulation | 39 |
| 7.3 Model parameters | 43 |
| 8. The NAM model | 44 |
| 8.1 Introduction | 44 |
| 8.2 Model formulation | 44 |
| 8.3 Model parameters | 48 |
| 9. A simple distributed model: the Grid Model | 50 |
| 9.1 Introduction | 50 |
| 9.2 Water balance in a grid square | 50 |
| 9.3 Isochrone-based kinematic wave routing scheme | 52 |
| 9.4 Some variants of the simple grid model | 54 |
| 10. Transfer Function models | 58 |
| 10.1 Introduction | 58 |
| 10.2 The Transfer Function (TF) model | 58 |
| 10.3 Physically Realisable Transfer Function (PRTF) model | 59 |
| 10.4 Other TF model variants | 63 |
| 11. New modelling approaches | 65 |
| 11.1 Introduction | 65 |
| 11.2 Neural network models | 65 |
| 11.3 Fuzzy rule-based modelling | 67 |
| 11.4 Nearest neighbour forecasting | 69 |
| 12. Model updating methods | 70 |
| 12.1 Introduction | 70 |
| 12.2 State correction | 70 |
| 12.3 Error prediction | 74 |
| 13. Overview of models, conclusions and recommendations | 78 |
| 13.1 Overview of models | 78 |
| 13.2 Conclusions and recommendations | 80 |
| References | 81 |
| Appendix A: Nonlinear storage models | 86 |
| A.1 General | 86 |
| A.2 Linear storage model | 87 |
| A.3 Quadratic storage model | 87 |
| A.4 Exponential storage model | 89 |
| A.5 Cubic storage model | 89 |
| A.6 General storage model in recession | 90 |

| | Page |
|---|------|
| A.7 Groundwater abstraction, negative storage and ephemeral flows | 91 |
| Appendix B: Parallel TF models and equivalent single TF and parallel linear storage models | 92 |

LIST OF TABLES AND FIGURES

| | | |
|--------------|--|----|
| Table 2.2.1 | Rainfall-runoff models used for flood forecasting in the EA regions | 3 |
| Table 2.2.2 | Provisional list of candidate rainfall-runoff models for evaluation | 4 |
| Table 3.4.1 | Parameters in the Thames Catchment Model | 12 |
| Table 4.3.1 | Parameters in the Midlands Catchment Runoff Model | 20 |
| Table 5.5.1 | Parameters of the PDM model | 33 |
| Table 6.2.1 | Parameters of the Isolated Event Model | 37 |
| Table 7.3.1 | Parameters of the NWS Model | 43 |
| Table 8.3.1 | Parameters of the NAM Model | 49 |
| Table 9.3.1 | Parameters of the Grid Model | 55 |
| Figure 3.2.1 | Representation of a hydrological response zone within the Thames Catchment Model. | 8 |
| Figure 3.2.2 | Representation of actual evaporation, E_a , as a function of potential evaporation, E , and soil moisture deficit. | 8 |
| Figure 4.1.1 | The Midlands Catchment Runoff Model. | 14 |
| Figure 4.2.1 | Rapid runoff, percolation and rapid drainage functions in the Midlands Catchment Runoff Model. | 16 |
| Figure 5.1.1 | The PDM rainfall-runoff model. | 21 |
| Figure 5.2.1 | Definition diagrams for the probability-distributed interacting storage capacity component. | 23 |
| Figure 5.2.2 | The storage capacity distribution function used to calculate basin moisture storage, critical capacity, and direct runoff according to the probability-distributed interacting storage capacity model. | 27 |
| Figure 5.2.3 | The Pareto distribution of storage capacity. | 27 |
| Figure 5.2.4 | Rainfall-runoff relationship for the probability-distributed interacting storage capacity model, using the Pareto distribution of storage capacity | 28 |
| Figure 5.4.1 | Conceptualisation of extended nonlinear storage. | 31 |
| Figure 7.1.1 | The US National Weather Service Sacramento Rainfall-Runoff Model. | 40 |
| Figure 8.1.1 | The NAM rainfall-runoff model. | 45 |
| Figure 9.2.1 | A typical grid storage illustrating the components of the water balance | 51 |
| Figure 9.3.1 | Catchment with superimposed weather radar grid and inset showing Isochrone areas in grid square j. | 53 |
| Figure 9.3.2 | The Simple Grid Model. | 54 |

| | | Page |
|---------------|---|------|
| Figure 11.2.1 | Feed-forward neural network with an hidden layer. | 65 |
| Figure 11.3.1 | Triangular membership function for rainfall. | 68 |
| Figure B.1 | Parallel configuration of TF models. | 92 |
| Figure B.2 | Two linear reservoirs in parallel. | 93 |

EXECUTIVE SUMMARY

Choosing a rainfall-runoff model for use in flood forecasting is not a straightforward decision and indeed may involve the selection of more than one. The aim of this Part 1 report is to provide a literature review of models in order to furnish a basic understanding of the types of model available, highlighting their similarities and differences. A sub-set of those reviewed are selected for more detailed assessment using data from a range of catchments. The results of this model intercomparison are presented in the Part 2 report.

Whilst there is a plethora of “brand name” models they involve a relatively small set of model functions which are configured in a variety of different ways. This is illustrated by the models reviewed here. The initial selection of models for review is guided by those already in use for flood forecasting in the UK. To this are added well-known models developed overseas and those with a distributed formulation. From this menu of models are selected the following eight models for intercomparison in Part 2: the Thames Catchment Model (TCM), the Midlands Catchment Runoff Model (MCRM), the Probability Distributed Moisture (PDM) model, the Isolated Event Model (IEM), the US National Weather Service Sacramento model, the Grid Model, the Transfer Function (TF) model and the Physically Realisable Transfer Function (PRTF) model. The first six are conceptual soil moisture accounting models, with the Grid Model having a distributed formulation, whilst the TF and PRTF are “black box” time-series models. Also selected for review in Part 1 are the Input-Storage-Output or ISO-function model and the NAM model, which are both conceptual approaches. An outline review of some newer, general approaches to forecasting are given which include neural network (NN), fuzzy rule-based and nearest neighbour methods.

An important aspect of the use of rainfall-runoff models in a real-time forecasting environment is the ability to incorporate recent observations of flow in order to improve forecast performance. The available methods for forecast updating are reviewed with particular reference to state correction and error prediction techniques. The latter aim to adjust, for example, the water contents of conceptual stores in a model and are usually tailored for a specific model. In contrast, error prediction operates independently of the rainfall-runoff model structure by exploiting the dependence in model errors to predict future ones. Parameter adjustment techniques are considered separately in the context of the simple TF and PRTF models.

The Part 1 report ends with an overview of the models reviewed. This includes consideration of the ease of use of different models in calibration and in an operational forecasting environment. In conclusion, the didactic rather than judgmental approach adopted in the review is justified. It is inherently dangerous to judge the efficacy of a model by the variety of functionality it supports or processes it purports to represent. The Part 2 report presents the results of the intercomparison of models across a range of catchments. These results provide an objective basis on which to make judgements concerning the choice of models. Guidelines on model choice are presented in terms of forecast accuracy for different types of catchment together with other factors, such as ease of calibration and operational use, considered only partially in this Part 1 report.

KEYWORDS

Rainfall-runoff, Floods and flooding, Flood forecasting, Flood warning, Modelling (Hydrological)

1. INTRODUCTION

1.1 Background

The Environment Agency employs a range of rainfall-runoff models for flow forecasting and there are others, in this country and abroad, which might service the needs of the EA as well if not better. They range in type from transfer function (empirical black box), through lumped conceptual to more physically-based distributed models. The rainfall-runoff models also are often accompanied by updating techniques for taking account of recent measurements of flow so as to improve the accuracy of model predictions in real-time. Against this variety of available modelling technique the EA is seeking guidance on the appropriate choice, as it relates to catchment characteristics (size, lithology, soils, land use, relief, etc.), storm type and available real-time data (including radar as well as raingauge measurements of rainfall). Of importance is the appropriate model choice in relation to the speed of response of the catchment, the forecast lead time required and the accuracy and consistency of the forecast. The problem of appropriate choice of model is addressed in this study in two parts. In Part 1, reported here, a literature review of rainfall-runoff models is carried out. This provides a foundation for the model assessment that follows in Part 2.

In order to focus on a comparison of models the use of rainfall forecasts is not considered in this study; previous R&D Notes have addressed this issue (Moore *et al.*, 1993, 1995). Perfect foreknowledge of measured rainfall is assumed to avoid the uncertainty associated with rainfall forecasts confounding the analysis. Also, a review of snowmelt models and an assessment of forecasts during snowmelt conditions are outside the scope of the present study and the subject of an ongoing EA R&D project (Moore *et al.*, 1996).

1.2 Forecasting Requirements

The needs of the EA for rainfall-runoff models are spread across a range of water management functions and include both real-time operational applications and off-line uses for design and planning. Forecasting systems which operate in real-time generally have flood warning as the dominant requirement to serve but are designed to forecast over the full range of flows, where possible, in support of a variety of functions. Also in design and planning increasing use is being made of continuous simulation models for flood and drought estimation and impact assessment studies, and where consideration of the choice of rainfall-runoff model can be important. Whilst the choice of rainfall-runoff model for flood warning forms the focus to this study, the literature review here and model assessment of Part 2 is considered to have wider relevance for these reasons.

1.3 Previous Model Intercomparisons

There have been few comprehensive model intercomparison studies that are relevant to the UK flow forecasting problem. The World Meteorological Organisation's intercomparison of real-time forecasting models in 1987 (WMO, 1992) is now ten years old and was biased towards rather large catchments and model time increments, relative to the typical UK situation. Of the three catchments considered only the Orgeval in France was comparable,

with an areal extent of 104 km² and 1 hour data interval, whilst the two North American catchments both exceeded 1000 km² and used either daily or 6 hourly data.

Of much greater relevance here is the study undertaken by the Institute of Hydrology in 1992 (Moore *et al.*, 1993) which compared three models used operationally by the EA for flood forecasting across nine catchments employing 30 flood events. Whilst the primary focus of this study was an assessment of radar rainfall forecasts from the Met Office's Frontiers and IH's local (HYRAD) systems an important byproduct was an assessment of the different models and associated updating schemes which used both observed and forecast estimates of rainfall. This work was further consolidated in an Operational Guidance Note for the NRA (Moore *et al.*, 1995) which extended to consider the relative performance of a simple distributed conceptual model configured on the radar grid (Moore *et al.*, 1994). It also provided a commentary on previous experience with transfer function models and recursive updating schemes.

However, the formal assessment was restricted to catchments within the Thames basin, and whilst these were varied in terms of catchment area, land use and lithology, they lacked some of the stronger topographical controls on runoff experienced in the smaller catchments of upland Britain. Also, whilst the assessment did consider catchments with strong groundwater controls this did not extend to explicitly incorporate information on groundwater levels or pumped abstractions. This points to the need to carry out an assessment of models using catchments both in upland and lowland Britain, and also where regimes of natural recharge and artificial abstraction can exert a primary control on flood generation, for example as is the case in the South Downs (notably Chichester) and the Yorkshire Wolds (notably Bridlington).

1.4 Purpose and Outline of the Report

The purpose of this Part 1 report is to provide a broad literature review of existing models from which to select a restricted set chosen to be representative of particular approaches to forecasting. Section 2 first identifies the rainfall-runoff models used by the EA for flood forecasting at the present time. These models together with selected models developed outside the UK, and models having a distributed formulation, are used to form a menu of models for more detailed review and assessment. Models selected from this menu are reviewed in Sections 3 to 10. The relevance to flood forecasting of more recent modelling developments - including neural network, fuzzy rule-based and nearest neighbour approaches - are considered in Section 11. Methods of model updating, where recent observations of flow are used to improve flow forecast performance, are reviewed in Section 12. An overview of the models together with conclusions and recommendations are presented in the final Section 13.

2. SELECTION OF RAINFALL-RUNOFF MODELS FOR REVIEW AND ASSESSMENT

2.1 Introduction

This review aims to help provide the improved understanding of rainfall-runoff models that the EA requires in order to support decisions on the choice of models for flood forecasting. Whilst there is a plethora of models, with a variety of “brand names”, there are in reality comparatively few different generic approaches to forecasting. Such genericism is exploited in the choice of models to be carried through to formal assessment utilising the catchment datasets which is the subject of the Part 2 report. This serves to contain the scope of the intercomparison whilst preserving the generality of the conclusions drawn from the results of the project.

Model selection for more detailed review and assessment is the concern of this Section. The approach followed is to initially identify models in current use by the EA for flood forecasting. To this list is added selected overseas models, and models with distributed formulations, in order to have a menu of models encompassing a range of model types. A priority list of models is then identified from this menu for more detailed review and assessment. Additional “new approaches” not included in the list are reviewed later. Methods of updating, which may form an integral part of a given rainfall-runoff model or operate largely independent of it, are also considered in a later Section.

2.2 Choice of Models to Review and Assess

Table 2.2.1 below summarises the main models used for flood forecasting in each of the eight EA regions.

Table 2.2.1 Rainfall-runoff models used for flood forecasting in the EA regions

| EA Region | Models in use |
|------------------|----------------------|
| Anglian | TF, PDM |
| Midlands | MCRM |
| North East | PDM |
| North West | ISO, TF, PRTF |
| Southern | ISO |
| South West | TF, PRTF |
| Thames | TCM, IEM, PDM |
| Welsh | ISO |

The seven models identified are the following:

| | |
|------|---|
| TCM | Thames Catchment Model |
| MCRM | Midlands Catchment Runoff Model |
| PDM | Probability Distributed Moisture model |
| IEM | Isolated Event Model |
| ISO | Input-Storage-Output model |
| TF | Transfer Function model |
| PRTF | Physically Realisable Transfer Function model |

To this list may be added a few well-known models from outside the UK, and our choice is:

| | |
|-----|---|
| NWS | US National Weather Service (Sacramento) model |
| HBV | HBV model (Swedish Met. and Hydrological Institute) |
| NAM | NAM model (Danish Hydraulics Institute). |

There is a need to consider distributed models that may be practical for real-time flood forecasting; our choice is:

| | |
|------------|--|
| Grid Model | Developed by IH for the NRA |
| Topmodel | Developed by Beven, University of Lancaster. |

This provisional short-list of models is summarised in Table 2.2.2, which makes a distinction between EA operational and other candidates, and aggregates the ISO/IEM models as models of similar class. There are various variants of the TF model in use. The Physically Realisable Transfer Function (PRTF) developed by Han (1991) is an important special case and should be considered as an additional candidate for assessment purposes. Note that the PDM encompasses a range of model structures utilising the probability-distributed storage principle, and is representative of other models of this type such as the ARNO (Todini, 1996) and Xinanjiang models (Zhao *et al.*, 1980).

Table 2.2.2 Provisional list of candidate rainfall-runoff models for evaluation

| | Model |
|---------------------------|-----------------------------------|
| EA operational candidates | 1. MCRM |
| | 2. TCM |
| | 3. PDM |
| | 4. TF (and PRTF) |
| | 5. ISO (and IEM) |
| Other candidates | 6. Grid (or Topmodel) distributed |
| | 7. NWS (or HBV or NAM) overseas |

The short-list of models in Table 2.2.2 is considered to be still too wide ranging and in need of further reduction. The NWS, HBV and NAM models are classic lumped conceptual rainfall-runoff models, in the same class for example as the MCRM and TCM. Choosing the NWS model as the main overseas model candidate is favoured as a well structured model, a known good performance and source code in the public domain. Of the two distributed models, retaining the Grid Model is favoured since this was developed with flood warning in mind, can accommodate grid-square radar rainfall, and encompasses the topographic index formulation of runoff production employed by Topmodel as one model variant. A limit of 8 models was agreed with the EA as sensible to restrict the scope of the project to a sensible size. Omitting the ISO from the full intercomparison, as largely encompassed by the PDM, TCM and IEM model formulations, would appear sensible. The final choice of models to intercompare is the following:

| | |
|------------|--|
| TCM | Thames Catchment Model |
| MCRM | Midlands Catchment Runoff Model |
| PDM | Probability Distributed Moisture model |
| IEM | Isolated Event Model |
| NWS | US National Weather Service (Sacramento) model |
| TF | Transfer Function model |
| PRTF | Physically Realisable Transfer Function model |
| Grid Model | Developed by IH for the NRA. |

Snowmelt model components are available for four of these: MCRM, PDM, NWS and Grid Model. However, these are not reviewed here as snowmelt modelling is outside the scope of the present project and the subject of an ongoing EA R&D project. Also, model performance is not assessed during snowmelt periods in the Part 2 report.

2.3 Forecasting Methods for Review

The eight models above feature in the assessment of rainfall-runoff models in the Part 2 report. These models are reviewed here in detail, as background to the assessment, in Sections 3 to 10. The ISO-function model is included in the review of nonlinear storage models, along with the IEM (Section 6). Newer modelling approaches – including artificial neural network (ANN), fuzzy rule-based and nearest neighbour methods – are outlined in Section 11. Procedures for updating the model forecasts with reference to recent observations of flow are reviewed in Section 12, placing particular emphasis on the methods available for use with the eight models selected for assessment. The report ends with an overview of the models considered and a set of conclusions and recommendations arising from the literature review.

The data needs for the different models are similar in all requiring rainfall and flow data, the latter for initialisation and updating and off-line for model calibration and performance assessment. Whilst explicit soil moisture accounting models employ evaporation as an additional input, this can take the form of a simple sine curve over the seasons of the year or a standard annual profile but can utilise near real-time evaporation estimates from an automatic weather station if available. The data requirements of different models are reviewed in Section 13.1 of the concluding section when considering ease-of-use issues.

The review of each model is deliberately presented in a style that is didactic rather than judgmental. A model with greater functionality is not necessarily better and different models may prove more appropriate for different circumstances. Thus the emphasis is on gaining an understanding of how a model works and not on its strengths and weaknesses. This approach also serves to highlight the similarities of different “brand name” models. The assessment that follows in Part 2 will provide the objective basis for making judgements on an appropriate choice of model or models.

3. THE THAMES CATCHMENT MODEL

3.1 Introduction

The structure of the Thames Catchment Model, or TCM (Greenfield, 1984), is based on subdivision of a basin into different response zones representing, for example, runoff from aquifer, clay, riparian and paved areas and sewage effluent sources. Within each zone the same vertical conceptualisation of water movement is used, the different characteristic responses from the zonal areas being achieved through an appropriate choice of parameter set, some negating the effect of a particular component used in the vertical conceptualisation. The zonal flows are combined, passed through a simple routing model (optional), and go to make up the basin runoff.

A given response zone may be considered to represent a combination of sub-areas within a catchment having similar hydrological characteristics. In some catchments a single geographical area will account for most or all of a zone, and the overall model will thus contain elements of a semi-distributed description of the catchment. Reflecting this possibility, a facility is available in the TCM to provide different rainfall inputs to the hydrological response zones. However in this study the same, catchment-average, rainfall is used for all zones. This is partly because the TCM is not designed to be a semi-distributed model (for instance, there is no differential time delay between zones).

3.2 Zone Structure

The conceptual representation of a hydrological response zone in the TCM is illustrated in Figure 3.2.1 and its constituent parts are described below. Nomenclature used in the figure and description below relates to an aquifer zone. However, the same structure applies to all types of zone but with changes to the nomenclature; for example, for other zones percolation is better described as rainfall excess.

1. *Soil moisture*

Within a given zone, water movement in the soil is controlled by the classical Penman storage configuration (Penman, 1949) in which a near-surface storage, of depth related to the rooting depth of the associated vegetation and to the soil moisture retention characteristics of the soil (the root constant depth), drains only when full into a lower storage of notional infinite depth (Figure 3.2.1). Evaporation occurs at the Penman potential rate, E , whilst the upper store contains water and at a lower rate, E_a , when only water from the lower store is available (Figure 3.2.2). The Penman stores are replenished by rainfall, but a fraction ϕ (typically 0.15, and usually only relevant to aquifer zones) is bypassed to contribute directly as percolation to a lower “unsaturated storage”. Percolation occurs from the Penman stores only when the total soil moisture deficit has been made up.

2. *Unsaturated and saturated stores*

Within each zone, the total percolation forms the input to the unsaturated storage which behaves as a linear reservoir, with the outflow rate q being related to its store of water s

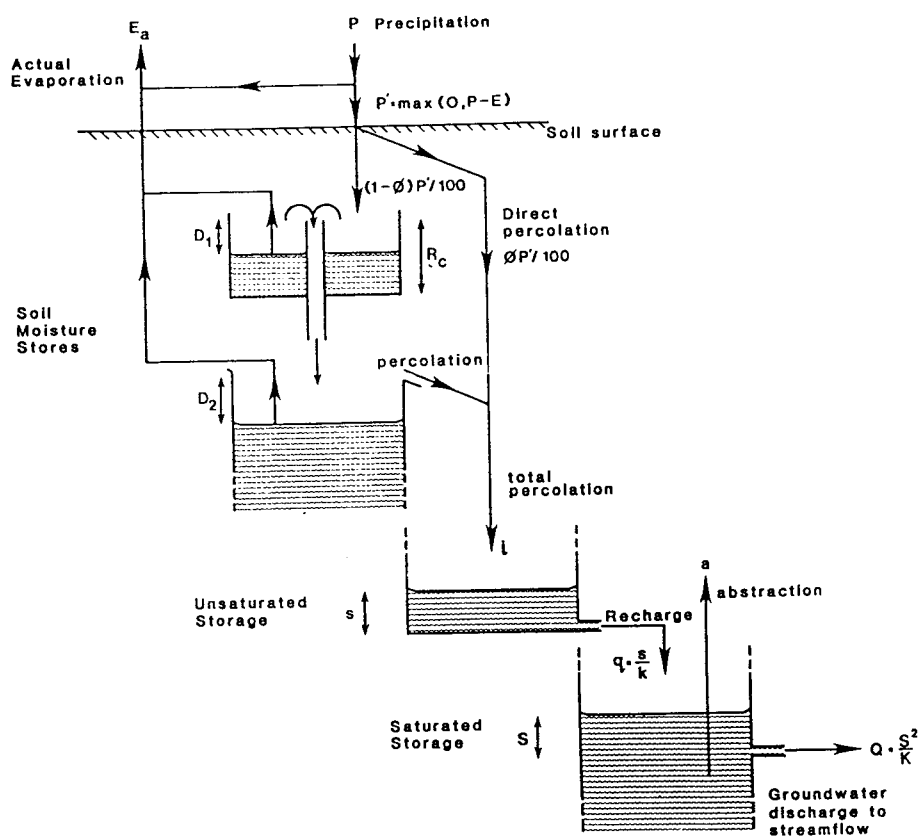


Figure 3.2.1 Representation of a hydrological response zone within the Thames Catchment Model.

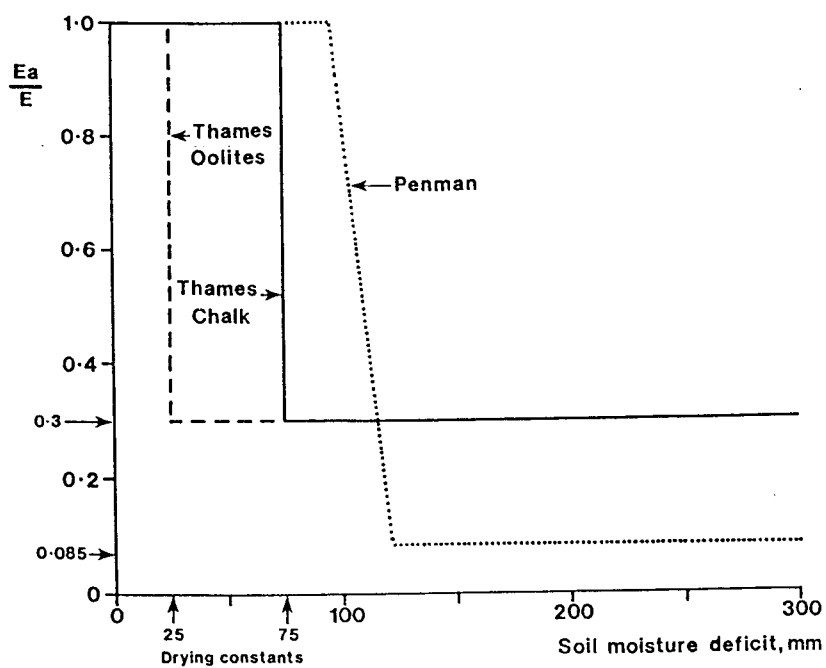


Figure 3.2.2 Representation of actual evaporation, E_a , as a function of potential evaporation, E , and soil moisture deficit.

through the relation $q=s/k$, where k is the time constant of the reservoir. This outflow, or more correctly the integrated volume over an interval, acts as an input called “recharge” to a further storage representing storage of water below the phreatic surface in an aquifer. Withdrawals are allowed from this storage to allow pumped groundwater abstractions to be represented. A quadratic storage representation is used here where the outflow rate, Q , is related to the storage of water, S , through the relation $Q=S^2/K$ where K is a nonlinear storage constant. The actual algebraic expressions in each of these two storages are presented below and a review of the theoretical background of nonlinear storage models is given in Annex I.

3. *Linear reservoir*

The function defining outflow, q , from the linear reservoir is

$$q = \frac{1}{k} s, \quad (3.2.1)$$

where s is the volume in storage and k is a constant (with units of time).

For a time interval $(t-T, t)$ at the start of which the outflow is q_{t-T} , and during which there is a constant input (flow from the soil zone) of i_t , it can be shown that the mean outflow during the period is given by

$$\bar{q}_t = \frac{k}{T} (1 - \exp(-T/k)) q_{t-T} + \left\{ 1 - \frac{k}{T} (1 - \exp(-T/k)) \right\} i_t. \quad (3.2.2)$$

The final outflow, q_t , is given by

$$q_t = \exp(-T/k) q_{t-T} + (1 - \exp(-T/k)) i_t. \quad (3.2.3)$$

The calculations are normally performed with i_t and q_t in units of mm/day or mm/hour. To obtain a volumetric flow rate it is necessary to multiply by the area of the zone being considered.

4. *Quadratic reservoir*

The function defining outflow, Q , from the quadratic reservoir is

$$Q = \frac{1}{K} S^2, \quad (3.2.4)$$

where S is the volume in storage, and K is a constant (with units of volume time).

The net inflow into this storage, I , is the difference between mean outflow \bar{q} from the linear reservoir and any abstraction, a . It is possible to derive analytical solutions for the outflow Q_t at the end of a time interval $(t-T, t)$, during which the net inflow is I_t (assumed constant over the interval) and the initial outflow is Q_{t-T} .

To find Q_t , the differential equation to be solved is

$$\frac{dS}{dt} = I - \frac{S^2}{K}. \quad (3.2.5)$$

Using the transformed variable, $v = S/\sqrt[3]{IK}$, the differential equation may be written

$$\frac{1}{1-v^2} dv = \sqrt[3]{I/k} dt, \quad (3.2.6)$$

with solution

$$\tanh^{-1} v_t = \tanh^{-1} v_{t-T} + \frac{\sqrt[3]{I_t}}{K} T, \quad (3.2.7)$$

where $v_t = S_t/\sqrt[3]{(I_t K)} = \sqrt[3]{(Q_t/I_t)}$. Taking hyperbolic tangents, and letting $\tau = \sqrt[3]{(I/K)}T$ gives the result

$$Q_t = I_t \left(\sqrt[3]{(Q_{t-T}/I_t)} + \tanh \tau \right)^2 / \left(1 + \sqrt[3]{(Q_{t-T}/I_t)} \tanh \tau \right)^2. \quad (3.2.8)$$

If I_t is negative due to abstractions exceeding recharge then a valid solution may be sought using the transformed variable $v = S/\sqrt[3]{(-IK)}$, which gives the differential equation

$$\frac{1}{1+v^2} dv = -\sqrt[3]{(-I/K)} dt, \quad (3.2.9)$$

with solution

$$\tan^{-1} v_t = \tan^{-1} v_{t-T} - \sqrt[3]{(-I_t/K)} T, \quad (3.2.10)$$

where $v_t = S_t/\sqrt[3]{(-I_t K)} = \sqrt[3]{(Q_t/(-I_t))}$. This yields the result

$$Q_t = I_t \tan^2 \left\{ \tan^{-1} \sqrt[3]{(Q_{t-T}/(-I_t))} - \sqrt[3]{(-I_t/K)} T \right\}. \quad (3.2.11)$$

Note that in this case flow will cease at time

$$T' = \sqrt[3]{(K/(-I_t))} \tan^{-1} \sqrt[3]{(Q_{t-T}/(-I_t))} \quad (3.2.12)$$

when the expression in curly brackets in Equation (3.2.11) falls below zero and a volume deficit begins to build up, which at the end of the interval $(t-T, t)$ is

$$V_t = I_t (T - T') \quad (3.2.13)$$

The solution for $I=0$ may be readily obtained by solving the differential equation

$$\frac{dS}{dt} = -\frac{S^2}{K} \quad (3.2.14)$$

which yields the result

$$Q_t = \left(\frac{1}{\sqrt{Q_{t-T}}} + t/\sqrt{K} \right)^{-2}. \quad (3.2.15)$$

3.3 Basin Runoff and Channel Flow Routing

Total basin runoff derives from the sum of the flows from the quadratic store of each zonal component of the model delayed by a time τ_d . Provision is also made to include a constant contribution from an effluent zone if required. A more recent extension of the model passes the combined flows through an additional channel flow routing component if required. This component of the model derives from the channel flow routing model developed by the Institute of Hydrology (Moore and Jones, 1978; Jones and Moore, 1980) which, in its basic form, takes the kinematic wave speed as fixed. The model employs a finite difference approximation to the kinematic wave model with lateral inflow

$$\frac{\partial Q}{\partial t} + c \frac{\partial Q}{\partial x} = cq \quad (3.3.1)$$

such that the flow at time t out of the n 'th sub-reach is given by

$$Q_t^n = \left(1 - c \frac{\Delta t}{\Delta x} \right) Q_{t-1}^n + c \frac{\Delta t}{\Delta x} (Q_{t-1}^{n-1} + q_{t-1}^n) \quad (3.3.2)$$

where c is the kinematic wave speed and q_t^n is the lateral inflow to the n 'th sub-reach. The quantities Δx and Δt are the space and time steps associated with the discretisation and $c < \Delta x / \Delta t$ is a requirement for stability. This model is used to represent routing of flows through a reach of length L sub-divided into N sub-reaches so that $\Delta x = L/N$. Note that both N and c control the delay and attenuation of the flood wave through the reach. In practice the model employs the dimensionless wave speed $\theta = c\Delta t / \Delta x$ for the purposes of parameter estimation with $0 < \theta < 1$.

3.4 Model Parameters

A summary of the model parameters used in the Thames Catchment Model is presented in Table 3.4.1 together with the units used in the IH implementation of the model.

Table 3.4.1 Parameters in the Thames Catchment Model

| Parameter name | Unit | Description |
|-------------------------|--------------------------------|---|
| <i>Zone parameters</i> | | |
| A | km ² | Area of hydrological response zone |
| γ | none | Drying rate in lower soil zone (usually $\gamma=0.3$) |
| R _c | mm | Depth of upper soil zone (drying or root constant) |
| R _ℓ | mm | Depth of lower soil zone (notionally infinite) |
| ϕ | none | Direct percolation factor (proportion of rainfall bypassing soil storage) |
| k | h | Linear reservoir time constant |
| K | mm h | Quadratic reservoir time constant |
| a | m ³ s ⁻¹ | Abstraction rate from quadratic reservoir |
| <i>Other parameters</i> | | |
| n _z | none | Number of zones |
| q _c | m ³ s ⁻¹ | Constant flow (effluent or river abstraction) |
| τ_d | h | Time delay |
| N | none | Number of channel sub-reaches |
| θ | none | Dimensionless wave speed, $c\Delta t/\Delta x$ |

4. THE MIDLANDS CATCHMENT RUNOFF MODEL

4.1 Introduction

The rainfall-runoff catchment model used in the Midlands Flood Forecasting System (M-FFS) is based on classical conceptual soil moisture accounting principles. An outline of the model, previously known as the Severn-Trent Catchment Runoff Model, is provided by Bailey and Dobson (1981) and Wallingford Water (1994). A schematic of the model structure is shown in Figure 4.1.1. The model comprises three main stores: an interception store, a soil moisture store and a groundwater store. Rapid runoff is generated from the soil moisture store, the proportion of the input to the store becoming runoff increasing exponentially with decreasing soil moisture deficit. “Percolation” to the groundwater store occurs when the soil is supersaturated, increasing as a linear function of the negative deficit. When supersaturation exceeds a critical value, “rapid drainage” also occurs as a power function of the negative deficit in excess of the critical value (the so-called excess water). This rapid drainage along with rapid runoff forms the soil store runoff. Evaporation occurs preferentially from the interception store at a rate which is a fixed proportion of the catchment potential evaporation. A proportion of any residual evaporation demand is then met by water in the soil store, the proportion varying as a function of the soil moisture deficit. Drainage of the groundwater store to baseflow varies as a power function of water in storage, the exponent being fixed at 1.5. The total output, made up of baseflow and soil store runoff, is then lagged and spread evenly over a specified duration to represent the effect of translation of water from the ground to the catchment outlet. Finally, the flow is smoothed using two nonlinear storage functions, one for routing in-bank flow and the other out-of-bank flow, the two components being summed to give the catchment model outflow.

The more detailed operation of each component of the Midlands Catchment Runoff Model will be considered in the description of the model formulation which follows.

4.2 Model Formulation

1. *Interception store*

The interception store operates as a simple bucket having a capacity, S_{\max} , and with water in storage, S , increasing through the addition of rainwater, P , until full when overflows, q_T , enter the soil store as throughflow. A proportion, f , of the catchment atmospheric demand for evaporation, E_c referred to here as the catchment evaporation, is met by water in the interception store, or by a lesser amount if storage S is not sufficient. Thus we have the following sequential water balance operations for the interception store (dropping time suffixes for simplicity):

$$\text{Interception Storage} \quad S = S + P \quad (4.2.1)$$

$$\text{Throughflow} \quad q_T = \begin{cases} S - S_{\max} & S > S_{\max} \\ 0 & \text{otherwise} \end{cases} \quad (4.2.2)$$

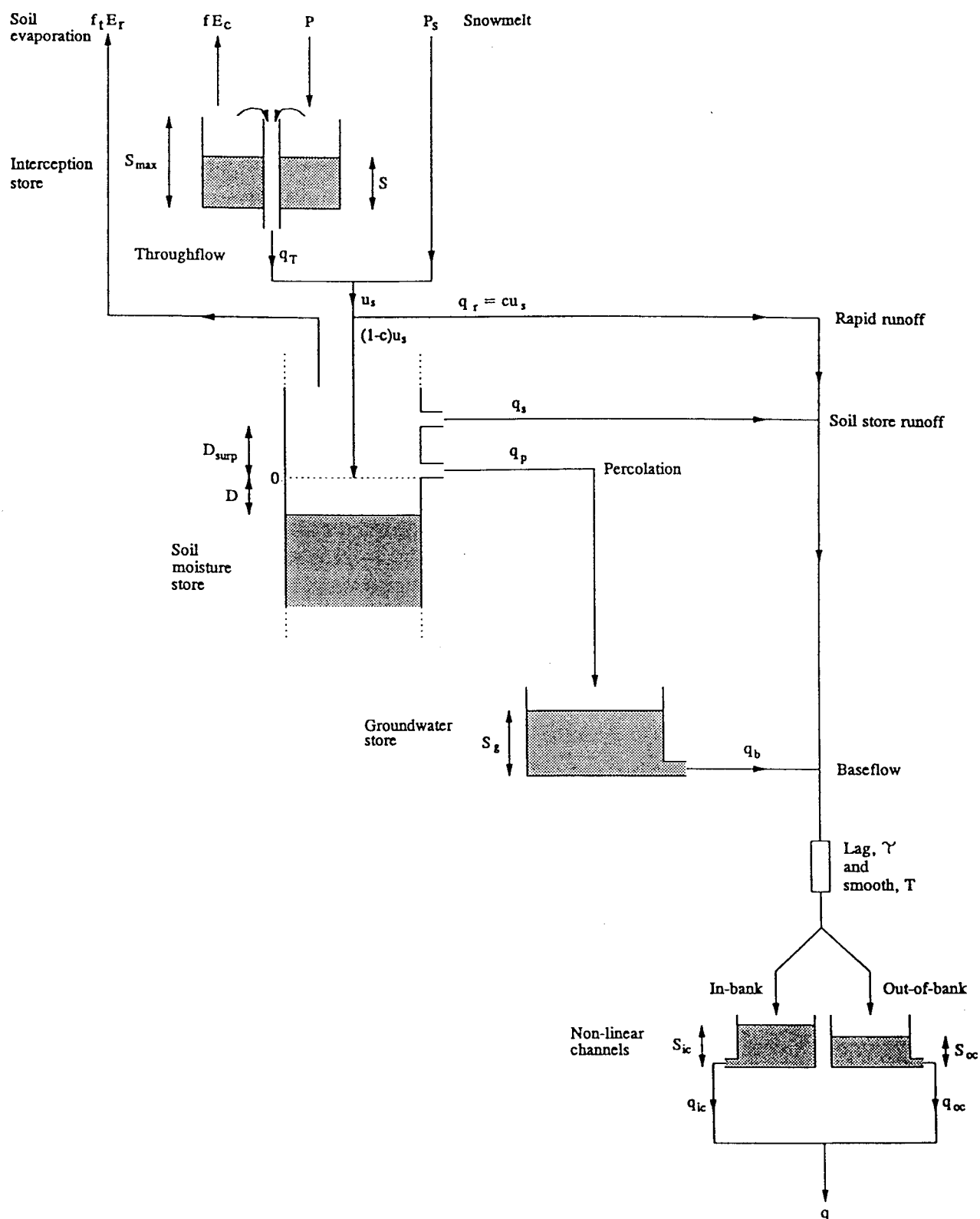


Figure 4.1.1 The Midlands Catchment Runoff Model.

$$\text{Potential interception evaporation } E_p = f E_c \quad (4.2.3)$$

$$\text{Residual evaporation demand } E_r = \begin{cases} E_p - \frac{S}{f} & E_p > S > 0 \\ 0 & E_p \leq S \leq 0 \\ E_c & S \leq 0 \end{cases} \quad (4.2.4)$$

$$S = \begin{cases} 0 & E_p > S > 0 \\ S - E_p & E_p \leq S; S > 0. \end{cases}$$

2. Soil store

The soil store has no defined capacity, calculations proceeding on the basis of the amount of water in deficit, D . Input to the soil store, u_s , is made up of throughflow, q_T , from the interception store plus any melt, P_s , from the snowmelt component, so that $u_s = q_T + P_s$. A proportion of the input, c , does not enter the store but forms rapid runoff. This proportion increases as an exponential function of the negative deficit, from a minimum value c_0 up to a maximum value c_{\max} under the control of parameter c_1 (Figure 4.2.1a); thus

$$\text{Rapid runoff proportion } c = \min(c_{\max}, c_0 \exp(-c_1 D)) \quad (4.2.5)$$

$$\text{Rapid runoff } q_r = c u_s \quad (4.2.6)$$

$$\text{Soil moisture deficit } D = D - (1 - c) u_s. \quad (4.2.7)$$

In practice the calculation is carried out incrementally, for each unit of input u_s , and the q_r values summed to account more accurately for the nonlinear dependence of the runoff proportion on the negative deficit.

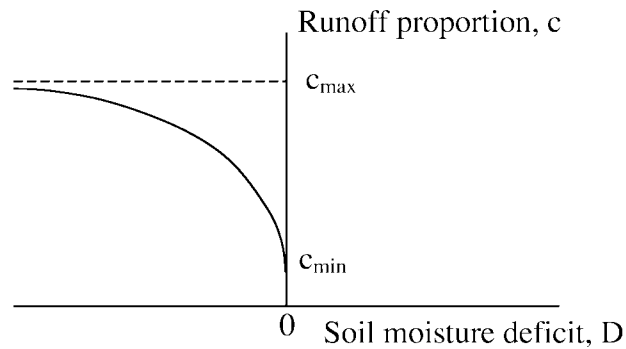
Percolation to groundwater occurs only for negative deficits ($D < 0$) when it is governed by the equation

$$q_p = \begin{cases} \frac{q_p^{\max} D}{-D_{\text{surp}}} & -D_{\text{surp}} < D \leq 0 \\ q_p^{\max} & D \leq -D_{\text{surp}} \end{cases} \quad (4.2.8)$$

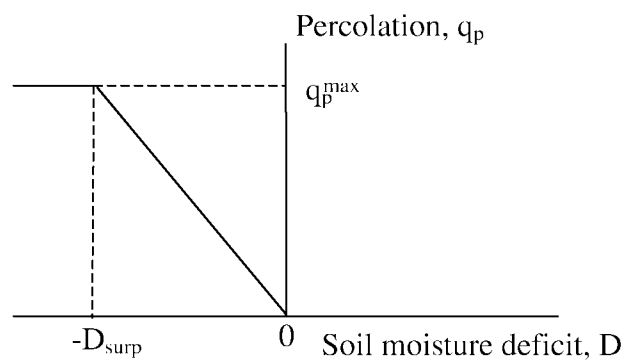
where q_p^{\max} is the maximum percolation rate parameter and D_{surp} is the soil store moisture surplus parameter. Figure 4.2.1b illustrates the form of the percolation function. The deficit is updated using

$$D = D + q_p. \quad (4.2.9)$$

- (a) **Rapid runoff proportion as a function of negative soil moisture deficit (moisture surplus)**



- (b) **Percolation to groundwater as a function of negative soil moisture deficit (moisture surplus)**



- (c) **Rapid drainage as a function of (negative) soil moisture deficit, D (or excess water, $W = - (D_{\text{surp}} + D)$)**

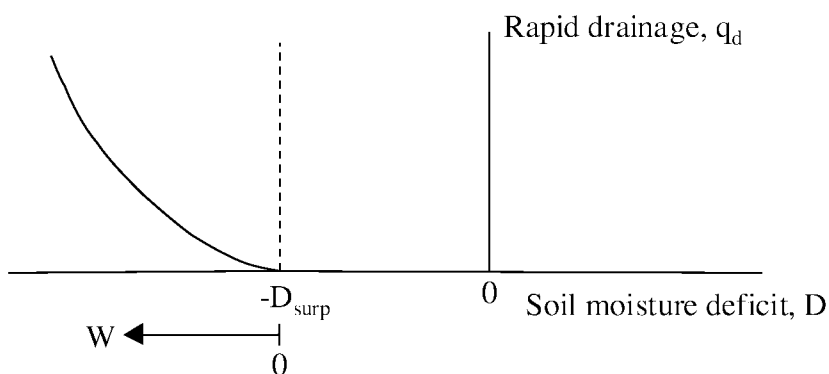


Figure 4.2.1 Rapid runoff, percolation and rapid drainage functions in the Midlands Catchment Runoff Model.

Rapid drainage, q_d , which like rapid runoff bypasses the groundwater store, is generated when the negative deficit exceeds a critical value, D_{surp} , and gives rise to “excess water” conditions. Excess water is given by

$$W = -(D_{surp} + D) \quad D < -D_{surp} \quad (4.2.10)$$

and rapid drainage is governed by the power function

$$q_d = \frac{W^{\gamma_d}}{k_d} \quad (4.2.11)$$

where γ_d is a soil function exponent and k_d is a soil function coefficient. Figure 4.2.1c illustrates the form of the rapid drainage function. The deficit is updated using

$$D = D + q_d. \quad (4.2.12)$$

Soil store runoff, q_s , is then

$$q_s = q_r + q_d. \quad (4.2.13)$$

Finally, the soil store is further depleted by any residual evaporation demand, E_r , according to the soil water evaporation function which gives soil evaporation as

$$E_s = f_t E_r \quad (4.2.14)$$

where the transpiration factor, f_t , is given by

$$f_t = \begin{cases} T_p & D < E_{\max}^D \\ T_m & D > E_{\min}^D \\ T_p - \frac{(D - E_{\max}^D)(T_p - T_m)}{E_{\min}^D - E_{\max}^D} & \text{otherwise} \end{cases} \quad (4.2.15)$$

with $T_m \leq f_t \leq T_p$. Here T_p and T_m are the potential and minimum transpiration parameters and E_{\max}^D and E_{\min}^D the corresponding deficit values at which these limiting conditions first apply.

Finally, the soil moisture deficit is updated using

$$D = D + E_s. \quad (4.2.16)$$

3. Groundwater store

The groundwater store behaves as a nonlinear storage with an exponent value of 1.5. It receives percolation, q_p , from the soil moisture store as input and output is baseflow, q_b . The groundwater storage is updated according to

$$S_g = S_g + q_p \quad q_p > 0 \quad (4.2.17)$$

and baseflow is given by the storage function

$$q_b = \frac{S_g^{1.5}}{1000K_g} \quad (4.2.18)$$

with parameter K_g . Adjustment to the storage then follows as

$$S_g = \begin{cases} S_g - q_b & S_g > 0 \\ 0 & \text{otherwise.} \end{cases} \quad (4.2.19)$$

4. *Lag and spread of catchment runoff*

The total runoff is the sum of baseflow and soil store runoff, $q_b + q_s$. This is lagged by a fixed time interval, τ , and spread evenly over a specified duration, T , in order to represent the translation of water from the ground to the catchment outlet.

5. *Nonlinear smoothing of catchment runoff*

The last operation in the Midlands Catchment Runoff Model is the application of a nonlinear smoothing function to produce a smooth catchment outflow hydrograph. Nonlinear storage functions are used for in-bank and out-of-bank flows, which are treated separately as follows. After first adding the lagged runoff to the in-channel storage, S_{ic} , the out-of-bank component of the input and in-channel storage are calculated as

$$u_{oc} = \begin{cases} S_{ic} - S_{bf} & S_{ic} > S_{bf} \\ 0 & \text{otherwise} \end{cases} \quad (4.2.20)$$

$$S_{ic} = S_{bf} \quad S_{ic} > S_{bf}.$$

The in-channel outflow is given by the nonlinear storage function

$$q_{ic} = \begin{cases} k_{cr} S_{ic}^{\gamma_{cr}} & q_{ic} \leq .75 S_{ic} \\ .75 S_{ic} & \text{otherwise} \end{cases} \quad (4.2.21)$$

where k_{cr} and γ_{cr} are the in-channel routing coefficient and exponent. A similar expression is used to obtain the out-of-bank outflow, q_{oc} , from the out-of-bank storage, S_{oc} . Updating of the in-channel storage follows

$$S_{ic} = S_{ic} - q_{ic} \quad (4.2.22)$$

and for the out-of-channel store

$$S_{oc} = S_{oc} + u_{oc} \quad (4.2.23)$$

Finally, the total catchment outflow is calculated as

$$q = q_{ic} + q_{oc} . \quad (4.2.24)$$

4.3 Model Parameters

A summary of the model parameters used in the Midlands Catchment Runoff Model is presented in Table 4.3.1 together with the units used in the model.

Table 4.3.1 Parameters in the Midlands Catchment Runoff Model

| Parameter | Unit | Description |
|----------------------|--|---|
| f_c | none | Rainfall factor |
| S_{\max} | mm | Capacity of interception store |
| f | none | Fraction of catchment evaporation potentially met by interception storage |
| c_0 | none | Minimum value of rapid runoff proportion |
| c_1 | mm^{-1} | Parameter in rapid runoff proportion function |
| c_{\max} | none | Maximum value of rapid runoff proportion |
| q_p^{\max} | mm h^{-1} | Maximum percolation rate |
| D_{surp} | mm | Maximum soil store moisture surplus |
| γ_d | none | Soil function exponent controlling rapid drainage |
| k_d | h mm^{γ_d-1} | Soil function coefficient controlling rapid drainage |
| T_p | none | Potential transpiration factor |
| T_m | none | Minimum transpiration factor |
| E_{\max}^D | mm | Deficit below which potential transpiration factor applies |
| E_{\min}^D | mm | Deficit above which minimum transpiration factor applies |
| K_g | $\text{h mm}^{0.5}$ | Time constant in baseflow storage function |
| τ | h | Time lag applied to total runoff |
| T | h | Duration of time spread applied to total runoff |
| S_{bf} | mm | Channel storage at bankfull |
| k_{cr} | $\text{h}^{-1} \text{mm}^{1-\gamma_{\text{cr}}}$ | In-channel routing storage coefficient |
| γ_{cr} | none | In-channel routing storage exponent |
| k_{or} | $\text{h}^{-1} \text{mm}^{1-\gamma_{\text{or}}}$ | Out-of-bank channel routing storage coefficient |
| γ_{or} | none | Out-of-bank channel routing storage exponent |

5. THE PROBABILITY DISTRIBUTED MOISTURE MODEL

5.1 Introduction

The Probability Distributed Moisture model or PDM is a fairly general conceptual rainfall-runoff model which transforms rainfall and evaporation data to flow at the catchment outlet. Figure 5.1.1 illustrates the general form of the model. Runoff production at a point in the catchment is controlled by the absorption capacity of the soil to take up water: this can be conceptualised as a simple store with a given storage capacity. By considering that different points in a catchment have differing storage capacities and that the spatial variation of capacity can be described by a probability distribution, it is possible to formulate a simple runoff production model which integrates the point runoffs to yield the catchment surface runoff into surface storage. Groundwater recharge from the soil moisture store passes into subsurface storage. The outflow from surface and subsurface storages, together with any fixed flow representing, say, compensation releases from reservoirs or constant abstractions, forms the model output. The components of the PDM model are described in more detail below.

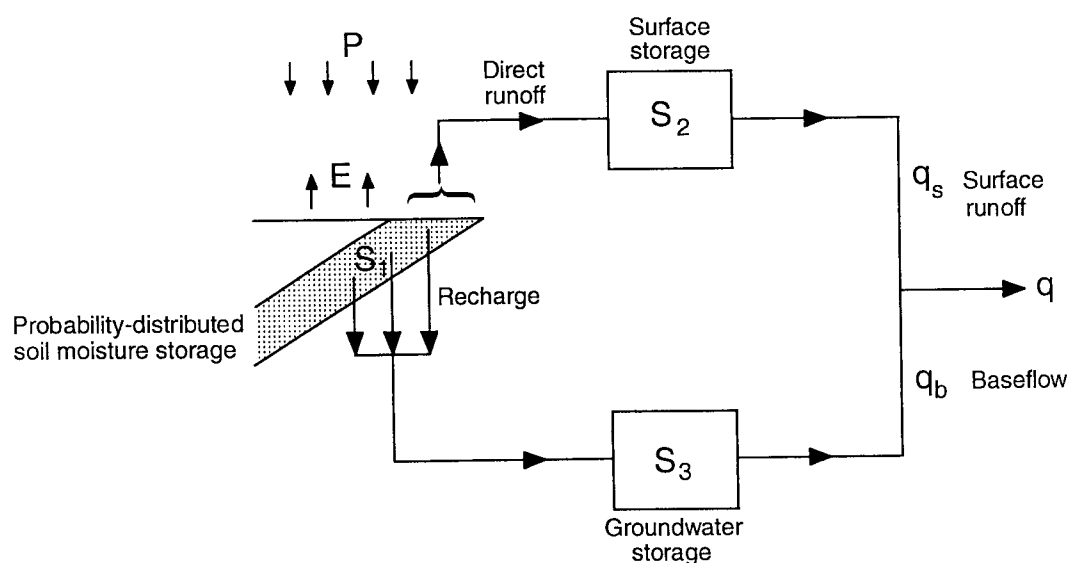


Figure 5.1.1 The PDM rainfall-runoff model.

5.2 Soil Moisture Store

Consider that runoff production at any point within a river basin may be conceptualised as a single storage, or tank, of capacity c' , representing the absorption capacity of the soil column at that point. The storage takes up water from rainfall, P , and loses water by evaporation, E , until either the storage fills and spills, generating direct runoff, q , or empties and ceases to lose water by evaporation. Figure 5.2.1(a) depicts such a storage, whose behaviour may be expressed mathematically by

$$q = \begin{cases} P - E - (c' - S_0) & P > c' + E \\ 0 & P \leq c' + E \end{cases} \quad (5.2.1)$$

where S_0 is the initial depth of water in storage, and where P , E and q represent the depth of rainfall, evaporation and the resulting direct runoff over the interval being considered. Now consider that runoff production at every point within a river basin may be similarly described, each point differing from another only with regard to the storage capacity. The storage capacity at any point, c , may then be considered as a random variate with probability density function, $f(c)$, so that the proportion of the river basin with depths in the range $(c, c+dc)$ will be $f(c)dc$.

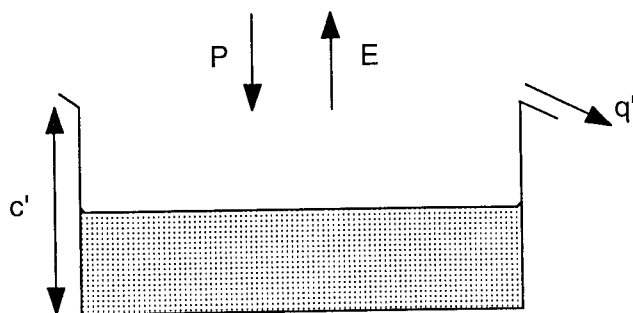
The water balance for a river basin assumed to have storage capacities distributed in this way may be constructed as follows. First imagine that stores of all possible different depths are arranged in order of depth and with their open tops arranged at the same height: this results in a wedge-shaped diagram as depicted in Figure 5.2.1(b). If the basin is initially dry so that all stores are empty and rain falls at a net rate P for a unit duration, then stores will fill to a depth P unless they are of lesser depth than P when they will fill and spill. During the interval the shallowest stores will start generating direct runoff and at the end of the interval stores of depth P will just begin to produce runoff, so that the hachured triangular area denotes the depth produced from stores of different depth over the unit interval. Since, in general, there are more stores of one depth than another the actual runoff produced over the basin must be obtained by weighting the depth produced by a store of a given depth by its frequency of occurrence, as expressed by $f(c)$. Now, at the end of the interval stores of depth less than P are generating runoff: let this critical capacity below which all stores are full at some time t be denoted by $C^* \equiv C^*(t)$ ($C^* = P$ in the present example). The proportion of the basin containing stores of capacity less than or equal to C^* is

$$\text{prob}(c \leq C^*) = F(C^*) = \int_0^{C^*} f(c)dc. \quad (5.2.2)$$

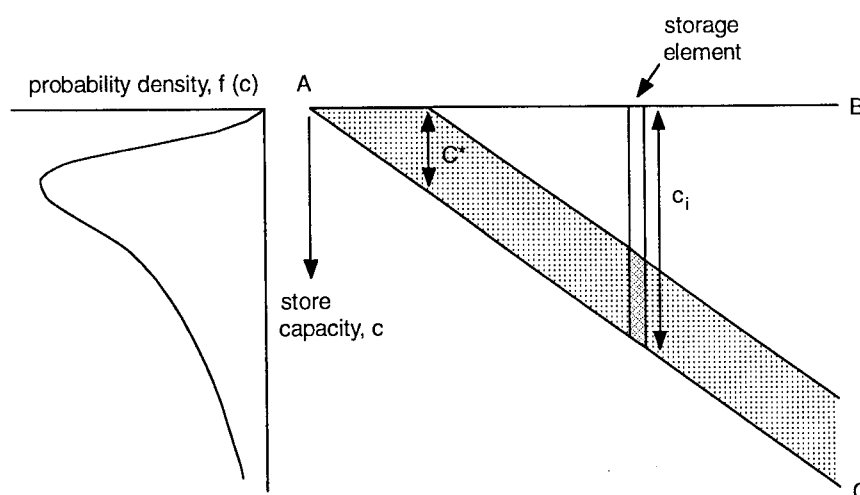
The function $F(\cdot)$ is the distribution function of store capacity and is related to the density function, $f(c)$, through the relation $f(c) = dF(c)/dc$. This proportion is also the proportion of the basin generating runoff, so that the contributing area at time t for a basin of area A is

$$A_c(t) = F(C^*(t))A. \quad (5.2.3)$$

(a) Point representation of runoff production by a single store



(b) Basin representation by storage elements of different depth and their associated probability density function



(c) Direct runoff production from a population of stores

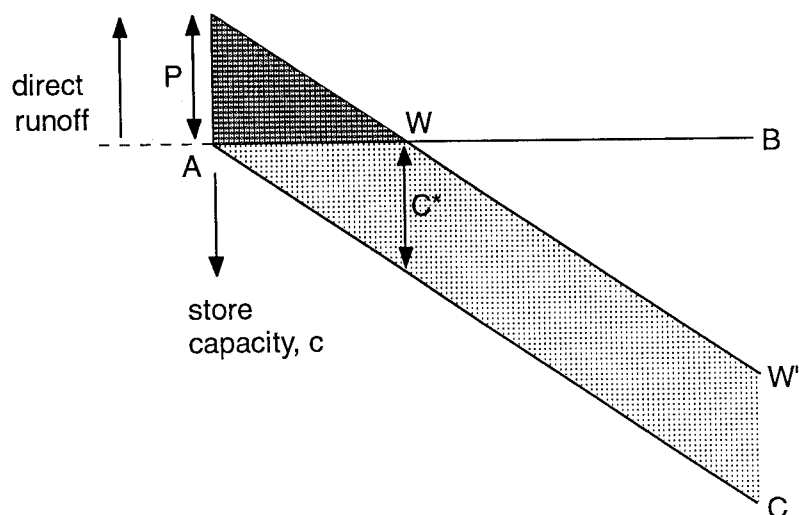


Figure 5.2.1 Definition diagrams for the probability-distributed interacting storage capacity component.

The instantaneous direct runoff rate per unit area from the basin is the product of the net rainfall rate, $\pi(t)$, and the proportion of the basin generating runoff, $F(C^*(t))$; that is

$$q(t) = \pi(t) F(C^*(t)). \quad (5.2.4)$$

During the i 'th wet interval, $(t, t+\Delta t)$, suppose rainfall and potential evaporation occur at constant rates P_i and E_i , so that net rainfall $\pi_i = P_i - E_i$. Then the critical capacity, $C^*(\tau)$, will increase over the interval according to

$$C^*(\tau) = C^*(t) + \pi_i(\tau - t) \quad t \leq \tau \leq t + \Delta t, \quad (5.2.5)$$

the contributing area will expand according to (5.2.3), and the volume of basin direct runoff per unit area produced over this interval will be

$$V(t + \Delta t) = \int_t^{t+\Delta t} q(\tau) d\tau = \int_{C^*(t)}^{C^*(t+\Delta t)} F(c) dc. \quad (5.2.6)$$

During dry periods potential evaporation will deplete the water content of each storage. It will be assumed during such depletion periods that water moves between storages of different depths so as to equalise the depth of stored water at different points within the basin. Thus at any time all stores will have a water content, C^* , irrespective of their capacity, unless this is less than C^* when they will be full: the water level profile across stores of different depths will therefore always be of the simple form shown in Figure 5.2.2(c). The assumption which allows redistribution of water between storages of different size during depletion periods is particularly important for real-time applications of the model where the possibility of updating the store contents is envisaged. Moore (1985) shows how this assumption, when not invoked, leads to a more complex water accounting procedure which is less amenable to real-time empirical state adjustment schemes. Particularly important is that a unique relationship exists between the water in storage over the basin as a whole, $S(t)$, and the critical capacity, $C^*(t)$, and in turn to the instantaneous rate of basin runoff production, $Q(t)$. Specifically, and referring to Figure 5.2.2(c), it is clear that the total water in storage over the basin is

$$\begin{aligned} S(t) &= \int_0^{C^*(t)} cf(c)dc + C^*(t) \int_{C^*(t)}^{\infty} f(c)dc \\ &= \int_0^{C^*(t)} (1 - F(c))dc. \end{aligned} \quad (5.2.7)$$

For a given value of storage, $S(t)$, this can be used to obtain $C^*(t)$ which allows the volume of direct runoff, $V(t+\Delta t)$, to be calculated using equations (5.2.6) together with (5.2.5).

The dependence of evaporation loss on soil moisture content is introduced by assuming the following simple function between the ratio of actual to potential evaporation, E'_i/E_i , and soil moisture deficit, $S_{\max} - S(t)$:

$$\frac{E'_i}{E_i} = 1 - \left\{ \frac{(S_{\max} - S(t))}{S_{\max}} \right\}^{b_e}; \quad (5.2.8)$$

either a linear ($b_e=1$ so $E'_i=(S(t)/S_{\max})E_i$) or quadratic form ($b_e=2$) is usually assumed. Here, S_{\max} is the total available storage, and is given by

$$S_{\max} = \int_0^{\infty} cf(c)dc = \int_0^{\infty} (1 - F(c))dc = \bar{c}, \quad (5.2.9)$$

where \bar{c} is the mean storage capacity over the basin.

Further loss as recharge to groundwater may be introduced by assuming that the rate of drainage over the interval, d_i , depends linearly on basin soil moisture content at the start of the interval i.e.

$$d_i = k_r (S(t) - S_i)^{b_r} \quad (5.2.10)$$

where k_r is a drainage time constant with units of inverse time, b_r is an exponent (usually set to 1) and S_i is the threshold storage below which there is no drainage, water being held under soil tension. An alternative formulation is available which allows recharge to depend on both soil and groundwater storage for use in catchments where soil/groundwater interactions are important. Consider recharge into a groundwater store of maximum capacity S_g^{\max} . Then a groundwater deficit ratio may be defined as

$$g(t) = \frac{S_g^{\max} - S_g(t)}{S_g^{\max}} \quad (5.2.11)$$

where $S_g(t)$ denotes the groundwater storage at time t . This ratio can be used to define a groundwater demand factor between 0 and 1:

$$f(t) = \begin{cases} \left(\frac{g(t)}{\alpha} \right)^{\beta} & g(t) < \alpha \\ 1 & \text{otherwise} \end{cases} \quad (5.2.12)$$

which achieves a maximum for values of the deficit ratio $g(t)$ in excess of α . It is then reasonable to suppose that the recharge depth over the interval, D_i , will increase with soil storage, $S(t)$, and with the groundwater demand factor, $f(t)$, according to

$$D_i = (D_{sat} + (S_{\max} - D_{sat})f(t)) \frac{S(t)}{S_{\max}}. \quad (5.2.13)$$

Here the maximum possible recharge depth $D_{sat}=q_{sat}\Delta t$, with q_{sat} the outflow from the groundwater storage when $S_g(t)$ equals S_g^{\max} . Note that the drainage rate over the interval is $d_i=D_i/\Delta t$. There are thus only three parameters: α , β and q_{sat} (with S_g^{\max} thereby implied from its storage function). It is seen that, for a saturated soil store, recharge is diminished when the groundwater demand factor is less than α , when the soil ceases to be freely draining. This formulation derives from a reparameterised form of percolation model used in the National Weather Service rainfall-runoff model (Burnash *et al.*, 1973; Gupta and Sarooshian, 1983).

A third recharge formulation is available which assumes that there is no soil drainage, d_i . Direct runoff is split between a fraction α which goes to make up surface runoff and a fraction $(1-\alpha)$ going to groundwater storage.

With both losses to evaporation and recharge, the net rainfall, π_i , may be defined in general as

$$\pi_i = P_i - E'_i - d_i . \quad (5.2.14)$$

During a period when no runoff generation occurs then, for this general case, soil moisture storage accounting simply involves the calculation

$$S(\tau) = S(t) + \pi_i (\tau - t) \quad t \leq \tau \leq t + \Delta t, 0 \leq S(\tau) \leq S_{\max} . \quad (5.2.15)$$

When runoff generation does occur then the volume of runoff produced, $V(t+\Delta t)$, is obtained using (5.2.6), and then continuity gives the replenished storage as

$$S(t + \Delta t) = \begin{cases} S(t) + \pi_i \Delta t - V(t + \Delta t) & S(t + \Delta t) \leq S_{\max} \\ S_{\max} & \text{otherwise} \end{cases} \quad (5.2.16)$$

If basin storage is fully replenished within the interval $(t, t+\Delta t)$ then $V(t+\Delta t)$ should be computed from continuity as

$$V(t + \Delta t) = \pi_i \Delta t - (S_{\max} - S(t)). \quad (5.2.17)$$

The above completes the procedure for soil moisture accounting and determining the value of runoff production according to a probability-distributed storage capacity model. Figure 5.2.2 provides a graphical representation of this procedure for a wet interval $(t, t+\Delta t)$ during which soil moisture storage is added to by an amount $\Delta S(t+\Delta t) = \pi_i \Delta t - V(t+\Delta t)$, and a volume of direct runoff, $V(t+\Delta t)$, is generated.

A specific application of the procedure can be developed for a given choice of probability density function. Analytical solutions of the integrals in the probability-distributed storage capacity model component (specifically equations (5.2.6) and (5.2.7)) are presented in Institute of Hydrology (1992) for a range of possible distribution types. After a number of trials on alternative distributions, a Pareto distribution of storage capacity is now most widely used in practice and will be used here to illustrate application of the method. The distribution function and probability density function for this distribution are

$$F(c) = 1 - (1 - c/c_{\max})^b \quad 0 \leq c \leq c_{\max} \quad (5.2.18)$$

$$f(c) = \frac{dF(c)}{dc} = \frac{b}{c_{\max}} \left(1 - \frac{c}{c_{\max}} \right)^{b-1} \quad 0 \leq c \leq c_{\max} \quad (5.2.19)$$

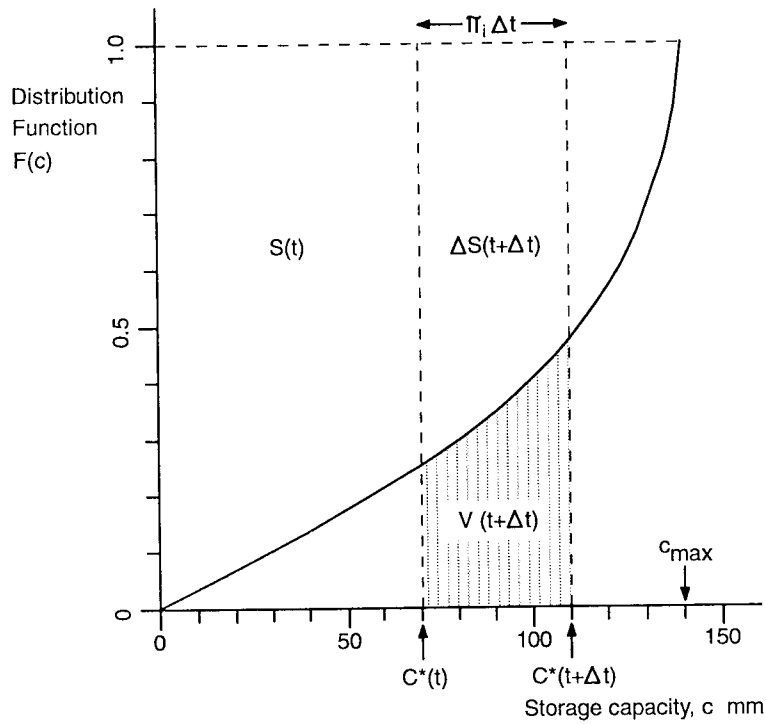


Figure 5.2.2 The storage capacity distribution function used to calculate basin moisture storage, critical capacity, and direct runoff according to the probability-distributed interacting storage capacity model.

(a) Probability density function

(b) Distribution function

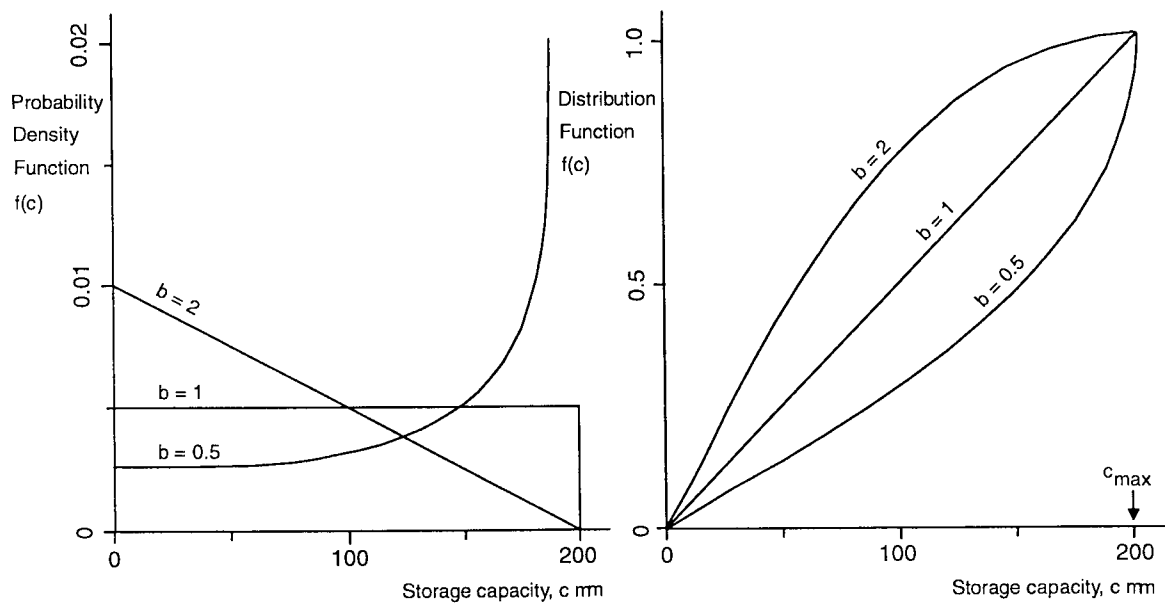


Figure 5.2.3 The Pareto distribution of storage capacity.

where parameter c_{\max} is the maximum storage capacity in the basin, and parameter b controls the degree of spatial variability of storage capacity over the basin. These functions are illustrated in Figure 5.2.3: note that the rectangular distribution is obtained as a special case when $b=1$, and $b=0$ implies a constant storage capacity over the entire basin. The following relations apply for Pareto distributed storage capacities:-

$$S_{\max} = c_{\max} / (b + 1), \quad (5.2.20a)$$

$$S(t) = S_{\max} \left\{ 1 - (1 - C^*(t)/c_{\max})^{b+1} \right\}, \quad (5.2.20b)$$

$$C^*(t) = C_{\max} \left\{ 1 - (1 - S(t)/S_{\max})^{1/(b+1)} \right\}, \quad (5.2.20c)$$

$$V(t + \Delta t) = \pi_i \Delta t - S_{\max} \left\{ (1 - C^*(t)/c_{\max})^{b+1} - (1 - C^*(t + \Delta t)/c_{\max})^{b+1} \right\}. \quad (5.2.20d)$$

The relationship between rainfall and runoff implied by the above expressions, for given conditions of soil moisture, is presented in Figure 5.2.4. A related, if not similar, procedure forms the basis of the Xinanjiang model developed by Ren Jun Zhao and co-workers in China (Zhao and Zhuang, 1963; Zhao *et al.*, 1980) and most recently popularised and extended by Todini, 1996) in the form of the Arno model in Italy. Indeed, Moore (1985) traces back the origins of such probability-distributed principles in hydrology to the pioneering contribution of Bagrov in 1950, working in what was then the USSR.

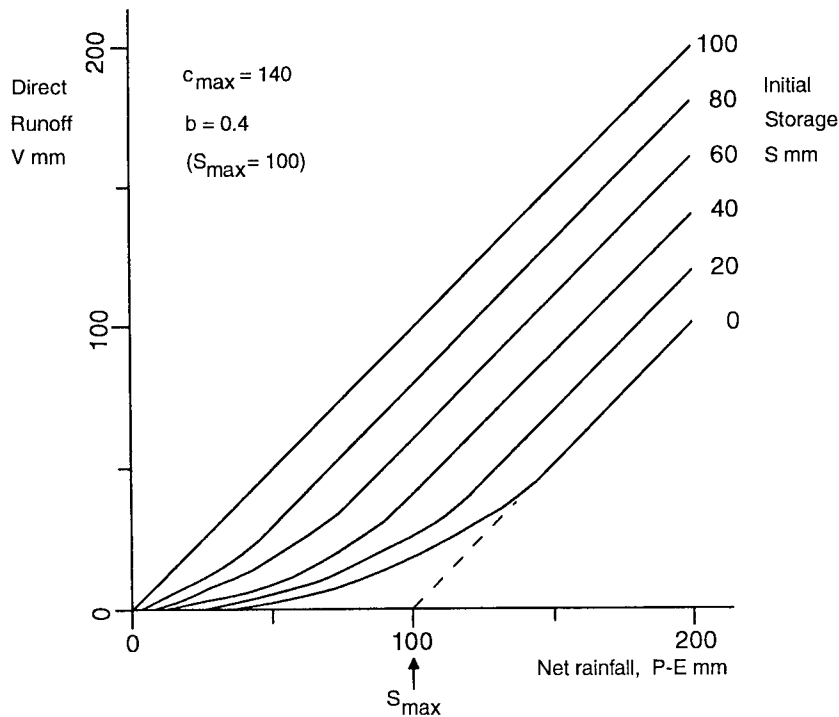


Figure 5.2.4 Rainfall-runoff relationship for the probability-distributed interacting storage capacity model, using the Pareto distribution of storage capacity.

5.3 Surface and Subsurface Storages

The probability-distributed store model partitions rainfall into direct runoff, groundwater recharge and soil moisture storage. Direct runoff is routed through surface storage: a “fast response system” representing channel and other fast translation flow paths. Groundwater recharge from soil water drainage is routed through subsurface storage: a “slow response system” representing groundwater and other slow flow paths. Both routing systems can be defined by a variety of nonlinear storage reservoirs or by a cascade of two linear reservoirs (expressed as an equivalent second order transfer function model constrained to preserve continuity). The choice of nonlinear storage includes the linear and quadratic storages reviewed in the context of the TCM and IEM together with exponential, cubic and general nonlinear forms. A cubic form is usually considered most appropriate to represent the groundwater storage. In this case where $q=kS^3$ an approximate solution utilising a method due to Smith (1977) yields the following recursive equation for storage, given a constant input u over the interval $(t, t+\Delta t)$:

$$S(t + \Delta t) = S(t) - \frac{1}{3kS(t)^2} \left\{ \exp(-3kS(t)^2 \Delta t) - 1 \right\} (u - kS(t)^2). \quad (5.3.1)$$

Discharge may then be obtained simply using the nonlinear relation

$$q(t + \Delta t) = k S(t + \Delta t)^3. \quad (5.3.2)$$

Solutions for the other nonlinear forms are presented in Appendix A. When used to represent groundwater storage, the input u will be the drainage rate, d_i , from the soil moisture store and the output $q(t)$ will be the “baseflow” component of flow $q_b(t)$. Explicit allowance for groundwater abstractions is incorporated in a new extension of the PDM which can also make use of well level data. The theoretical basis of this extension is outlined in Section 5.4.

The most commonly used representation of the surface storage component is a cascade of two linear reservoirs, with time constants k_1 and k_2 , expressed as the discretely coincident transfer function model

$$q_t = -\delta_1 q_{t-1} - \delta_2 q_{t-2} + \omega_0 u_t + \omega_1 u_{t-1} \quad (5.3.3)$$

with

$$\begin{aligned} \delta_1 &= -(\delta_1^* + \delta_2^*), \quad \delta_2 = \delta_1^* \delta_2^*, \quad \delta_1^* = \exp(-\Delta t/k_1), \quad \delta_2^* = \exp(-\Delta t/k_2) \\ \omega_0 &= \frac{k_1(\delta_1^* - 1) - k_2 \delta_2^*}{k_2 - k_1} & k_1 \neq k_2 \\ \omega_1 &= \frac{k_2(\delta_2^* - 1)\delta_1^* - k_1(\delta_1^* - 1)\delta_1^*}{k_2 - k_1} & k_1 \neq k_2 \end{aligned} \quad (5.3.4)$$

$$\omega_0 = 1 - (1 + \Delta t/k_1) \delta_1^* \quad k_1 = k_2$$

$$\omega_1 = (\delta_1^* - 1 + \Delta t/k_1) \delta_1^* \quad k_1 = k_2.$$

Here Δt is the time interval between times $t-1$ and t and it is assumed that the input u_t is constant over this interval. In this case the input is the volume of direct runoff, $V(t)$, generated from the probability-distributed soil moisture store and the output q_t will be the surface flow component of the total basin runoff, $q_s(t)$. The total basin flow is given by $q_s(t)+q_b(t)$, plus a constant flow, q_c , representing any returns or abstractions.

5.4 Groundwater Losses

Water held in groundwater storage can be lost to the surface catchment by artificial pumped abstractions, by underflow below the gauged catchment outlet or by spring flow external to the surface catchment. Losses via underflow and spring flow will be considered later. In the case of abstractions, a , the nonlinear storage theory introduced in Section 5.3 requires extension to consider the case of negative net input to storage, u , and the possibility of storages being drawn down below a level at which flow at the catchment outlet ceases. This extension allows for the modelling of ephemeral streams typical of catchments on the English Chalk.

Formally, we can define the input to the nonlinear storage, u , as recharge d , less abstractions, a , dropping the time suffix for notational simplicity. With $u=d-a$, the prospect arises of negative inputs to storage leading to the cessation of flow. Consider the time interval $(t, t+\Delta t)$ within which cessation of flow occurs after a time T' . Using the cubic storage, $q=kS^3$, for the purposes of illustration, then equation (5.3.1) gives the time to flow cessation, T' , by solving

$$0 = S(t) - \frac{1}{3kS(t)^2} \left\{ \exp(-3kS(t)^2 T') - 1 \right\} (u - kS(t)^3)$$

which gives

$$T' = -\frac{1}{3kS(t)^2} \ln \left\{ 1 + \frac{3kS(t)^3}{u - kS(t)^3} \right\}. \quad (5.4.1)$$

Now consider an extended form of storage is conceptualised which, instead of emptying at zero flow, allows for further withdrawal of water for abstraction (Figure 5.4.1). Then the “negative storage” at the end of the interval can be calculated as

$$\begin{aligned}
S(t + \Delta t) &= u(\Delta T - T') \\
&= u\Delta t \left\{ 1 + \frac{1}{3kS(t)^2 \Delta t} \ln \left\{ 1 + \frac{3kS(t)^3}{u - kS(t)^3} \right\} \right\} \\
&= u\Delta t \left\{ 1 + \frac{1}{a\Delta t q(t)^{2/3}} \ln \left\{ 1 + \frac{3q(t)}{u - q(t)} \right\} \right\}
\end{aligned} \tag{5.4.2}$$

where $a = 3k^{1/3}$.

With further abstractions from storage the negative storage can be calculated by simple continuity. When recharge exceeds abstractions the storage is replenished and at some time flow is initiated once more. The time interval within the model interval Δt that this occurs is calculated by simple continuity and the residual time interval used in equation (5.3.1) in place of Δt (with $S(t)=0$). The normal calculations apply whilst the storage is in surplus. Expressions for the time to flow cessation, T' , and the initial negative storage, $S(t+\Delta t)$, for other types of nonlinear store are given in Appendix A.7.

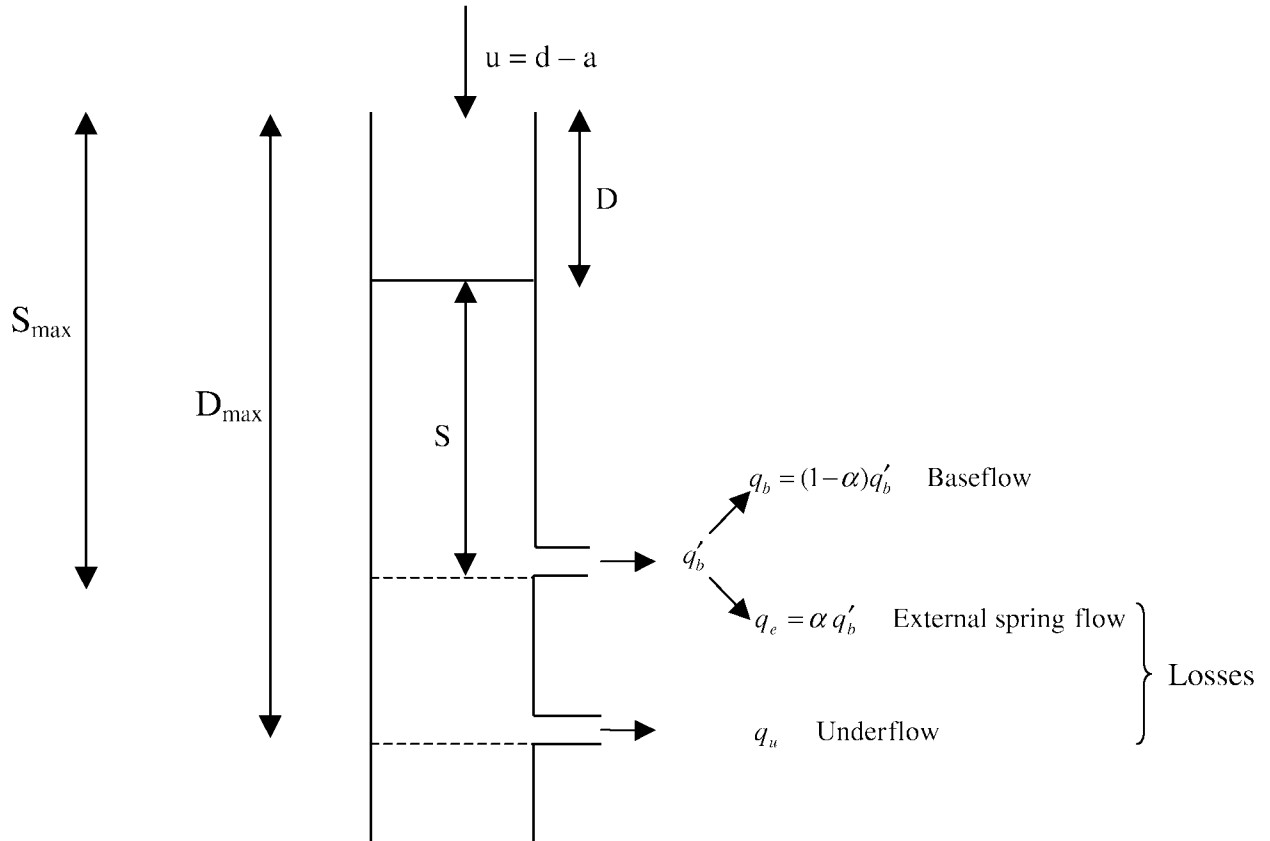


Figure 5.4.1 Conceptualisation of extended nonlinear storage.

If well measurements of groundwater level are available it is possible to relate the model storage, $S \equiv S(t)$, to the well level, $W^o \equiv W^o(t)$. Well measurements normally record the depth of the water table from the ground surface. By introducing a maximum groundwater storage, S_{\max} , then the groundwater storage deficit can be calculated as

$$D = S_{\max} - S \quad (5.4.3)$$

for both positive and negative values of S . This storage deficit can be used to calculate the depth to the water table as

$$W = Y_s D. \quad (5.4.4)$$

Here, Y_s is the specific yield of the groundwater reservoir, defined as the volume of water produced per unit aquifer area per unit decline in hydraulic head. This dimensionless parameter takes values typically in the range 0.01 to 0.3 (Freeze and Cherry, 1979). An additional datum correction may be required to relate W to observed well levels, W^o . The above provides the basis of incorporating well level measurements into both the model calibration process and the model state updating procedure. This will not be discussed further here.

Having extended the theory of nonlinear storage models to accommodate pumped abstractions, it is now appropriate to consider the conceptualisation of losses to underflow and external spring flow. Flow emerging from the catchment beneath the ground surface of the gauging station is referred to here as underflow. It is reasonable to suppose that underflow is controlled by the hydraulic head and thus the water in storage. If D_{\max} is the maximum deficit for underflow to occur then the rate of underflow can be defined as

$$q_u = k_u (D_{\max} - D), \quad (5.4.5)$$

where k_u is the underflow time constant (units of inverse time).

The normal outflow from the nonlinear reservoir, q_b , arising from positive values of storage, S , has been assumed to be the baseflow component of the flow at the catchment outlet. An extension allows a fraction, α , to contribute to springs external to the catchment whilst the remaining flow, $(1-\alpha)q$, contributes as baseflow at the catchment outlet.

5.5 Model Parameters

The parameter and structure options in the model are summarised in Table 5.5.1 below. Note that a rainfall factor, f_c , is incorporated in the model to allow conversion of a rainfall observation to rainfall, P , thereby compensating for effects such as lack of raingauge representativeness.

Table 5.5.1 Parameters of the PDM model

| Parameter name | Unit | Description |
|--------------------------------------|--------------------------------|---|
| f_c | none | rainfall factor |
| τ_d | h | time delay |
| <i>Probability-distributed store</i> | | |
| c_{min} | mm | minimum store capacity |
| c_{max} | mm | maximum store capacity |
| b | none | exponent of Pareto distribution controlling spatial variability of store capacity |
| <i>Evaporation function</i> | | |
| b_e | none | exponent in actual evaporation function |
| <i>Recharge function</i> | | |
| 1: Standard | | |
| k_g | h mm ^{bg-1} | groundwater recharge time constant |
| b_g | none | exponent of recharge function |
| S_t | mm | soil tension storage capacity |
| 2: Demand-based | | |
| α | none | groundwater deficit ratio threshold |
| β | none | exponent in groundwater demand factor function |
| q_{sat} | mm h ⁻¹ | maximum rate of recharge |
| 3: Splitting | | |
| α | none | runoff factor controlling the split of rainfall to surface and groundwater storage routing when no soil recharge is allowed |
| <i>Surface routing</i> | | |
| k_s | h | time constant of cascade of two equal linear reservoirs ($k_s=k_1=k_2$) |
| <i>Groundwater storage routing</i> | | |
| k_b | h mm ^{m-1} | baseflow time constant |
| m | none | exponent of baseflow nonlinear storage |
| q_c | m ³ s ⁻¹ | constant flow representing returns/abstractions |

6. NONLINEAR STORAGE MODELS: THE ISOLATED EVENT AND ISO FUNCTION MODELS

6.1 Introduction

Nonlinear storage models commonly occur as one or more elements in many conceptual models of the rainfall-runoff process. The outflow from a conceptual model store, $q \equiv q(t)$, is considered to be proportional to some power of the volume of water held in the storage, $S \equiv S(t)$, so that

$$q = kS^m, \quad k > 0, m > 0. \quad (6.1.1)$$

The storage, for example, could be a soil column or aquifer storage at the catchment scale. Combining the power equation (6.1.1) with the equation of continuity

$$\frac{dS}{dt} = u - q, \quad (6.1.2)$$

where $u \equiv u(t)$ is the input to the store (e.g. effective rainfall), gives

$$\frac{dq}{dt} = a(u - q)q^b, \quad q > 0, -\infty < b < 1, \quad (6.1.3)$$

where $a = mk^{1/m}$ and $b = (m-1)/m$ are two parameters. This ordinary differential equation has become known as the Horton-Izzard model (Dooze, 1973) and can be solved exactly for any rational value of n (Gill, 1976, 1977).

In this Section two specific nonlinear storage models developed and applied in the UK are reviewed. The first is the Isolated Event Model or IEM, originally developed for design use as part of the UK Flood Study (NERC, 1975), which employs a quadratic storage function ($m=2$ in (6.1.1)) so that $b=1/2$ in the Horton-Izzard equation. The second is the Input-Storage-Output or ISO-function model (Lambert, 1972) which employs a linear storage function ($m=0$, $b=0$), and/or an exponential storage function which yields the Horton-Izzard equation with $b=1$. The IEM and ISO-function models are reviewed in the next two sub-sections. Annex I provides further background on nonlinear storage models in general, including analytical derivations of the forecast equations for the linear, quadratic and exponential storage cases used in this Section.

6.2 The Isolated Event Model

6.2.1 Classical formulation

The Isolated Event Model, or IEM, was originally developed for design applications as part of the UK Flood Studies Project (NERC, 1975). In many respects it is very similar to the single zone representation of the Thames Catchment Model in using the Penman stores concept and a quadratic reservoir for routing. However, the use of the Penman stores concept is not done as part of an explicit soil moisture accounting procedure as is the case with the TCM. Rather

the soil moisture deficit it provides is used as an indicator of catchment wetness within an empirical equation which relates the proportion of rainfall that becomes runoff (the runoff coefficient) to the soil moisture deficit, D . Specifically the exponential function

$$f = \alpha \exp(-\beta D) \quad (6.2.1)$$

is used where β is a parameter with units $(\text{mm water})^{-1}$ and α is a dimensionless parameter. Note that the IEM uses as standard a Penman upper store of depth 75 mm, the root constant for short grass, with no bypassing ($\phi=0$). Because the original formulation was event-based and for design, the runoff coefficient, f , was applied to the whole storm and D was the soil moisture deficit at the start of the storm. The parameter α can be interpreted as a “gauge representativeness factor” since, with zero deficit (saturated conditions), a proportion α of the rain becomes runoff.

In the IEM approach the storm rainfall time series is multiplied by the factor f to give an “effective rainfall” series. This is then subject to a time delay before being used as input to the quadratic storage reservoir. The hyperbolic form of the solution (equation (3.2.8) or (I.10b)) is used to calculate the outflow from the reservoir which forms the IEM model flow prediction.

6.2.2 Real-time formulation

In real-time flood forecasting applications the concept of an “event” is often an awkward notion to work with. It becomes more natural then to define f as a time variant function of the deficit D , maintained as a water balance calculation throughout the storm. Thus we have

$$f_t = \alpha \exp(-\beta D_t). \quad (6.2.2)$$

The calculation of D_t throughout the storm can be achieved using the Penman stores employed within the Thames Catchment Model, and indeed can be calculated continuously between events. In practice the latter is most easily achieved (at least in off-line model calibration mode) using daily rainfall data and a daily time step, changing to the smaller interval of the flood event data at the start of each event. Note that in the IEM model formulation no use is made of the outflows from the Penman stores, only the deficit as an index of catchment wetness and its impact on the ensuing volume of flood runoff. In many respects the use of the IEM was as an engineering expedient at a time when continuous rainfall records were not widely available at the Institute of Hydrology and the soil moisture deficit calculated routinely at the Meteorological Office provided a readily available, and succinct, source of information on the antecedent conditions of selected flood events. In the 1990s there is no real justification for keeping these modelling components separate. It is also more attractive to use the Penman stores concept as part of an integrated, explicit water account model, as is done in the TCM, rather than through invoking an empirical function to account for “losses” as is the case with the IEM. However, whilst it may be more attractive it does not necessarily ensure superior forecast performance and it is one of the purposes of this study to assess the accuracy of the forecasts from the two models.

6.2.3 Further modifications

Further modifications of the classical IEM formulation resulted from trials undertaken in the context of the study by Moore *et al.* (1993). The first is to replace rainfall by net rainfall (rainfall less evaporation) prior to applying the factor f_t to yield effective rainfall.

Specifically, effective rainfall is defined as

$$u_t = \begin{cases} f_t(P - E) & P > E \\ 0 & P \leq E \end{cases} \quad (6.2.3)$$

where P and E denote storm rainfall and potential evaporation respectively.

The second modification is to replace the simple time delay on the effective rainfall by a triangular time delay function. Thus the inflow to the quadratic storage, I_t , is given by

$$I_t = \sum_{\tau=\tau_s}^{\tau_s+\tau_e} w_\tau u_{t-\tau} \quad (6.2.4)$$

where w_τ is the triangular weighting function defined by

$$w_\tau = \begin{cases} w(\tau - \tau_s) / \tau_p & \tau_s < \tau \leq (\tau_s + \tau_p) \\ w(\tau_s + \tau_e - \tau) / (\tau_e - \tau_p) & (\tau_s + \tau_p) < \tau \leq (\tau_s + \tau_e) \\ 0 & \text{elsewhere} \end{cases} \quad (6.2.5)$$

$$\sum_{\tau_s}^{\tau_s+\tau_e} w_\tau = 1$$

and the outflow, q_t , is calculated according to equation (3.2.8). The final modification is that a constant flow, q_c , can be added to q_t to give the total basin outflow, Q_t .

The EA Thames Region implementation of the IEM also uses a form of smoothing delay, but this differs in using a less general form of weighting function.

6.2.4 Model parameters

The similarity between the IEM and a single zone of the TCM has been exploited by implementing the IEM as a variant on the TCM. The IEM parameters are as for a TCM zone with $n=1$, A equal to the catchment area, $R_c=75$, $R_f=999$ and ϕ , k , a , τ_d and N set to zero. The remaining parameters, together with additional parameters specific to the IEM, are listed in Table 6.2.1.

Table 6.2.1 Parameters of the Isolated Event Model

| Parameter name | Unit | Description |
|----------------|--------------|--|
| α | none | Coefficient in runoff proportion equation |
| β | none | Exponent in runoff proportion equation |
| K | mm h | Quadratic storage constant |
| τ_s | h | Delay to start of smoothing triangle |
| τ_p | h | Delay from start to peak of smoothing triangle |
| τ_e | h | Delay from start to end of smoothing triangle |
| q_c | $m^3 s^{-1}$ | Constant flow |

6.3 ISO-Function Models

Lambert (1972) introduces a class of model which he refers to as ISO-function models, or Input-Storage-Output function models. The ISO-function model belongs to the class of models that are based on the Horton-Izzard equation, or nonlinear storage model given by the equation

$$\frac{dq}{dt} = a(u - q)q^b. \quad (6.3.1)$$

where q is the runoff rate, u is the input of rainfall over an interval and a and b are model parameters. This equation has been considered previously in relation to the IEM, TCM and PDM models and reviewed in detail in Appendix A. Specifically, Lambert (1972) considered the logarithmic storage function, $S = \kappa \ln q$, and the linear storage function, $S = \kappa q$, where κ is a model parameter appropriate to the two functions.

First, we will consider the logarithmic case. When $b=1$ in the nonlinear storage model (6.3.1) then Moore (1983) shows that the model derives from the exponential storage equation

$$\ln q = \gamma + aS \text{ or } q = \exp(\gamma + aS) \quad (6.3.2)$$

where a is the same parameter as appears in (6.3.1), and γ is an intercept parameter which differentiates out in the derivation of (6.3.1). The exponential storage equation of (6.3.2) is simply a generalised form of the logarithmic storage function $S = \kappa \ln q$ used by Lambert and both are encompassed by equation (6.3.1) with $b=1$. Note that the basis of the model is that the rate of change of storage is inversely proportional to the discharge since $dS/dt = \kappa/q$. Integrating equation (6.3.1) with $b=1$ gives the forecast equation

$$\begin{aligned} q_{t+T} &= \frac{q_t}{(q_t/u) + (1 - q_t/u)\exp(-aTu)} \\ &= \frac{q_t}{\exp(-aTu) + (q_t/u)(1 - \exp(-aTu))}. \end{aligned} \quad (6.3.3)$$

This is the “log-storage” model, or more properly the exponential storage model, derived by Lambert (1972), and which is in current use for flood forecasting on the River Dee (Central Water Planning Unit, 1977).

The linear case based on the storage function, $S=\kappa q$, is represented by the Horton-Izzard equation when $b=0$ and $a=k=\kappa^{-1}$ is a time constant with units of inverse time. Integrating (6.3.1) in this case gives the forecast equation

$$q_{t+T} = e^{-Tk} q_t + (1 - e^{-Tk})u. \quad (6.3.4)$$

In practice, allowance is made in the ISO-function model for a time delay, b , between rainfall and runoff so u is understood to refer to u_{t-b} in the forecast equations above.

For the recession case when the input, $u=0$, then the Horton-Izzard equation can be solved for $b \neq 0$ to give the forecast equation:

$$q_{t+T} = \left(q_t^{-b} + abT \right)^{-1/b} \quad b \neq 0; \quad (6.3.5)$$

which for the logarithmic case ($b=1$) gives

$$q_{t+T} = \left(q_t^{-1} + aT \right)^{-1}. \quad (6.3.6)$$

For the linear reservoirs case when $b=0$, then in recession when $u=0$ the forecast equation is

$$q_{t+T} = \exp(-kT) q_t. \quad (6.3.7)$$

A special feature of Lambert’s application of the ISO-function model is to allow the storage-discharge function to be made up of different segments, differing in terms of the type of storage function (linear or logarithmic) or the parameter value used. The choice of flow ranges and functions to be applied is guided by empirical storage-discharge curves obtained from recession analysis of historical hydrographs.

When the forecast equations are used in practice, observed values of the quantities (q and u) on the right hand side of the equation are employed to get the one-step ahead flow forecast. Forecasts for higher lead times are simply obtained in a recursive fashion by using the previous flow forecast in the right hand side for q . (It is assumed that some form of rainfall forecast is available for u in constructing forecasts with lead times beyond the time delay, b .) This form of recursive forecast construction incorporating the most recent observed flow is a simple case of state updating discussed further in Section 12.

7. US NATIONAL WEATHER SERVICE SACRAMENTO MODEL

7.1 Introduction

The US National Weather Service (NWS) rainfall-runoff model is also called the Sacramento Soil Moisture Accounting Model or simply the Sacramento Model. It was developed in the early 1970s at the NWS River Forecast Centre in Sacramento (California), principally by Bob Burnash and Larry Ferral, as a classic lumped, conceptual, soil moisture accounting model. The basic source document is the report by Burnash *et al.* (1973).

A schematic of the model is shown in Figure 7.1.1 which highlights that the model comprises three principal storages:

- (i) *unsaturated zone store* generating direct runoff to the basin outlet and rainfall excess feeding the saturated zone below after a proportion contributes to surface runoff;
- (ii) *saturated zone store* generating interflow and draining downwards as percolation to the groundwater zone; and
- (iii) *groundwater zone store* which is divided into water held under tension and water that is free to drain, both contributing to baseflow after losses have been taken into account.

An indicative account of the model formulation follows which, like the model schematic, may not be accurate in detail but serves to communicate the main form and function of the model.

7.2 Model Formulation

1. *Unsaturated zone store*

Evaporation from the unsaturated zone storage, E_s , reduces linearly with water in storage, S_u , from the potential rate, E , when the store is full to capacity, S_u^{\max} , to zero when empty, such that

$$E_s = E \frac{S_u}{S_u^{\max}}. \quad (7.2.1)$$

Direct runoff, q_d , is generated from the fraction of the catchment that is impervious, f , such that

$$q_d = fP \quad (7.2.2)$$

where P is rainfall. The impervious fraction f comprises the fixed fraction of the catchment that is impervious, f_i , together with the additional fraction which develops as tension water

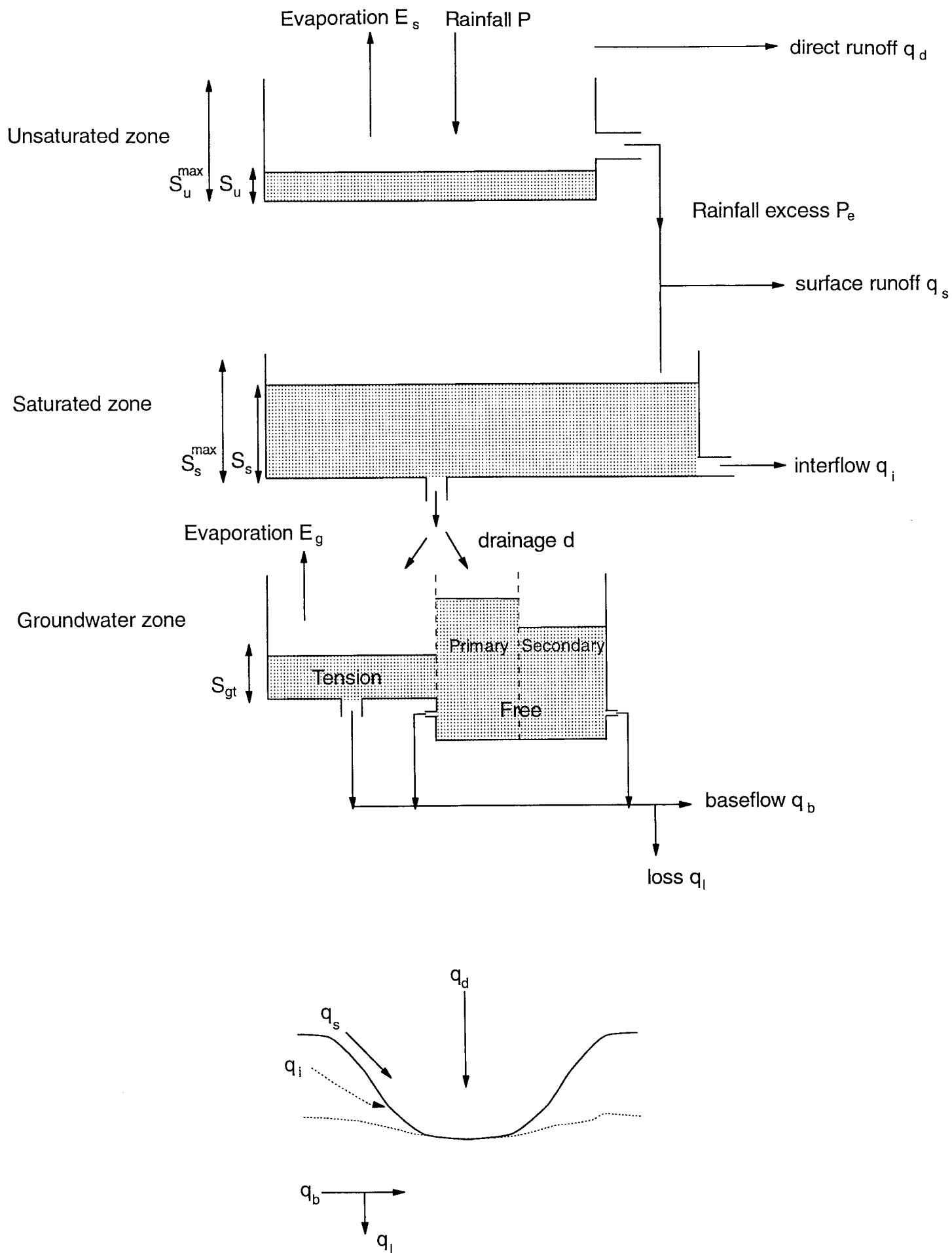


Figure 7.1.1 The US National Weather Service Sacramento Rainfall-Runoff Model.

requirements are met, f_w , so that $f=f_i+f_w$. Since f_w is limited to a maximum value f_w^{\max} , the potential (maximum) impervious fraction is $f_{\max}=f_i+f_w^{\max}$.

Rainfall excess is then calculated by continuity as

$$P_e = P - E_s - q_d \quad (7.2.3)$$

which passes downwards to the saturated zone store.

2. Saturated zone store

Surface runoff, q_s , is generated as a fraction $(1-f)$ of the rainfall excess

$$q_s = P_e(1-f) \quad (7.2.4)$$

leaving a residual rainfall excess to enter the saturated zone store, such that

$$P_e = P - E_s - fP = P(1-f) - E_s. \quad (7.2.5)$$

Interflow, q_i , from the saturated zone store is proportional to the water in the saturated zone store, S_s , with an adjustment for the potential impervious fraction f_{\max} such that

$$q_i = k_i S_s (1 - f_{\max}). \quad (7.2.6)$$

The lateral flows generated from the unsaturated and saturated zone storages are summed to give

$$q_{A+B} = q_d + q_s + q_i \quad (7.2.7)$$

and routed using a classical unit hydrograph convolution to give

$$Q_{A+B} = \int v(\tau) q_{A+B}(t - \tau) d\tau \quad (7.2.8)$$

where $v(\tau)$ is the impulse response function and t is time.

Channel evaporation is accounted for as a simple fraction, c , of the potential evaporation, so

$$E_c = cE. \quad (7.2.9)$$

Drainage (percolation) from the saturated zone into the groundwater zone occurs as a function of the degree of saturation in the saturated zone and the deficit in the groundwater zone, so

$$d = k_b \left(1 + \gamma \left[\frac{S_g^{\max} - S_g}{S_g^{\max}} \right]^\delta \right) \frac{S_s}{S_s^{\max}} \quad (7.2.10)$$

where $S_g^{\max} - S_g$ is the *total* deficit in the groundwater zone (all compartments) and k_b , γ and δ are model parameters.

3. Groundwater zone

Drainage (percolation) to groundwater is split between *tension water* S_{gt} and *free water* S_{gf} such that

$$S_{gt} = (1 - p)d \quad (7.2.11)$$

$$S_{gf} = pd \quad (7.2.12)$$

where p is a parameter determining the split. A proportion, r_s , of the free water in the groundwater zone is held in reserve and not used to replenish the tension water deficit.

Tension water supplies evaporation loss from groundwater as a function of the potential evaporation still to be satisfied and the proportion of total tension water storage that arises from the groundwater zone; that is

$$E_g = (E - E_s) \frac{S_{gt}}{S_{st}^{\max} + S_{gt}^{\max}} \quad (7.2.13)$$

Free water is split between primary and secondary compartments, with maximum storage capacities S_{gp}^{\max} and S_{gs}^{\max} respectively, and generating separate baseflows given by

(i) *primary baseflow*:

$$q_b^p = k_{gp} S_{gp}^{\max} (1 - f_{\max}) \quad (7.2.14)$$

(ii) *secondary baseflow*:

$$q_b^s = k_{gs} S_{gs}^{\max} (1 - f_{\max}). \quad (7.2.15)$$

Total baseflow is then given simply as

$$q_b = q_b^p + q_b^s. \quad (7.2.16)$$

Effective baseflow is calculated after taking into account losses, q_l , so

$$q_b^e = q_b - q_l. \quad (7.2.17)$$

The total flow at the basin outlet is given by the sum of the effective baseflow and the routed lateral flows from the unsaturated and saturated zone storages.

7.3 Model Parameters

A summary of the model parameters used in the NWS Model is presented in Table 7.3.1 together with the units used in the model.

Table 7.3.1 Parameters of the NWS Model

| Parameter | Unit | Description |
|-----------------|-------------------|---|
| r_f | none | Rainfall factor |
| f_i | none | Fraction of the catchment that is impervious |
| f_w^{\max} | none | Maximum additional fraction of impervious area which develops as tension water requirements are met |
| c | none | Fraction of the catchment covered by streams, lakes and riparian vegetation |
| S_u^{\max} | mm | Capacity of unsaturated zone tension water store |
| S_s^{\max} | mm | Capacity of unsaturated zone free water store |
| k_i | day^{-1} | Rate of interflow from saturated zone |
| γ | none | Proportional increase in percolation from saturated to dry conditions |
| δ | none | Exponent in equation for percolation rate |
| S_{gt}^{\max} | mm | Capacity of groundwater zone tension water store |
| S_{gs}^{\max} | mm | Capacity of groundwater zone secondary free water storage |
| k_{gs} | day^{-1} | Lateral drainage rate from secondary groundwater zone |
| S_{gp}^{\max} | mm | Capacity of groundwater zone primary free water storage |
| k_{gp} | day^{-1} | Lateral drainage rate from primary groundwater zone |
| p | none | Fraction of percolated water going directly to groundwater zone free water store in preference to tension water store |
| r_s | none | Fraction of groundwater zone free water not available for resupplying lower zone tension water store |

8. THE NAM MODEL

8.1 Introduction

The NAM Model is a classical lumped conceptual model of the rainfall-runoff process. NAM as an acronym stands for Nedbør-Afstrømnings-Model, Danish for precipitation-runoff-model, and was developed at the Technical University of Denmark. A schematic of the main features of the model is shown in Figure 8.1.1. This highlights that the model is made up of three main storage elements:

- (i) *upper zone storage* representing vegetation, depressions and near surface (cultivated) soil;
- (ii) *lower zone storage* representing the root zone and the main soil horizons; and
- (iii) *groundwater storage* representing water bearing rocks.

Overland flow together with interflow generated from the upper zone storage and baseflow generated from the groundwater storage experience additional routing and are summed to give the total model flow at the basin outlet.

8.2 Model Formulation

The following provides a summary of the mathematical functions employed in the different elements of the model. The precision of the summary reflects access to the Reference Manual but not the source code and the need for some interpretation as a result. Notation is clarified by avoiding the computer coding acronyms used by the Reference Manual.

1. *Evaporation*

Evaporation, E_a , occurs at the potential rate, E , given sufficient water in the upper storage, and then at a reduced rate proportional to the degree of saturation of the lower storage. Specifically,

$$E_a = \begin{cases} E & S_u \geq E \\ S_u + \frac{S_\ell}{S_\ell^{\max}}(E - S_u) & \text{otherwise} \end{cases} \quad (8.2.1)$$

where S_u and S_ℓ are the water storage depths in the upper and lower zone and S_ℓ^{\max} is the maximum capacity of the lower zone.

2. *Net rainfall and infiltration*

Net rainfall, P_n is not clearly defined by the NAM documentation (DHI, 1992) but appears to be given by

$$P_n = \max(0, P - E_a - q_i - (S_u^{\max} - S_u)) \quad (8.2.2)$$

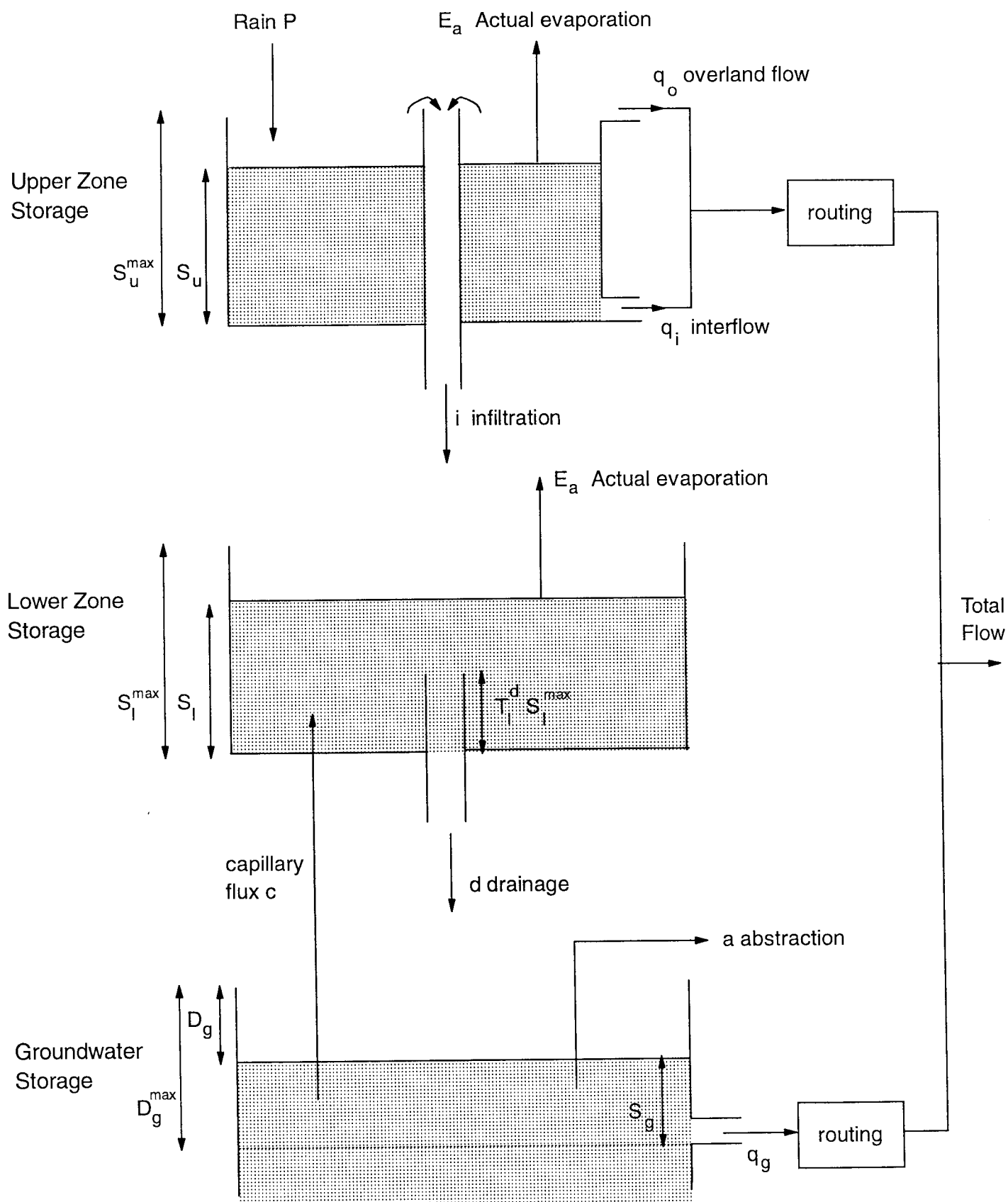


Figure 8.1.1 The NAM rainfall-runoff model.

where rainfall P is reduced by evaporation, E_a , interflow, q_i , and addition to storage $(S_u^{\max} - S_u)$. This leaves infiltration to the lower zone storage defined as

$$i = P_n - q_o \quad (8.2.3)$$

where q_o is overland flow

3. Overland flow

Overland flow only occurs when the saturated fraction of the lower storage, S_ℓ/S_ℓ^{\max} , exceeds a threshold proportion, T_ℓ^o . The magnitude is proportional to the degree of excess and the net rainfall, such that

$$q_o = \begin{cases} f P_n \left[\frac{(S_\ell/S_\ell^{\max} - T_\ell^o)}{1 - T_\ell^o} \right] & S_\ell/S_\ell^{\max} > T_\ell^o \\ 0 & \text{otherwise} \end{cases} \quad (8.2.4)$$

where f is the overland flow runoff coefficient, a dimensionless parameter in the range (0,1).

4. Interflow

Again, interflow only occurs when a critical saturation fraction of the lower storage is exceeded, the threshold in this case being denoted T_ℓ^i . The magnitude is directly proportional to the degree of excess such that

$$q_i = \begin{cases} k_i \left[\frac{(S_\ell/S_\ell^{\max} - T_\ell^i)}{1 - T_\ell^i} \right] & S_\ell/S_\ell^{\max} > T_\ell^i \\ 0 & \text{otherwise} \end{cases} \quad (8.2.5)$$

where k_i is the interflow storage coefficient.

The above must be subject to the constraint that there is sufficient water available to the upper store to sustain this interflow (the documentation does not make this clear). An alternative conjecture is that interflow is actually generated from water in the lower storage and that the model schematic is wrong.

5. Groundwater recharge

Drainage of water from the lower storage into the groundwater storage is referred to as groundwater recharge, d . It is directly related to the infiltration entering the lower storage, i , and its degree of saturation in excess of a critical threshold for drainage to occur, T_1^d , such that

$$d = \begin{cases} i \left\{ \frac{(S_\ell / S_\ell^{\max} - T_\ell^d)}{1 - T_\ell^d} \right\} & S_\ell / S_\ell^{\max} > T_\ell^d \\ 0 & \text{otherwise.} \end{cases} \quad (8.2.6)$$

Continuity gives the update equation (omitting time update notation for simplicity) for lower zone storage as

$$S_\ell = S_\ell + i - d. \quad (8.2.7)$$

6. Groundwater storage and baseflow

The groundwater storage releases water as baseflow in one of two ways. The simple scheme uses a linear reservoir conceptualisation such that baseflow

$$q_g = \begin{cases} k_g S_g & S_g \geq 0 \\ 0 & \text{otherwise} \end{cases} \quad (8.2.8)$$

where S_g is the water in groundwater storage above a zero reference (negative values are possible) and k_g is a time constant parameter. The second scheme aims to conceptualise a shallow reservoir typical of lowland catchments with little topographic variation and the potential for waterlogging. In this case baseflow is proportional to the water table depth above the maximum drawdown of the groundwater reservoir and is given by

$$q_g = \begin{cases} k_g Y_s (D_g^{\max} - D_g) & D_g \leq D_g^{\max} \\ 0 & \text{otherwise} \end{cases} \quad (8.2.9)$$

where D_g is the depth of the water table below a zero datum, attaining a maximum value of D_g^{\max} , k_g is a time constant parameter and Y_s is the specific yield of the groundwater reservoir.

7. Upward capillary flux

Water can transfer upwards from the groundwater reservoir to the lower zone storage by capillary action. The capillary flux, c , is proportional to the square root of the deficit in the lower zone storage and inversely proportional to the drawdown in the groundwater reservoir, such

$$c = \left(1 - \frac{S_\ell}{S_\ell^{\max}}\right)^{1/2} \left(\frac{D_g}{D_g^1}\right)^{-\alpha} \quad (8.2.10)$$

If c has units of mm day^{-1} then the parameter α is given by the empirical relation

$$\alpha = 1.5 + 0.45 D_g^1 \quad (8.2.11)$$

where D_g^1 is the depth of the groundwater table at which the capillary flux is 1 mm day^{-1} when $S_\ell=0$.

The depth to the water table is updated from continuity as

$$D_g = D_g - d + c + a + q_g \quad (8.2.12)$$

where a is an allowance for pumped abstractions.

8. *Routing of lateral flows*

Overland flow and interflow are summed and routed to represent translation through the catchment using two linear reservoirs in series with time constants k_1 and k_2 . To accommodate a linear response for near surface flows and a kinematic response for above surface flows (classic overland flow) at higher flow rates, the time constants are modified to follow the form

$$k = \begin{cases} k_p & q_o \leq q_o^{\min} \\ k_p \left[\frac{q_o}{q_o^{\min}} \right]^{-\beta} & \text{otherwise} \end{cases} \quad (8.2.13)$$

where q_o^{\min} is a threshold above which kinematic overland flow occurs and β is a parameter, set to 0.4 mm hr^{-1} and 0.33 respectively. Here, k_p denote the original linear parameterisation (k_1 or k_2).

As a final step all the lateral components of streamflow – overland flow, interflow and baseflow – are routed together through a final linear reservoir to obtain the total flow response at the basin outlet. This step is not made clear in the model schematic in the NAM Reference Manual. The NAM model also allows for feedback effects within the catchment where irrigation water from groundwater and/or river water can form an input to the model in addition to rainfall. This features within the irrigation module available for modelling catchments with major irrigation schemes: this is not reviewed further here.

8.3 Model Parameters

A summary of the model parameters used in the NAM Model is presented in Table 8.3.1 together with the units used in the model.

Table 8.3.1 Parameters of the NAM Model

| Parameter | Unit | Description |
|-----------------|--------------------|---|
| S_u^{\max} | mm | Maximum capacity of upper zone storage |
| S_ℓ^{\max} | mm | Maximum capacity of lower zone storage |
| D_g^{\max} | mm | Maximum capacity of groundwater storage |
| T_ℓ^o | none | Critical saturation fraction of lower storage above which overland flow occurs |
| f | none | Overland flow runoff coefficient |
| T_ℓ^i | none | Critical saturation fraction of lower storage above which interflow occurs |
| k_i | mm h ⁻¹ | Interflow storage coefficient |
| T_ℓ^d | none | Critical saturation fraction of lower storage above which drainage occurs |
| k_g | h ⁻¹ | Baseflow time constant |
| Y_s | none | Specific yield of groundwater reservoir |
| D_g^{\max} | mm | Maximum depth of water table below zero datum |
| D_g^l | mm | Depth of water table at which capillary flux is 1 mm day ⁻¹ when the lower zone storage is empty |
| k_1, k_2 | h ⁻¹ | Time constants of two linear reservoirs in series used to route the sum of overland flow and interflow |
| q_0^{\min} | mm h ⁻¹ | Threshold above which kinematic overland flow occurs |
| β | none | Exponent in kinematic overland flow threshold function |

9. A SIMPLE DISTRIBUTED MODEL: THE GRID MODEL

9.1 Introduction

In order to fully exploit the distributed nature of radar data the Grid Model (Moore *et al.*, 1992; Bell and Moore, 1998) is configured so as to share the same grid as that used by the weather radar. Each radar grid square is conceptualised in the catchment as a storage mechanism which receives water in the form of precipitation and loses water via overflow, evaporation and drainage. The storage mechanism used in the basic form of model is a simple store (tank or bucket) having a finite capacity S_{\max} . This capacity can be thought of as an absorption capacity of the grid encompassing surface detention, soil moisture storage, and the interception capacity of vegetation and other forms of land use. A fundamental idea used in the basic form of model is that absorption capacity is controlled by the average gradient, \bar{g} , of the topography in the grid square which can be calculated readily from a digital terrain model.

9.2 Water Balance in a Grid Square

Specifically, for a given grid square, the following linkage function is used to relate the maximum storage capacity, S_{\max} , and the average gradient, \bar{g} , within a grid square:

$$S_{\max} = \left(I - \frac{\bar{g}}{g_{\max}} \right) c_{\max} , \quad (9.2.1)$$

for $\bar{g} \leq g_{\max}$. The parameters g_{\max} and c_{\max} are upper limits of gradient and storage capacity respectively and act as “regional parameters” for the basin model. A measurement of the mean gradient within each grid square of the river basin can be obtained from the DTM (or a contour map if not available). Values of S_{\max} for all grid squares are determined using only the two model parameters, g_{\max} and c_{\max} , together with measurements of \bar{g} for each square.

A grid storage loses water in three possible ways. If the storage is fully saturated from previous rainfall then any net addition of water spills over and contributes to the fast catchment response. Drainage from the base of the store is controlled by the volume of water in store and contributes to the slow catchment response. Thirdly, water is lost via evaporation to the atmosphere. Figure 9.2.1 illustrates a typical grid storage and the components of the water balance involved.

Specifically, a water balance is maintained as follows for each grid square and time interval of duration Δt . (Time and space subscripts are omitted for notational simplicity.) Evaporation loss occurs at the rate, E_a , which is related to the potential evaporation rate, E , and the water in store, S , through the relation

$$E_a = \begin{cases} \left(1 - \frac{D - D^*}{S_{\max} - D^*} \right) E, & D \leq D^* \\ E, & D > D^*. \end{cases} \quad (9.2.2)$$

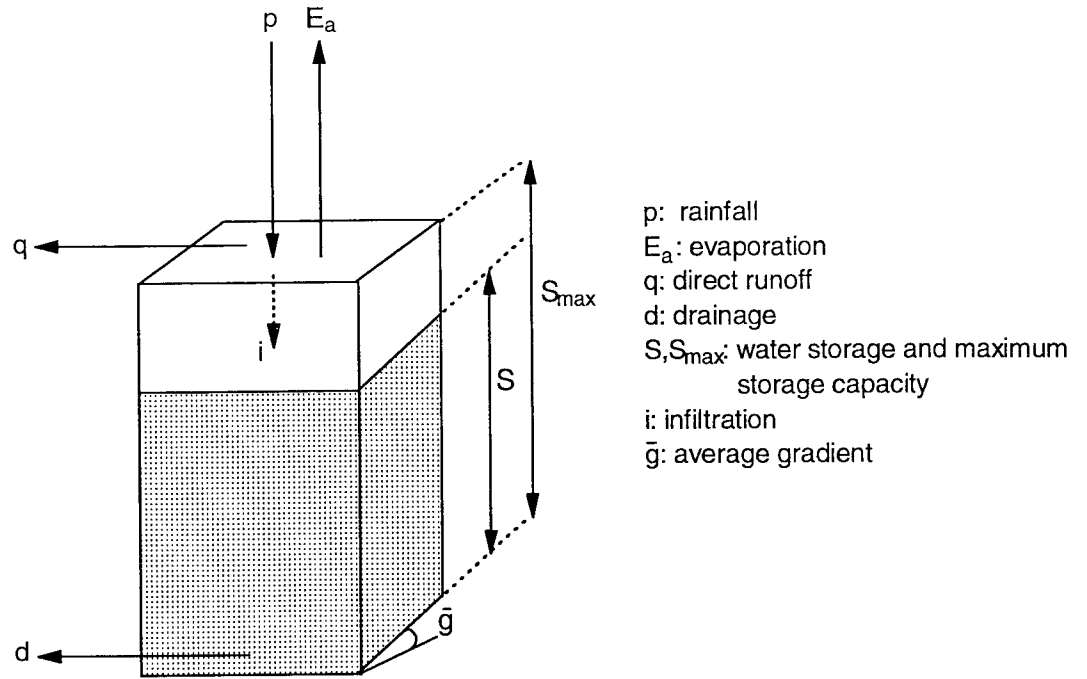


Figure 9.2.1 A typical grid storage illustrating the components of the water balance.

Here, $D = S_{\max} - S$ is the soil moisture deficit and D^* is the threshold deficit below which evaporation occurs at the potential rate. The value of D^* is common across grid squares.

Drainage from the grid storage, which contributes to the slow catchment response, occurs at the rate

$$d = \begin{cases} \alpha S^\beta, & S > 0 \\ 0, & \text{otherwise} \end{cases} \quad (9.2.3)$$

where α is the drainage storage constant and the drainage exponent β is a parameter (set here to 3).

A potential infiltration rate is given by

$$i_p = \left(1 - \frac{S}{S_{\max}} \right)^b i_{\max} \quad (9.2.4)$$

where i_{\max} is the upper limit of infiltration rate and S is the water in storage. Then the actual infiltration rate is given by

$$i = \min(p, i_p) \quad (9.2.5)$$

where p is the rainfall rate. The direct runoff generated by this infiltration excess mechanism is simply $q = p - i$. In practice i is set equal to p for modelling the humid temperate basins encountered in the UK, where saturation excess is the dominant runoff mechanism.

Finally, the updated water storage is given by

$$S = \max(0, S + i\Delta t - E_a \Delta t - d\Delta t) \quad (9.2.6)$$

and the direct runoff rate contributing to the fast basin response is calculated as

$$q = \max(0, S - S_{\max}) + p\Delta t - i\Delta t. \quad (9.2.7)$$

9.3 Isochrone-Based Kinematic Wave Routing Scheme

Water is routed from each grid square storage to the catchment outlet using DTM-derived isochrone pathways. The construction of isochrones – lines joining points of equal time of travel to the basin outlet – is achieved by assuming that water travels with only two velocities depending on whether the pathway involves a hillslope or a river channel. In this way it is relatively easy to construct isochrones by direct inference from the distance of a point to the basin outlet and the nature of the pathways involved. The catchment is subdivided into reaches according to these isochrones and water is routed along the reaches to the catchment outlet using a discrete kinematic wave routing procedure. This not only advects water between the reaches but also incorporates a diffusive component seen in observed hydrographs.

Figure 9.3.1 shows an idealised catchment with isochrones overlaid onto the grid squares. From the diagram it is clear that if $A_{\tau j}$ is the area of grid square j that lies in the catchment between isochrones $\tau-1$ and τ , then the sum of $A_{\tau j}$ over all m grid squares in the catchment is equal to the area between isochrones $\tau-1$ and τ in the catchment: that is, $A_{\tau} = \sum_{j=1}^m A_{\tau j}$ where $\tau=1,2,\dots,n$. Similarly, the area of the j^{th} grid square that lies in the catchment is given by $A_j = \sum_{\tau=1}^n A_{\tau j}$, $j=1,2,\dots,m$, and the total area of the catchment is $A = \sum_{\tau=1}^n A_{\tau} = \sum_{j=1}^m A_j$. Water storage accounting for any grid only partially inside the catchment is treated in the normal way and an adjustment made when accumulating the runoff/drainage across the catchment. Hence, the water input to isochrone τ at time t is

$$I_{\tau}(t) = \sum_{j=1}^m u_{\tau j} r_{\tau j}, \quad (9.3.1)$$

where $u_{\tau j} = A_{\tau j}/A$, and $r_{\tau j}$ is the grid square outflow rate. The latter can be the direct runoff rate, $q_{\tau j}$, the drainage rate, $d_{\tau j}$, depending on whether the routing scheme relates to the fast or slow response pathway to the catchment outlet.

Formally, convolution of the grid square outflow rate per unit area over a grid square, $r_{\tau j}$, from grid squares $j=1,2,\dots,m$, to obtain the basin runoff rate per unit area over the basin, Q_t , at time t may be achieved using

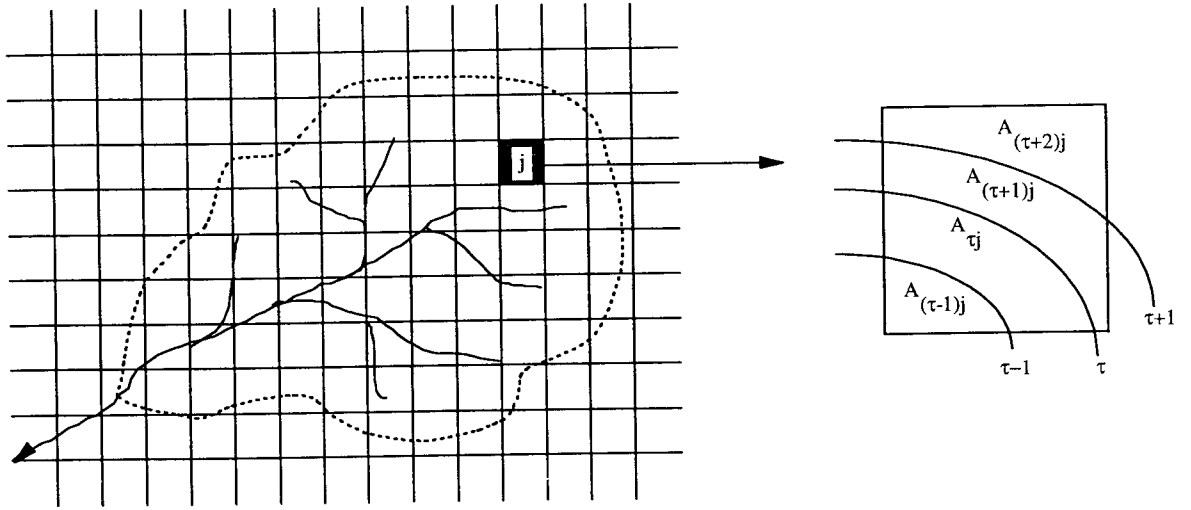


Figure 9.3.1 Catchment with superimposed weather radar grid and inset showing isochrone areas in grid square j.

$$Q_t = \sum_{j=1}^m \sum_{\tau=1}^n u_{\tau j} r_{(t-\tau)j} = \sum_{\tau=1}^n I_{\tau}(t-\tau). \quad (9.3.2)$$

This routing formulation can be interpreted as a distributed form of unit hydrograph. For uniform direct runoff (effective rainfall in a UH context) over the basin the underlying classical unit hydrograph is obtained as $v_{\tau} = A_{\tau}/A$, $\tau=1,2,\dots,n$, with catchment runoff given by the convolution $\sum_{\tau=1}^n v_{\tau} \tau_{(t-\tau)}$. The relation between $u_{\tau j}$ and v_{τ} is $u_{\tau j} = w_{\tau j} v_{\tau}$ where $w_{\tau j} = A_{\tau j}/A_{\tau}$.

Early versions of the model were based on the distributed unit-hydrograph formulation of equation (9.3.2). Initial trials revealed two weaknesses: the first was the computer time involved in computing the discrete form of convolution integral, particularly as part of a parameter optimisation process. A second weakness was the pure form of advection routing implied by the use of the isochrone method and the need to introduce a diffusive element to obtain the more attenuated catchment response seen in practice. A simple way of introducing diffusion into the isochrone formulation is to assume that each isochrone strip, instead of operating as a simple advection time delay, can be represented by a discrete kinematic wave. Specifically, the idea is to replace the n isochrone strips by a cascade of n reaches, with the outflow from the k 'th reach at time t represented by

$$q_t^k = (1-\theta)q_{t-1}^k + (q_{t-1}^{k+1} + r_t^k). \quad (9.3.3)$$

Here, r_t^k is the outflow rate from the k 'th isochrone strip calculated for the interval $(t-1, t)$ and serves as the lateral inflow to the k 'th reach. Parameter θ is a dimensionless wave speed taking values in the range 0 to 1. The flow rate q_t^1 corresponds to the total outflow from the

catchment. Moore and Jones (1978) show how this formulation may be derived from either a discrete form of the kinematic wave equation or a linear storage form of routing. The parameter θ is related to the kinematic wave speed, c , through $\theta = c\Delta t/\Delta x$ where Δt and Δx are the time and space intervals of the discretisation. For a reach of length L sub-divided into N reaches of equal length, $\Delta x = L/N$, then a condition for stability is $\theta < 1$ or $c < L/(N\Delta t)$.

The lateral inflow r_t^k can be defined as direct runoff or drainage which are routed separately using two parallel discrete kinematic wave models, characterised by different wave speeds θ_s and θ_b respectively. This routing formulation has been adopted for use in the basic Grid Model, referred to as the Simple Grid Model or SGM. A schematic depicting the overall structure of the Simple Grid Model is shown in Figure 9.3.2. Table 9.3.1 provides a summary of the SGM model parameters along with their units.

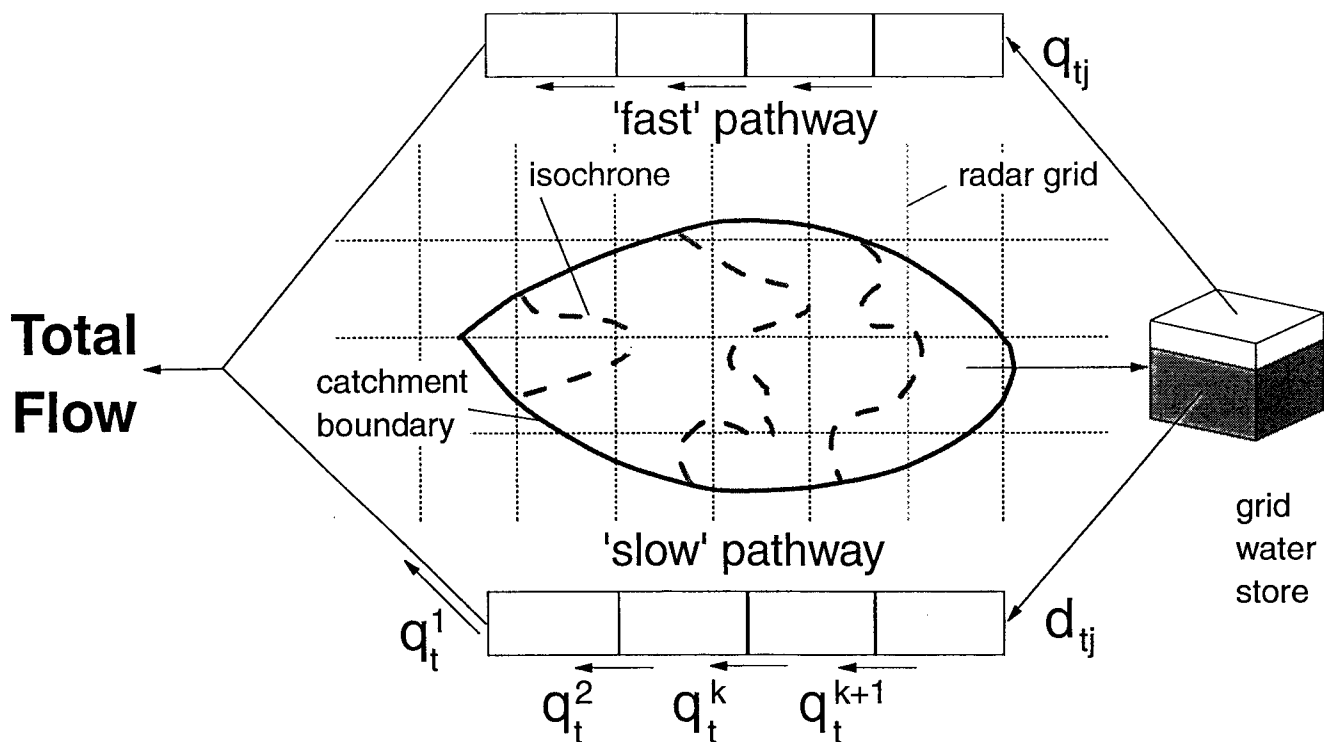


Figure 9.3.2 The Simple Grid Model.

9.4 Some Variants of the Simple Grid Model

The simplicity of the basic Grid Model structure permits the incorporation, and investigation of, a number of model variants. Two main variants will be considered here, the first affecting translation of water to the basin outlet and the second runoff production within each grid square. The translation variant considers drainage from each grid square travels to the basin outlet in a way governed by a separate set of isochrones determined by the path length and a Darcy velocity of flow. In the runoff production variant, spatial variability in runoff response

Table 9.3.1 Parameters of the Grid Model

| Parameter | Description | Unit |
|------------|--|----------------------------------|
| f_r | Rainfall correction factor | - |
| D^* | Storage threshold deficit (or root constant) in evaporation function | mm |
| S_0 | Proportion of total storage capacity initially full | - |
| g_{\max} | Regional upper limit of gradient | - |
| c_{\max} | Regional upper limit of storage capacity | mm |
| i_{\max} | Maximum infiltration rate | mm h ⁻¹ |
| k_d | Storage constant of (cubic) drainage function | h ⁻¹ mm ⁻² |
| θ_s | Wave speed parameter for routing direct runoff | - |
| θ_b | Wave speed parameter for routing drainage | - |
| v_L | Advection velocity of flow along land path | m s ⁻¹ |
| v_R | Advection velocity of flow along river path | m s ⁻¹ |

within each grid square is introduced. The simple linkage between storage capacity and mean gradient within a grid square is extended to a probability-distributed representation of gradient within a square which, through the linkage function, is used to derive a distribution of storage capacity for a square. This distribution of storage capacity is used to obtain the integrated runoff response from each grid square. Also, If classifications of urban area are available, such as obtained from an analysis of Landsat images, then these may be introduced into the SGM and its variants to delineate the fraction of each grid square that can be considered to have zero storage capacity. Other variants of the SGM, including a topographic index control of soil saturation and the use of integrated air capacity data obtained from soil surveys, are discussed in Moore *et al.* (1992).

9.4.1 Separate slow response pathway isochrones variant

A possible criticism of the Simple Grid Model formulation is that both the fast and slow (“baseflow”) response routing pathways are represented by isochrones whose derivation is based upon land and river velocities. To overcome this a model variant is introduced in which the slow response routing component is based upon a second set of isochrones derived using the Darcy velocity

$$v = Kdh/d\ell, \quad (9.4.1)$$

where v is the velocity of flow through a porous medium, K is the hydraulic conductivity (permeability), h is the piezometric head and ℓ is the thickness of the medium.

The Darcy velocity is estimated from the DTM by approximating the hydraulic gradient, $dh/d\ell$, by the local gradient of the terrain, g , so that

$$v = kg, \quad (9.4.2)$$

where k is a parameter which allows optimisation of the slow response isochrones. Time-of-travel of every point in the catchment to the outlet is then calculated from

$$t_i = \frac{1}{k} \sum_i \frac{d_i}{g_i} \quad (9.4.3)$$

where d_i is the distance between the i th and the $(i-1)$ th points on the flow path, g_i is the gradient between the points and k is the parameter found by calibration.

9.4.2 The Probability-distributed Grid Model variant

In the Probability-distributed Grid Model, or PGM, the simple empirical relation between gradient, g , and storage capacity, c , at a point

$$c = (1 - g/g_{\max})c_{\max}, \quad (9.4.4)$$

where g_{\max} and c_{\max} are the maximum gradient and storage capacity for the catchment, is used to develop a probability-distributed storage capacity formulation as an extension to the approach presented by Moore (1985). (Further details of this approach are given in Section 5 in the context of the Probability-Distributed Moisture model or PDM.) For a given distribution of gradient within a grid square, equation (9.4.1) can be used to derive the distribution of storage capacity over the square in terms of the parameters defining the distribution of gradient.

The choice of distribution can be guided by constructing frequency curves of gradient from DTM data, both for within-grid square areas and for the whole catchment. Particular distributions, such as truncated exponential or power, can be fitted to the gradient frequency curve data. Parameters defining these distributions may then be used in the derived distribution for storage capacity. The probability-distributed model theory presented by Moore (1985) can then be used to obtain the proportion of each grid square which is saturated and in turn the volume of runoff generated.

Central to this modelling approach, here applied to a grid square, is the unique relationship that exists between the total water in storage, $S(t)$, the critical capacity, $C^*(t)$, below which all stores are full, and the volume of total runoff, $V(t)$. Specifically, the total water in storage over the grid square is

$$S(t) = \int_0^{C^*(t)} (1 - F(c)) dc, \quad (9.4.5)$$

where the function $F(\cdot)$ is the distribution function of storage capacity. For a given value of total water in storage, $S(t)$, this can be used to obtain $C^*(t)$ which allows the volume of direct runoff from the square, $V(t+\Delta t)$, to be calculated from

$$V(t + \Delta t) = \int_{C^*(t)}^{C^*(t+\Delta t)} F(c) dc. \quad (9.4.6)$$

An overall distribution function for the catchment storage capacity is derived and applied to each grid square by calculating the appropriate distribution parameter for each square from information derived from the DTM. The derivation of the distribution function for a power function of gradient now follows.

Power function distribution of gradient

Consider gradients in the range $0 \leq g \leq g_{\max}$ which follow a power distribution of the form

$$F(g) = \text{Prob}(\text{slope} \leq g) = \left(\frac{g}{g_{\max}} \right)^b \quad 0 \leq g \leq g_{\max} \quad (9.4.7)$$

with the exponent b related to the mean gradient \bar{g} by

$$b = \frac{\bar{g}}{g_{\max} - \bar{g}}. \quad (9.4.8)$$

The distribution function of storage capacity may be derived, and can be shown to take the Pareto distribution form

$$F(c) = 1 - \left(1 - \frac{c}{c_{\max}} \right)^b \quad c \leq c_{\max}, \quad (9.4.9)$$

with the exponent b given by (9.4.8). Using (9.4.5) it then follows that the total water in storage, $S(t)$, and the critical capacity, $C^*(t)$, are related by

$$S(t) = \frac{c_{\max}}{b+1} \left[1 + \left(1 - \frac{C^*(t)}{c_{\max}} \right)^{b+1} \right] \quad (9.4.10)$$

and the maximum possible total water storage for the grid square is given by

$$S_{\max} = \frac{c_{\max}}{b+1}. \quad (9.4.11)$$

This is also the mean store capacity, \bar{c} .

This storage distribution is incorporated into the Grid Model as a variant in place of the simple single storage form of the basic model.

10. TRANSFER FUNCTION MODELS

10.1 Introduction

Transfer Function or TF models are a class of time-series models popularised by Box and Jenkins (1970). They are linear models with which an output variable can be forecast as a linear weighted combination of past outputs and inputs. In a rainfall-runoff context the output is usually flow and the input rainfall. Any residual model error can be represented through a noise model which is normally of autoregressive moving average (ARMA) form. The overall model is termed a Transfer Function Noise, or TFN, model.

An overview of the TF approach to forecasting is given next. This is followed by a review of a special variant, called the Physically Realisable Transfer Function or PRTF model, developed by Han (1991) specifically for use as a rainfall-runoff model. Other variants of the TF model and their application in the UK are outlined in the concluding section.

10.2 The Transfer Function (TF) Model

A linear transfer function model relates an output at time t , y_t , to r previous values of the output and s previous values of an input with delay b , u_{t-b} , such that

$$y_t = -\delta_1 y_{t-1} - \delta_2 y_{t-2} - \dots - \delta_r y_{t-r} + \omega_0 u_{t-b} + \omega_1 u_{t-b-1} + \dots + \omega_{s-1} u_{t-b-s+1} \quad (10.2.1)$$

where $\{\delta_i\}$ are r autoregressive parameters and $\{\omega_i\}$ are s moving average parameters operating on the past outputs and inputs respectively. With y_t as basin runoff (or baseflow separated runoff) and u_t as rainfall (or effective rainfall) this TF model can be used as a simple rainfall-runoff model. The notation TF(r,s,b) is used to indicate the order of the model in terms of the number of parameters and the time delay.

Equation (10.2.1) may be written in a more compact form through the introduction of the backward shift operator, B , defined by $B^r y_t = y_{t-r}$, and the polynomials in B

$$\begin{aligned} \delta(B) &= 1 + \delta_1 B + \delta_2 B^2 + \dots + \delta_r B^r \\ \omega(B) &= \omega_0 + \omega_1 B + \omega_2 B^2 + \dots + \omega_{s-1} B^{s-1}. \end{aligned} \quad (10.2.2)$$

It then follows that equation (10.2.1) can be written as

$$\delta(B) y_t = \omega(B) u_{t-b} \quad (10.2.3)$$

and rearranging gives

$$y_t = \frac{\omega(B)}{\delta(B)} u_{t-b}. \quad (10.2.4)$$

This is the transfer function model written in operator form and with $\omega(B)/\delta(B)$ defining the form of the transfer function. An equivalent form is given by

$$v(B) = \frac{\omega(B)}{\delta(B)} \quad (10.2.5)$$

with

$$v(B) = v_0 + v_1 B + v_2 B^2 + \dots \quad (10.2.6)$$

a polynomial in B of infinite order, so that

$$\begin{aligned} y_t &= v(B)u_{t-b} \\ &= v_0 u_{t-b} + v_1 u_{t-b-1} + v_2 u_{t-b-2} + \dots \end{aligned} \quad (10.2.7)$$

The polynomial $v(B)$ defines the impulse response function (equivalent to the unit hydrograph for effective rainfall as input and baseflow separated runoff as the output). In general the number of parameters $s+r$ in the transfer function representation is far fewer than in the impulse function representation: this is strictly infinite although in practice can be treated to correspond to a significant memory length. The transfer function model thus offers a parsimonious parameterisation of a linear system response.

The model output, y_t , can be related to the observed output, Y_t , through the relation

$$Y_t = y_t + \eta_t = \frac{\omega(B)}{\delta(B)} u_{t-b} + \eta_t \quad (10.2.8)$$

where $\eta_t = Y_t - y_t$ is the simulation model error. This model error may be represented by an ARMA error predictor (see Section 12) to obtain real-time updated forecasts. In this form, the overall model is referred to as a Transfer Function Noise (TFN) model as popularised by Box and Jenkins (1970). An alternative formulation, referred to as Autoregressive Moving Average on exogenous inputs or ARMAX, is given by

$$\delta(B)Y_t = \omega(B)u_t + \xi_t \quad (10.2.9)$$

where ξ_t also represents model error and can be represented by an ARMA noise model structure. This is a special case of the TFN model formulation with $\xi_t = \delta(B) \eta_t$.

10.3 Physically Realisable Transfer Function (PRTF) Model

The basic idea in formulating the Physically Realisable Transfer Function, or PRTF, model (Han, 1991) is to choose a parameterisation which constrains the impulse response function, $v(B)$, to have a physically realistic form in a hydrological context. Principally, this means that it should be positive and not exhibit oscillatory behaviour (it is stable). Han (1991) considers the impulse response function

$$v(B) = \frac{\omega(B)}{\delta(B)} = \frac{\sum_{i=0}^{s-1} \omega_i B^i}{\delta(B)} \quad (10.3.1)$$

and restricts attention to the special case where the polynomial $\delta(B)$ of order r has equal roots β so that

$$\delta(B) = (1 - \beta^{-1} B)^r = (-\beta)^{-r} (B - \beta)^r = 1 + \delta_1 B + \delta_2 B^2 + \dots + \delta_r B^r. \quad (10.3.2)$$

This gives a stable impulse response function for $\beta > 1$.

First note the expansion

$$(B - \beta)^r = B^r + rB^{r-1}(-\beta) + \frac{r(r-1)}{2!} B^{r-2}(-\beta)^2 + \dots + \frac{r(r-1)\dots(r-(k-1))}{k!} B^{r-k}(-\beta)^k + \dots + (-\beta)^r$$

and the definition of a combinatorial as

$$C_k^r = \frac{r!}{(r-k)!k!} = \frac{r(r-1)\dots(r-k+1)}{k!}.$$

Then equating terms in $(r-k)$ in (10.3.2) gives

$$(-\beta)^{-r} C_k^r B^{r-k} (-\beta)^k = \delta_{r-k} B^{r-k}$$

so

$$\delta_{r-k} = (-\beta)^{k-r} C_k^r.$$

and, in general, it follows that

$$\delta_i = (-\beta)^{-i} C_{r-i}^r. \quad (10.3.3)$$

An important feature of the equal root parameterisation is that it allows the r autoregressive parameters of the TF model to be reduced to one, the root β , through the use of the above relation. However, the form of TF model is restricted as a result.

It is of interest to note special cases of the above. For dependence on one past output ($r=1$) we have $\delta_1 = -1/\beta$ and for two past outputs ($r=2$) $\delta_1 = -2/\beta$ and $\delta_2 = 1/\beta^2$. From a consideration of (10.3.1) and (10.3.2) it follows that the impulse response function for a single, unlagged input ($s=1, b=0$), so that $v(B) = 1/\delta(B)$

$$v(t) = C_t^{r-1+t} \beta^{-t} \quad (10.3.4)$$

which gives $v(t) = \beta^{-t}$ for $r=1$ and $v(t) = (1+t) \beta^{-t}$ for $r=2$.

Han (1991) suggests that choosing r to be 2 or 3 provides sufficient flexibility of the impulse response function, provided the moving average parameters $\{\omega_i\}$ can take on negative values so as to lower the recession limb. To make the model more physically intuitive the equal root parameterisation β is substituted by the time to peak, t_{peak} , of the impulse response function of $v(B) = 1/\delta(B)$ as given by equation (10.3.4). This is obtained from the solution of $dv(t)/dt = 0$ for t . For $r=2$ when $v(t) = (1+t)\beta^{-t}$ we have the solution

$$t_{peak} = \frac{1}{\ln \beta} - 1 \quad (10.3.5)$$

giving the reparameterisation

$$\beta = \exp \left\{ \frac{1}{(1+t_{peak})} \right\}. \quad (10.3.6)$$

For $r=3$ when $v(t) = (2+t)(1+t)\beta^{-t}/2$ we have the solution

$$t_{peak} = \frac{1}{2} \left\{ \frac{2}{\ln \beta} - 3 + \sqrt{\left(3 - \frac{2}{\ln \beta}\right)^2 - 4\left(2 - \frac{3}{\ln \beta}\right)} \right\} \quad (10.3.7)$$

giving the reparameterisation

$$\beta = \exp \left\{ \frac{2t_{peak} + 3}{(t_{peak}^2 + 3t_{peak} + 2)} \right\}. \quad (10.3.8)$$

Higher order solutions may be sought by solving the general relation

$$\ln \beta = \sum_{k=1}^{r-1} (r - k + t)^{-1} \quad (10.3.9)$$

for t and chosen values of r .

Han (1991) recognises that the TF model, with its fixed impulse response function, will not provide an adequate representation of the rainfall-runoff process which is both nonlinear and time variant. He chooses to address this problem by adjusting the form of the impulse response function to reflect each flood situation as it is encountered in real-time. To ease this task Han introduces three types of adjustment factor designed to alter the volume, shape and time response of the TF model. For volume adjustment the moving average parameters, $\{\omega_i\}$,

are scaled using a factor α , the proportion of volume change, such that the adjusted parameters are given by

$$\omega_i^* = (1 + \alpha)\omega_i \quad i = 0, 1, \dots, s-1. \quad (10.3.10)$$

Note that the autoregressive parameters, $\{\delta_i\}$, are not affected by this adjustment.

The shape of the impulse response function is changed with reference to a shift in the position of the peak of the $1/\delta(B)$ part of the impulse response function. The shape adjustment factor, γ , is defined as

$$\gamma = t_{peak}^* - t_{peak} \quad (10.3.11)$$

where t_{peak}^* denotes the adjusted peak time. For $r=2$ this may be expressed in terms of the equal root parameterisation, β of the original model and the adjusted model β^* , using equation (10.3.5) to give

$$\gamma = \frac{1}{\ln \beta^*} - \frac{1}{\ln \beta}, \quad (10.3.12)$$

so

$$\beta^* = \exp \left\{ \left(\gamma + \frac{1}{\ln \beta} \right)^{-1} \right\}. \quad (10.3.13)$$

It follows that the adjusted autoregressive parameters are obtained by substituting the above in

$$\delta_i^* = (-\beta^*)^{-i} C_{r-i}^r. \quad (10.3.14)$$

Similarly, for $r=3$ and using equation (10.3.7) it follows that

$$\gamma = \frac{1}{2} \left\{ \frac{2}{\ln \beta^*} - 3 + \sqrt{\left(3 - \frac{2}{\ln \beta^*} \right)^2 - 4 \left(2 - \frac{3}{\ln \beta^*} \right)} \right. \\ \left. - \frac{2}{\ln \beta} - 3 + \sqrt{\left(3 - \frac{2}{\ln \beta} \right)^2 - 4 \left(2 - \frac{3}{\ln \beta} \right)} \right\} \quad (10.3.15)$$

and

$$\beta^* = \exp \left\{ \frac{2\psi + 3}{(\psi^2 + 3\psi + 2)} \right\} \quad (10.3.16)$$

where

$$\psi = \gamma + \frac{1}{2} \left\{ \frac{2}{\ln \beta} - 3 + \sqrt{\left(3 - \frac{2}{\ln \beta} \right)^2 - 4 \left(2 - \frac{3}{\ln \beta} \right)} \right\}. \quad (10.3.17)$$

The adjusted autoregressive parameters are obtained by substituting (10.3.16) into (10.3.14). The third form of adjustment is to time shift the impulse response system. This simply involves a change to the pure time delay parameter, b , used to delay the rainfall inputs to the transfer function model (see equation (10.2.1)).

Wedgwood (1993) recognised the difficulty of implementing such simple adjustments, especially for fast responding catchments and where forecasts from many catchments may be required. He explored knowledge based procedures which employ logical rules, developed from an analysis of synthetic and historical storm data, to automate the adjustment of the PRTF model. The IF-THEN rules were based on the extent, position and direction of rainfall fields together with catchment status. Having established the extent and type of rainfall, rules employing rainfall intensity relationships were used to adjust the PRTF model. Relationships controlling the shape factor were expressed as linear regressions on the logarithm of average rainfall intensity whereas the time delay changed according to discrete thresholds of rainfall intensity. Volume adjustment involved only allowing rainfall to contribute to flow once a threshold value for the catchment antecedent precipitation index had been exceeded. The adjustments obtained provided better forecasts than those from a simple TF model in 14 of the 23 events considered, although with significant errors in the timing of peaks and occasional fluctuations in the forecast hydrographs. A drawback of the approach is the initial acquisition of knowledge concerning the thresholds, linkages and relationships involved.

10.4 Other TF Model Variants

If the input-output pair of a TF model is rainfall-runoff then the nonlinearity known to exist by hydrologists is clearly not represented explicitly. This problem has been addressed by using a nonlinear loss function to transform rainfall to “direct runoff” or “effective rainfall” and using this as the input variable u_t . Functionally, the transfer function serves as a simple linear routing function. Alternatively, a parallel system of two transfer function models can be envisaged together with a partitioning rule which directs rainfall to the two functions which operate as slow and fast translation pathways. A variety of nonlinear loss functions and parallel TF model functions were investigated in the UK for use in flood forecasting (Moore, 1980, 1982). Most recently, an improved estimation scheme for this class of parallel TF model has been developed (for example, see Young, 1992, Jakeman *et al.*, 1990) which overcomes some of the problems encountered in this earlier work. Appendix B provides insights into this class of model based on lecture notes by Moore (1989).

Other workers have sought to circumvent the shortcomings of the linear transfer function by allowing the parameters to be time-variant and tracking the variation using a recursive estimation scheme. For example, Cluckie and Owens (1987) employ a TF model in such a way that a single gain parameter, G_t , controlling the proportion of rainfall that becomes baseflow separated runoff, is recursively estimated. Specifically, they use the reparameterised TF model in state corrected form

$$y_t = (1 - \delta(B))Y_t + G_{t-1}\omega(B)u_{t-b} \quad (10.4.1)$$

for forecasting, with the time-varying model gain parameter calculated as

$$G_t = \mu G_{t-1} + (1 - \mu) \frac{\delta(B)Y_t}{\omega(B)u_{t-b}}. \quad (10.4.2)$$

Here, μ is a smoothing factor in the range (0,1) used to dampen out erratic fluctuations in G_t . This form of TF model with time-varying model gain, but without baseflow separation, is included in the assessment of models using catchment data presented in the Part 2 report. Page (1991) documents its use in the Anglian region of the EA where the output, Y_t , is taken to be baseflow separated runoff and two sets of model parameters are used to cope with different responses under “fast response” and “average” conditions. It is suggested that an initial value for G_t should be in the range (0.2, 3.8) with 0.2 a typical value. The model time-step for Anglian catchments is suggested as 1 to 6 hours, with 4 hours being typical. In Southern region the approach is used without baseflow separation as part of the flow forecasting model for the Leigh Barrier Scheme on the River Medway (Pollard, undated).

Transfer function models also form the basis of the Nith flood forecasting system in Scotland, developed at the University of Lancaster in association with the Solway River Purification Board (Lees *et al.*, 1993). They are used to relate upstream level to downstream level and smoothed effective rainfall (defined by a nonlinear operation involving the product of rainfall and the previous river level) to river level. The model steady state gains were found to be time variant and are tracked using recursive least squares, assuming a random walk process for the parameter variability, in a similar way to the approach adopted by Owens and Cluckie in north-west England. A drawback of this recursive approach is that the variation is merely “tracked” and not “anticipated”. Our understanding of hydrological science, for example, tells us that antecedent wetness can influence the model gain or runoff proportion and that soil moisture accounting model components can be used to anticipate this effect. This leads one to recognise that the role of the transfer function is primarily that of a linear routing operation and can be incorporated as such into a conceptual model as merely one component form.

11. NEW MODELLING APPROACHES

11.1 Introduction

The modelling approaches considered so far have either used storage models, in lumped or distributed form, to conceptualise the rainfall-runoff process or used simple linear transfer function models as general time-series modelling tools. This section considers three newer approaches which can be used for general forecasting purposes: neural network models, fuzzy rule-based models and nearest neighbour forecasting. They are reviewed briefly here with application to rainfall-runoff modelling and flood forecasting specifically in mind. Knowledge-based systems have been considered previously in the context of PRTF models in Section 10.3. It is outside the scope of the present project to include these new approaches in the model assessment using catchment data that forms the focus of the Part 2 report. There is clearly an opportunity for further work in this area.

11.2 Neural Network Models

Neural Networks (NN) can be thought of as a nonlinear form of transfer function model and are really no more than nonlinear regression models when used in a forecasting context. Unfortunately, much mystique surrounds their development and application. This is not helped by a voluminous literature, much marketing hype and an arguably overzealous use of the brain as an analogue. The aim here is to provide a simple but precise introduction to NNs for forecasting purposes, to review some examples of their application for rainfall-runoff modelling and to conclude with a critical commentary on their use for flood forecasting.

To introduce NNs it is helpful to choose one particular form that is commonly used for forecasting applications and from which generalisations are hopefully self-evident. This form is the so-called *feed-forward NN with an hidden layer* illustrated in Figure 11.2.1 for a simple

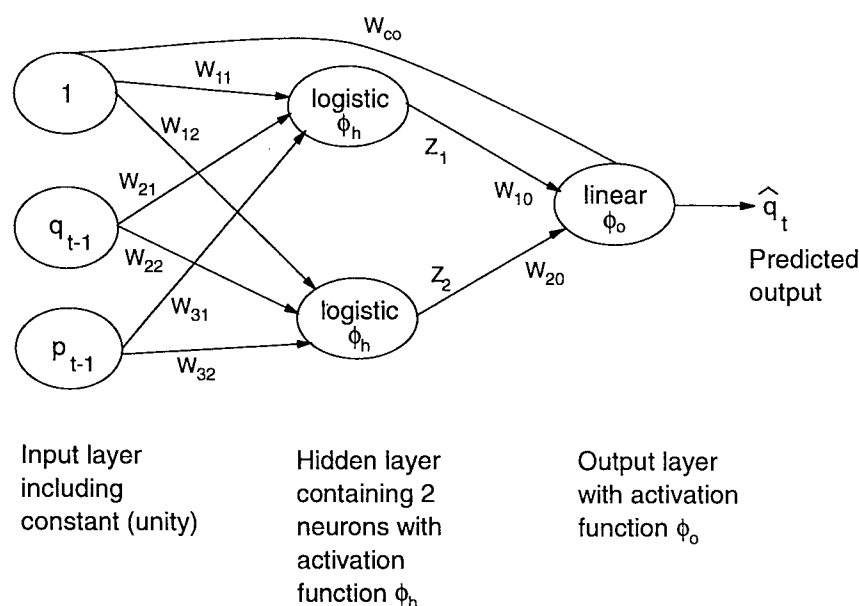


Figure 11.2.1 Feed-forward neural network with an hidden layer.

rainfall-runoff model application. The model involves three inputs - a constant (equal to 1) and lagged values of runoff, q_{t-1} and rainfall p_{t-1} at time $t-1$ - and one output, the model forecast of flow q_t . The inputs are weighted and summed as they pass to a *hidden layer* of *neurons (units)* via *connection* pathways. Specifically, the input to the j th neuron is given by the linear weighted sum

$$v_j = \sum w_{ij} y_i , \quad (11.2.1)$$

where w_{ij} is the weight of the connection between the i th input, y_i , and the j th neuron; here $\{y_1, y_2, y_3\} = \{1, q_{t-1}, p_{t-1}\}$. In the example the hidden layer contains two neurons which contain *activation functions*, ϕ_h . The normal form of activation function employed is the *logistic function*

$$z_j = \phi_h(v_j) = \frac{1}{1 + \exp(-v_j)} , \quad (11.2.2)$$

a function with a sigmoidal shape which contains the value of z_j to the range (0,1). The output from each neuron, together with the constant input, are weighted and summed to form the input to the *output layer*. The activation function of the output layer, ϕ_o , is normally taken to be a simple identity (no change). Thus the forecast runoff from the NN model is

$$\hat{q}_t = w_{co} + \sum w_{j0} z_j , \quad (11.2.3)$$

where w_{co} is the weight of the direct connection linking the constant input and the output and w_{j0} is the weight of the connection linking the j th neuron with the output. Note that the use of a constant unity input serves to introduce a *bias* or *intercept term* on each unit, essentially allowing these to be estimated via their associated weights.

The weights form the NN model parameters which are estimated by minimising the sum of the squares of the one-step ahead forecast errors, $\sum (q_t - \hat{q}_t)^2$. This is normally accomplished using the *back-propagation algorithm* to compute the first derivatives of the objective function which are then used in a *quasi-Newton method* of optimisation. Since NNs typically involve the estimation of many weights, the optimisation problem is far from trivial with problems of local minima, slow convergence, lack of identifiability and overfitting. Scaling of data prior to modelling and the choice of initial values for the weights can often prove important issues. Once an optimal parameter set has been found the NN model may be used for forecasting, using observed past inputs to predict one-step ahead, and substituting subsequent inputs for forecasts in a recursive fashion to obtain forecasts at higher lead times. Alternatively, a NN predictor may be configured with lagged inputs chosen to yield forecasts for a specific lead time, although this approach may lead to a proliferation of models.

The example above has illustrated the use of NNs for flood forecasting for a particular NN architecture. Choice of architecture can clearly be an important concern, and include decisions on the number of neurons to use within a hidden layer and become more complicated when multiple hidden layers are entertained. A good choice of input variables is clearly critical and demands an appreciation of the system being modelled along with NN theory and alternative modelling and time series analysis approaches. The example uses lagged runoff and rainfall as inputs, but clearly values of these for larger lags, along with indices of soil moisture deficit and other factors, present a wide range of alternative options to explore. It is not a methodology which is automatic and for which no experience is needed, as is sometimes

claimed. Also, being a black box approach, a particular NN model is generally difficult to understand and interpret. An important advantage over simple linear transfer function models is the ability of NNs to represent nonlinear behaviour; however, this may not prove to be important for some applications or might be accommodated in other ways.

11.3 Fuzzy Rule-based Modelling

It is beyond the scope of the present review of approaches to rainfall-runoff modelling to address fuzzy rule-based modelling in any detail. The reader is referred to the book by Bardossy and Duckstein (1995) for an accessible account with example applications. An indication of the modelling approach will be provided through an example of its use for rainfall-runoff modelling in a flood forecasting context given by Zhu and Fujita (1994). Interestingly, this paper provides a comparison of the approach with a neural network model.

Consider the problem of forecasting runoff three steps ahead. A model can be constructed in terms of the runoff increments, $q_t = Q_t - Q_{t-1}$, where Q_t denotes the runoff at time t . If R_t denotes rainfall in the interval $(t-1, t)$ then a simple forecasting procedure for some model function, $f(\cdot)$, is

$$\hat{q}_{t+3} = f(\hat{q}_{t+2}, \hat{q}_{t+1}, r_t) \quad (11.3.1)$$

where the circumflex indicates a forecast quantity. The underlying model to this forecast is

$$q_t = f(q_{t-1}, q_{t-2}, r_{t-3}). \quad (11.3.2)$$

The forecast procedure can be formulated as a fuzzy rule-based model by considering R and q to take on membership functions, M_R and M_q , rather than crisp real values. Triangular membership functions are assumed and that for rainfall, R_t , shown in Figure 11.3.1. This indicates that rainfall for time t lies in the range $(R_t - \delta_R, R_t + \delta_R)$ with the central value of R_t being most likely and δ_R indicating the possible degree of deviation from this value. The membership function essentially expresses the vagueness associated with the quantity to which it relates.

The model of equation (11.3.2) can now be recast as a fuzzy model having the proposition:

$$\text{If } R_{t-3} \text{ is } M_{R_{t-3}} \text{ and } q_{t-1} \text{ is } M_{q_{t-1}} \text{ and } q_{t-2} \text{ is } M_{q_{t-2}} \text{ then } q_t \text{ is } M_{q_t}. \quad (11.3.3)$$

A fuzzy model forecast can now be implemented by the following steps:

1. The fuzzy relation, P_t , is obtained from the proposition as:

$$P_t = M_{R_{t-3}} \wedge M_{q_{t-1}} \wedge M_{q_{t-2}} \wedge M_{q_t} \quad (11.3.4)$$

where \wedge is the minimum operator. This is used to define the time series of fuzzy relations $\{P_i, i=1, 2, \dots, t\}$.

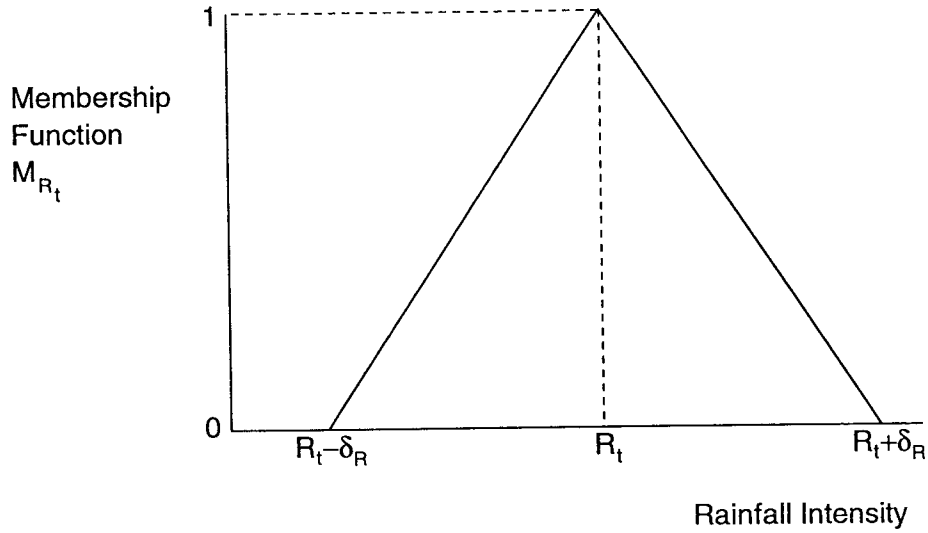


Figure 11.3.1 Triangular membership function for rainfall.

2. The whole fuzzy relation, Π_t , is obtained as

$$\Pi_t = P_1 \vee P_2 \vee \dots \vee P_t \quad (11.3.5)$$

where \vee is the maximum operator. In the case that previous records exist which allow Π_0 to be obtained then this can be used for initialisation to give the modified expression

$$\Pi_t^* = \Pi_0 \vee P_1 \vee P_2 \vee \dots \vee P_t. \quad (11.3.6)$$

3. The membership function of the 1-step forecast based on Π_t^* is

$$M_{\hat{q}_{t+1}} = \Pi_t^* \odot M_{R_{t-2}} \odot M_{R_{t-3}} \odot M_{q_t} \quad (11.3.7)$$

where \odot is the max-min operator. Membership functions for the 2- and 3-step forecasts are obtained in a similar way.

4. Now apply a defuzzy procedure to obtain the real values $\hat{q}_{t+1}, \hat{q}_{t+2}, \hat{q}_{t+3}$ based on the centre of gravity of the predicted membership functions.
5. Finally calculate 1-, 2- and 3-step forecasts of runoff from the runoff increments as follows:

$$\begin{aligned} \hat{Q}_{t+1} &= Q_t + \hat{q}_{t+1} \\ \hat{Q}_{t+2} &= \hat{Q}_{t+1} + \hat{q}_{t+2} \\ \hat{Q}_{t+3} &= \hat{Q}_{t+2} + \hat{q}_{t+3}. \end{aligned} \quad (11.3.8)$$

Whilst the computational detail of each step is omitted it is hoped that this outline sequence conveys an idea of the fuzzy rule-based modelling approach in a rainfall-runoff modelling context.

11.4 Nearest Neighbour Forecasting

The nearest neighbour approach to forecasting is a form of pattern recognition based on a nonparametric regression method for time series. A feature vector which encompasses information relevant to a succeeding flow is defined for each time point in the record. The closest k feature vectors to the current feature vector are identified and the succeeding flows to each of these vectors are averaged to form a forecast of the succeeding flow from the current time.

For example, the feature vector may contain r present at past flows, $\{q_t\}$ and s present at past rainfalls, $\{p_t\}$, such that $x(t) = (q_t, q_{t-1}, \dots, q_{t-r+1}, p_t, p_{t-1}, \dots, p_{t-s})$, defines the vector at time t . The “succeeding flow” to be forecast at time t will be q_{t+1} , for a one-step ahead forecast. A measure of “closeness” is required to identify the k nearest neighbour feature vectors in the historical record. Karlsson and Yakowitz (1967) suggest using a weighted Euclidean norm with weights chosen to adjust for the scale of the measurements (flow and rainfall in this example) and to give greater weight to more recent measurements. There is much scope for experimentation in choice of feature vector, closeness measure, number of nearest neighbours and optimisation method.

A drawback of the approach in its basic form is that a flow forecast can never exceed the maximum flow in the historical record because the forecast is constructed as an average of k flows selected from the record. However, Karlsson and Yakowitz (1987) and Shamseldin and O'Connor (1996) both present ways of overcoming this shortcoming. Karlsson and Yakowitz (1987) using 12 hour data and Galeate (1990) using daily data both find the method gives comparable performance to special forms of transfer function noise model.

A related approach to nearest neighbour forecasting in which floods are treated as quasi-replicates is developed by Cooper (1983). Such nonparametric methods are particularly well suited to situations where long historical records exist and where the hydrological response of the catchment has not changed appreciably over time.

12. MODEL UPDATING METHODS

12.1 Introduction

If observed flows are not used, except for initialisation, a model is said to be operating in *simulation mode*, acting as a function which transforms rainfall and evaporation to river flow. A model which has been calibrated in simulation mode may be extended to use observed flows by addition of further structure and associated parameters. These might take the form of rules for adjusting model states (*state correction*) or predicting future errors (*error prediction*). The former are heavily dependent on the structure of the simulation mode model, whilst the latter are essentially independent. Also model parameters and inputs can be adjusted with reference to observed flows. *Parameter-adjustment* has already been considered in the context of the PRTF model in Section 10.3 and the TF model with time-varying gain in Section 10.4. The view is taken that this approach confuses the issue of correct model identification, which is properly carried out through a controlled calibration procedure. Parameter variability is better addressed by improving the structural form of the model than by tracking its variation in real-time. *Input-adjustment* is not considered here since, in general, errors in the input (notably rainfall) aggregate together in the water content of conceptual storages which are better adjusted using state-correction. The time lags involved in input-adjustment are largely circumvented if a state-correction approach is followed.

A model incorporating observed flows through state-correction, error-prediction or some other scheme will be said to be operating in *updating mode*. An assessment of updating methods for flood forecasting purposes forms a secondary objective of this model intercomparison study.

12.2 State Correction

State correction for the PDM

The term “state” is used to describe a variable of a model which mediates between inputs to the model and the model output (Szollosi-Nagy, 1976). In the case of the PDM rainfall-runoff model the main input is rainfall and basin flow is the model output. Typical state variables are the water contents of the surface and groundwater stores, S_2 and S_3 , and of the probability-distributed soil storage, S_1 (using the notation of Figure 5.1.1). The flow rates out of the conceptual stores can also be regarded as state variables: examples are q_s , the flow out of the surface storage, and q_b , the flow out of the groundwater storage.

When an error, $\epsilon = Q - q = Q - (q_s + q_b)$, occurs between the model prediction, q , and the observed value of basin runoff, Q , it would seem sensible to “attribute the blame” to mis-specification of the state variables and attempt to “correct” the state values to achieve concordance between observed and model predicted flow. Mis-specification may, for example, have arisen through errors in rainfall measurement which, as a result of the model water accounting procedure, are manifested through the values of the store water contents, or equivalently the flow rates out of the stores. A formal approach to state correction is provided by the Kalman filter algorithm (Jazwinski, 1970; Gelb, 1974; Moore and Weiss, 1980a,b). This provides an optimal adjustment scheme for incorporating observations, through a set of linear operations, for linear dynamic systems subject to random variations which may not necessarily be Gaussian

in form. For nonlinear dynamic models, such as the PDM, an extended form of Kalman filter based on a linearisation approximation is required which is no longer optimal in the adjustment it provides. The implication of this is that simpler, intuitive adjustment schemes can be devised which potentially provide better adjustments than the more complex and formal extensions of the Kalman filter which accommodate nonlinear dynamics through approximations. We will call such schemes which make physically sensible adjustments *empirical state adjustment schemes*. A simple example is the apportioning of the error, ε between the surface and groundwater stores of the PDM in proportion to their contribution to the total flow. Mathematically this may be expressed as

$$q_b^* = q_b + \alpha g_b \varepsilon \quad (12.2.1a)$$

$$q_s^* = q_s + (1 - \alpha) g_s \varepsilon \quad (12.2.1b)$$

where

$$\alpha = q_b / (q_s + q_b) \quad (12.2.2)$$

and the superscript * indicates the value after adjustment. The “gain” coefficients, g_b and g_s , when equal to unity yield the result that $q_b^* + q_s^*$ equals the observed flow, Q , thus achieving exact correction of the model flow to equal the observed value. Values of the coefficients other than unity allow for different adjustments to be made, and g_b and g_s can be regarded as model parameters whose values are established through optimisation to achieve the “best” fit between state-adjusted forecasts and observed flows. A generalisation of the above is to define α to be

$$\alpha = \frac{q_b}{\beta_1 q_s + \beta_2 q_b} \quad (12.2.3)$$

and to choose the incidental parameters β_1 and β_2 to weight the apportionment towards or away from one of the flow components; in practice β_1 and β_2 are assigned values of 10 and 0.1 to apportion more of the error adjustment to the surface store. Note that the adjustment is carried out at every time step and the time subscripts have been omitted for notational simplicity. The scheme with α defined by (12.2.2) is referred to as the proportional adjustment scheme and that defined by (12.2.3) is the super-proportional adjustment scheme. Replacing α and $(1 - \alpha)$ in (12.2.1) by unity yields the simplest non-proportional adjustment scheme.

Other state variables within the PDM can also be adjusted. With the surface store characterized by the cascade of two linear reservoirs and represented by a discretely coincident TF model (Section 5.3) the outflows from the two reservoirs can be identified as q_{s1} and q_s . Then q_{s1} can be adjusted according to the rule

$$q_{s1}^* = q_{s1} + (1 - \alpha) g_{s1} \varepsilon. \quad (12.2.1c)$$

An adjustment may also be made to the direct runoff, $u_s \equiv V$, entering the surface store; this takes the form

$$u_s^* = u_s + (1 - \alpha) g_u \varepsilon . \quad (12.2.1d)$$

Finally, an adjustment to the probability-distributed soil moisture, $S \equiv S_1$, may be made, either of the proportional form

$$S^* = S + \alpha g_s \varepsilon \quad (12.2.1e)$$

or the direct form of gain with α equal to unity.

It should be noted that all the above forms of adjustment utilize the same basic form of adjustment employed by the Kalman filter in which an updated state estimate is formed from the sum of the current state value and the model error multiplied by a gain coefficient. However, instead of defining the gain statistically, as the ratio of the uncertainty in the observation to that of the current state value, it is first related to a physical apportionment rule multiplied by a gain factor. This gain factor acts as a relaxation coefficient which is estimated through an off-line optimisation using past flood event data.

State correction is essentially a form of negative feedback, and, although usually very effective, this feedback can sometimes give rise to an over- or under-shooting behaviour characterized by high accuracy at short lead times but with degraded accuracy at moderate lead times before a recovery in accuracy at longer lead times. This behaviour appears to be associated with a combination of some or all of the following: large gain factors, time lags between the correction of a state value and the appearance of an effect on the modelled flow, and rapid increases in the model error (often due to timing errors on the rising limb). The latter is also a problem for error prediction schemes. Optimal values for the gain factors tend to be greater than unity (over-relaxation) whilst time lags can occur because correction of soil moisture may not affect runoff until the next wet period.

State correction for the TCM and IEM

An essentially similar form of empirical state correction to that used in the PDM model has been used by Moore *et al.* (1989b) to update the Thames Catchment Model. Adjustments to the storages controlling the output from the zonal components of flow are made in proportion to their contribution to the total flow. However, the incorporation of a kinematic wave channel flow routing model into the most recent version of the TCM makes the use of state correction problematical. The time lag introduced by the channel flow routing component gives rise to an extreme oscillatory instability if correction of the zonal outflows is attempted. For this reason only error prediction is used with the TCM in this study. A scheme for state correction of a flow routing component has recently been developed for use in the Grid Model and this is described below. State correction of the IEM is particularly straightforward since only the quadratic storage is a candidate for correction. Adjustment of its outflow is made using the standard form of adjustment expressed by (12.2.1a) with α equal to unity.

State correction for the Grid Model

The Grid Model reviewed in Section 9 has two separate routing components, one representing fast translation typically along channel paths and the other slow translation associated with sub-surface paths. Since the routing procedure is similar for both, and based on a cascade of

discrete kinematic reaches, the same form of state updating scheme can be used. For simplicity of presentation a single routing path is assumed below.

Consider the one-step ahead forecast for time $t+1$ made from a time origin t . For the kinematic reach model (Bell and Moore, 1998; Moore *et al.*, 1994), the flow out of the j 'th reach at time $t+1$ is given by

$$q_{t+1}^j = (1 - \theta) q_t^j + \theta q_t^{j+1} + \theta r_t^j \quad (12.2.4)$$

for $j=1,2,...,N$. Here, N is the number of reaches with each reach chosen to be coincident with an isochrone band. It is possible to update this simulation forecast of flow using the observed simulation error at the time origin t , $\varepsilon = Q_t - q_t^1$, where Q_t is the measured flow at the catchment outlet and q_t^1 the model simulation. The form of adjustment is to modify the flows out of each reach so that the adjusted model outflow equals the measured outflow; that is

$$q_t^* \equiv (q_t^j)^* = Q_t = q_t^j + \varepsilon. \quad (12.2.5)$$

Also, the adjustments to upstream reach outflows are chosen to decrease smoothly as a power function to zero at the topmost (N 'th) reach, such that at time t

$$q_j^* = q_j + f_p(j) \varepsilon \quad j = 1, 2, \dots, N \quad (12.2.6)$$

where

$$f_p(j) = \left(\frac{N - j}{N - 1} \right)^p. \quad (12.2.7)$$

and the exponent p is a constant parameter.

The updated forecast corresponding to equation (8) is then given by

$$(q_{t+1}^j)^* = q_{t+1}^j + \{(1 - \theta) f_p(j) + \theta f_p(j+1)\} \varepsilon \quad (12.2.8)$$

where the last term is the correction that is applied to the forecast obtained using (12.2.4). This completes the development for a single channel path and for "total" adjustment to match the observed flow.

In practice two parallel channels, representing "surface" runoff q_s and "baseflow" q_b , are used in the normal form of Grid Model. The adjustment follows equations (12.2.1) to (12.2.3) allowing for partial adjustment, proportional adjustment or super-proportional adjustment, but with g_b (and similarly for g_s) replaced by

$$g_b' = \{(1 - \theta_b) f_p(j) + \theta_b f_p(j+1)\} g_b \quad (12.2.9)$$

with g_b (and g_s) are gain coefficients estimated by optimisation; here, θ_b denotes the dimensionless wave speed of the “groundwater” channel path.

It is also possible to formulate an adjustment to the water contents of the soil/vegetation stores in the Grid Model. The form of adjustment investigated, for a given grid square with capacity S_{\max} and water content S , is

$$S^* = S + \alpha \frac{S}{S_{\max}} g_s \varepsilon \quad (12.2.10)$$

with g_s a regional storage gain parameter and α allowing for proportional, super-proportional and direct (equal to unity) adjustments as before. Initial trials indicated that adjustment of the soil/vegetation store of the Grid Model provided little improvement and this approach is not normally used. This lack of success may be attributed to the time delays in the routing components of the Grid Model making allocation of errors to the soil/vegetation stores problematic.

12.3 Error Prediction

State correction techniques have been developed based on adjustment of the water content of conceptual storage elements in the belief that the main cause of the discrepancy between observed and modelled runoff will arise from errors in estimating basin average rainfall, which in turn accumulate as errors in water storage content. Rather than attribute the cause directly and devise empirical adjustment procedures we can analyse the structure of the errors and develop predictors of future errors based on this structure which can then be used to obtain improved flow forecasts. A feature of errors from a conceptual rainfall-runoff model is that there is a tendency for errors to persist so that sequences of positive errors (underestimation) or negative errors (overestimation) are common. This dependence structure in the error sequence may be exploited by developing error predictors which incorporate this structure and allow future errors to be predicted. Predictions of the error are added to the deterministic model prediction to obtain the updated model forecast of flows. In contrast to the state correction scheme, which internally adjusts values within the model, the error prediction scheme is wholly external to the deterministic model operation. The importance of this is that error prediction may be used in combination with any model, be it of TF, conceptual or “physics-based” form, and for representing rainfall-runoff or channel flow processes.

Error prediction is now a well established technique for forecast updating in real-time (Box and Jenkins, 1970; Moore, 1982). Error prediction is available as an alternative to empirical state correction in the PDM software and the PSM software used to implement the IEM and TCM models. A form of error prediction is also used in the Midlands Conceptual Runoff Model. A critical review by Wallingford Water (1994) has identified shortcomings in the formulation; for the purposes of this study the standard approach to error prediction outlined here is used instead. The error prediction approach is developed in detail below.

Consider that $q_{t+\ell}$ is the forecast of the observed flow, $Q_{t+\ell}$, at some time $t+\ell$, made using, for example, a conceptual rainfall-runoff model. Since $q_{t+\ell}$ will have essentially been obtained by transformation of rainfall into flow through some model conceptualisation of the catchment, it

will not have used previous observed values of flow, except perhaps for the purposes of model initialisation. It will consequently be referred to as a simulation-mode forecast to distinguish it from a real-time, updated forecast which incorporates information from observed flows.

The error, $\eta_{t+\ell}$, associated with this simulation-mode forecast is defined through the relation

$$Q_{t+\ell} = q_{t+\ell} + \eta_{t+\ell}. \quad (12.3.1)$$

If the simulation-mode error $\eta_{t+\ell}$ may be predicted using an error predictor which exploits the dependence structure of these errors, then an improved forecast may be obtained.

Let $\eta_{t+\ell|t}$ denote a prediction of the simulation-mode error, $\eta_{t+\ell}$, made ℓ steps ahead from a forecast origin at time t using an error predictor. (The suffix notation $t+\ell|t$ should be read as $q_{t+\ell|t}$ being a forecast of the value at time $t+\ell$ given information up to time t .) Then a real-time forecast, $q_{t+\ell|t}$, made ℓ time units ahead from a forecast origin at time t may be expressed as follows:

$$q_{t+\ell|t} = q_{t+\ell} + \eta_{t+\ell|t}. \quad (12.3.2)$$

The real-time forecast error is

$$a_{t+\ell|t} = Q_{t+\ell} - q_{t+\ell|t} \quad (12.3.3)$$

which, depending on the performance of the error predictor, should be smaller than the simulation-mode forecast error

$$\eta_{t+\ell} = Q_{t+\ell} - q_{t+\ell}. \quad (12.3.4)$$

Turning now to an appropriate form of error predictor it is clear that a structure which incorporates dependence on past simulation-mode errors is required. Thus the autoregressive (AR) model

$$\eta_t = -\phi_1 \eta_{t-1} - \phi_2 \eta_{t-2} - \dots - \phi_z \eta_{t-z} + a_t \quad (12.3.5)$$

is an obvious candidate, where a_t is the residual error (uncorrelated), and $\{\phi_i\}$ are parameters. However, a more parsimonious form of model is of the autoregressive-moving average (ARMA) form

$$\eta_t = -\phi_1 \eta_{t-1} - \phi_2 \eta_{t-2} - \dots - \phi_p \eta_{t-p} + \theta_1 a_{t-1} + \theta_2 a_{t-2} + \dots + \theta_q a_{t-q} + a_t \quad (12.3.6)$$

which incorporates dependence of past residual errors, a_{t-1}, a_{t-2}, \dots .

In general, the number of parameters $p+q$ associated with the ARMA model will be less than the number z associated with the AR model, in order to achieve as good a level of approximation to the true simulation-mode error structure. The ARMA model may be used to give the following error predictor

$$\begin{aligned} \eta_{t+\ell|t} = & -\phi_1 \eta_{t+\ell-1|t} - \phi_2 \eta_{t+\ell-2|t} - \dots - \phi_p \eta_{t+\ell-p|t} + \theta_1 a_{t+\ell-1|t} + \theta_2 a_{t+\ell-2|t} \\ & + \dots + \theta_q a_{t+\ell-q|t}, \quad \ell = 1, 2, \dots \end{aligned} \quad (12.3.7)$$

where

$$a_{t+\ell-i|t} = \begin{cases} 0 & \ell - i > 0 \\ a_{t+\ell-i} & \text{otherwise} \end{cases} \quad (12.3.8)$$

and $a_{t+\ell-i}$ is the one-step ahead prediction error

$$\begin{aligned} a_{t+\ell-i} & \equiv a_{t+\ell-i|t+\ell-i-1} = \eta_{t+\ell-i} - \eta_{t+\ell-i|t+\ell-i-1} \\ & = Q_{t+\ell-i} - q_{t+\ell-i|t+\ell-i-1}, \end{aligned} \quad (12.3.9)$$

and

$$\eta_{t+\ell-i|t} = \eta_{t+\ell-i} = Q_{t+\ell-i} - q_{t+\ell-i} \quad \text{for } \ell - i \leq 0. \quad (12.3.10)$$

The prediction equation (12.3.7) is used recursively to produce the error predictions $\eta_{t+1|t}$, $\eta_{t+1|t}$, ..., $\eta_{t+\ell|t}$, from the available values of a_t , a_{t-1} , ... and η_t , η_{t-1} ,

Using this error predictor methodology, the conceptual model simulation-mode forecasts, $q_{t+\ell}$, may be updated using the error prediction $\eta_{t+\ell|t}$, obtained from (12.3.7) (and the related equations (12.3.8)-(12.3.10)), to calculate the required real-time forecast, $q_{t+\ell|t}$, according to equation (12.3.2). Note that this real-time forecast incorporates information from the most recent observations of flow through the error predictor, and specifically through calculation of the one-step ahead forecast errors, $a_{t+\ell-i}$, according to equation (12.3.9).

Alternative error predictor schemes may be devised by working with other definitions of the basic errors: for example by using proportional errors. One such scheme can be formulated by starting with the logarithmic model so that the simulation-mode error is now defined as

$$\log Q_{t+\ell} = \log q_{t+\ell} + \eta_{t+\ell} \quad (12.3.11)$$

$$\eta_{t+\ell} = \log(Q_{t+\ell} / q_{t+\ell}). \quad (12.3.12)$$

An error predictor for $\eta_{t+\ell}$ may be formulated in the normal way using equations (4.6.10) and (12.3.8) with the one-step ahead prediction error given by

$$a_{t+\ell-i} = \eta_{t+\ell-i} - \eta_{t+\ell-i|t-i-1}. \quad (12.3.13)$$

Instead of equation (12.3.2) the real-time forecast, $q_{t+\ell|t}$, takes the form

$$q_{t+\ell|t} = q_{t+\ell} \exp(\eta_{t+\ell|t}). \quad (12.3.14)$$

The Transfer Function Noise (TFN) Modelling Package is used to identify the form of ARMA error predictor and to estimate its parameter values. Also a means exists within IH's TSCAL (Time Series CALibration) calibration shell program to estimate the ARMA error predictor parameters for an assumed model structure. Often a third order autoregressive, with dependence on three past model errors, provides an appropriate choice for UK conditions and a 15 minute model/data time interval.

Whilst error prediction provides a general technique which is easy to apply, its performance in providing improved forecasts will depend on the degree of persistence in the model errors. Unfortunately in the vicinity of the rising limb and peak of the flood hydrograph this persistence is least and errors show a tendency to oscillate rapidly and most widely; dependence is at its strongest for errors on the falling limb, where improved forecast performance matters least. In addition, timing errors in the model forecast may lead to erroneous error predictions being made, a problem which is also shared by the technique of state correction. The general applicability and popularity of error prediction as an updating tool commends its use as an "off-the-shelf" technique, but empirical state adjustment schemes should also be considered as viable alternatives to the use of error prediction.

13. OVERVIEW OF MODELS, CONCLUSIONS AND RECOMMENDATIONS

13.1 Overview of Models

Eight conceptual models of the rainfall-runoff process have been selected for more extensive review, all of which transform rainfall and evaporation time-series into time-series of total catchment outflow. Five of these are used operationally for flood forecasting in the UK: the Thames Catchment Model (TCM), the Midlands Catchment Runoff Model (MCRM), the Probability Distributed Moisture model (PDM), the Isolated Event Model (IEM) and the ISO-function model. Two of the models were developed overseas: the US National Weather Service Sacramento Model and the NAM model, developed in Denmark. The eighth conceptual model, the Grid Model, represents a simple distributed model specifically developed for flood forecasting. All the conceptual models are based on the combination of a soil moisture store (used indirectly by the IEM) with one or more linear or nonlinear reservoirs, a pure time delay, and (for the IEM) a smoothing function. The ISO-function model is the simplest and the TCM, which allows multiple zones, is the most complex. The PDM is rather more sophisticated than any one zone of the TCM, whilst requiring only a modest number of parameters.

Two classes of model are considered which do not attempt to represent the catchment conceptually and are often referred to as “black box” modelling approaches: these are Transfer Function (TF) models and Neural Network (NN) models. The Physically Realisable Transfer Function or PRTF model is presented as a variant of a TF model with a somewhat greater conceptual interpretation. Also considered are new classes of model based on fuzzy rule-based and nearest neighbour approaches to forecasting. More complex, physically-based models are not reviewed, being considered more appropriate for impact assessment studies than for flood forecasting.

An important feature of models used for real-time forecasting is the ability to update the modelled flows using observed flows in such a way as to improve the accuracy of forecast flows. Two ways of achieving this, through correction of model states or prediction of model errors, have been reviewed in Section 12.

Ease of use of models has not been considered explicitly within the review. The models to be carried through to the assessment of Part 2 will be accommodated within the calibration environment provided by IH’s TSCAL (Time Series CALibration) Program. This is the Model Calibration Facility of the River Flow Forecasting System or RFFS (Moore and Jones, 1991; Moore, 1999). Thus ease of use in calibration will be primarily a function of model complexity and particularly the number of parameters and their interdependence.

The TSCAL calibration shell program provides the following functionality:

- i) specification, via a single control file, of model parameters and structure, input data, and output results;
- ii) retrieval of input data from a database;

- iii) if required, interactive and/or automatic adjustment of model parameters whilst displaying the resulting hydrographs;
- iv) if required, generation of a contour plot of the objective function for any two parameters;
- v) input of forecast rainfall data from a file;
- vi) output of flow forecasts and other time series data for subsequent display and analysis; and
- vii) output of statistics to describing model performance.

Various utility programs are used to collate, display and analyse results from the output files generated.

The simplicity and linear form of the Transfer Function model make this the easiest to calibrate, although the model order and time delay to use requires some experimentation. The Thames Catchment Model is arguably the most difficult on account of its multiple use of the same model components to represent different response zones within a catchment. In operational mode no model is so complex as to be burdensome computationally. However, the mode of use of the Physically Realisable Transfer Function model involving manual adjustment of the volume, shape and time response is seen as potentially too burdensome for larger forecasting systems, even given the most well developed interactive visualisation tools to support the task. Use as a decision support tool for catchments of special concern might provide a satisfactory compromise. Automation of the adjustment using a knowledge based approach (Section 10.3) provides another possible option.

All models have similar demands for data with rainfall and flow data being the minimum, and normal, requirement. Flow data are used operationally for model initialisation and forecast updating and are also used off-line for calibration and model assessment. Explicit soil moisture accounting models require some form of evaporation estimate over the seasons of a year. They can utilise real-time evaporation estimates from an automatic weather station if available but a simple sine curve, representing the variation of evaporation over the year, can suffice. The conceptual soil-moisture accounting models require continuous inputs of rainfall data to maintain their water balance and generally are operated routinely (automatically) once a day in order to update their state variables. This is not a significant problem and provision can be made to accommodate for loss of rainfall data, or its delayed receipt, through data substitution schemes. The problem is more acute for distributed models, such as the Grid Model, and where radar data are used to maintain a distributed water balance of the catchment. Such models may also require Digital Terrain Model data to support their configuration and parameterisation, and also for certain variants access to land use and soil survey data. Greater use of data, particularly in this context, can of course be seen as a benefit in making greater use of available information and opening up the possibility of forecasting for ungauged catchments. The simpler nonlinear storage and transfer function models are readily state initialised using no more than a few recent observations of flow and rainfall, allowing them to quickly recover from data loss.

13.2 Conclusions and Recommendations

The review of models has served to highlight the similarities of the various “brand name” conceptual rainfall-runoff models. They differ greatly in complexity depending on which processes are explicitly represented or are represented in aggregate, “effective” form. It is inherently dangerous to judge the efficacy of a model by the variety of functionality it supports or processes it purports to represent. Thus this report has adopted a didactic rather than judgmental approach to model review. The assessment of models is deferred to the Part 2 report with the benefit of having results on model performance obtained across nine catchments and for many storm events, including the significant flood of Easter 1998. This will facilitate an objective assessment of flood forecasting methods.

A consideration of models in use in the UK and abroad, along with new distributed formulations, has led to the recommendation to include eight models in the model assessment using catchment data in Part 2. These models are: the Thames Catchment Model, the Midlands Catchment Runoff Model, the Probability-Distributed Moisture model, the Isolated Event Model, the US National Weather Service Sacramento model, the Grid Model, the Transfer Function model and the Physically Realisable Transfer Function model.

Some of the selected eight models have integral methods for forecast updating based on state correction, and in two cases parameter adjustment, whilst others employ error prediction. Where no existing or acceptable updating method exists, error prediction is used in the assessment for Part 2, since this operates independent of a specific model structure.

This review has identified new forecasting methods based on neural network, fuzzy rule-based and nearest neighbour approaches which deserve further consideration. It has not been possible to encompass these within the scope of the present assessment of forecasting methods. These could feature in a future extension of the project and benefit from the model benchmark performance statistics which feature in the Part 2 report.

REFERENCES

- Bailey, R.A. and Dobson, C. (1981) Forecasting for floods in the River Severn catchment. *J. Inst. Water Eng. and Scientists*, 35(2), 168-178.
- Bardossy, A. and Duckstein, L. (1995) *Fuzzy rule-based modelling with applications to geophysical, biological and engineering systems*, 232pp, CRC Press.
- Bell, V.A. and Moore, R.J. (1998) A grid-based distributed flood forecasting model for use with weather radar data. 1. Formulation. *Hydrology and Earth System Sciences*, 2(2-3), 265-281.
- Box, G.E.P. and Jenkins, G.M. (1970) *Time series analysis forecasting and control*, 553pp, Holden-Day.
- Brunsdon, G.P. and Sargent, R.J. (1982) The Haddington flood warning system, in *Advances in Hydrometry (Proc. Exeter Symp.)*, IAHS Publ. no. 134, 257-272.
- Burnash, R.J.C., Ferral, R.L. and McGuire, R.A. (1973) *A generalized streamflow simulation system: conceptual modelling for digital computers*, Report of the Joint Federal State River Forecast Centre, U.S. National Weather Service and California Department of Water Resources, Sacramento.
- Central Water Planning Unit (1977) *Dee Weather Radar and Real-time Hydrological Forecasting Project*. Report by the Steering Committee, 172 pp.
- Chow, V.T. (1959) *Open-channel hydraulics*, 680 pp, McGraw-Hill.
- Cluckie, I.D. and Owens, M.D. (1987) Real-time rainfall-runoff models and use of weather radar information. In: V.C. Collinge and C. Kirby (eds), *Weather Radar and Flood Forecasting*, 171-190, J. Wiley.
- Cooper, D.M. (1983) Short term flood forecasting for small catchments. In: Anderson, O.D. (ed.), *Time series analysis: theory and practice 3*, North Holland, 251-258.
- Ding, J.Y. (1967) Flow routing by direct integration method, *Proc. Int. Hydrology Symp., Fort Collins*, 1, 113-120.
- Dooge, J.C.I. (1973) *Linear theory of hydrologic systems*, Tech. Bull. 1468, Agric. Res. Service, US Dept. Agric., Washington, 327 pp.
- Galeati, G. (1990) A comparison of parametric and non-parametric methods for runoff forecasting. *Hydrological Sciences Journal*, 35 (1,2), 79-94.
- Gelb, A. ed. (1974) *Applied optimal estimation*, 374 pp, MIT Press.
- Gill, M.A. (1976) Exact solution of gradually varied flow, *J. Hydraulics Div., ASCE*, 102, HY9, 1353-1364.

Gill, M.A. (1977) Algebraic solution of the Horton-Izzard turbulent overland flow model of the rising hydrograph, *Nordic Hydrology*, 8, 249-256.

Gill, P.E., Murray, W. and Wright, M.H. (1981) *Practical Optimisation*, Academic Press.

Greenfield, B.J. (1984) *The Thames Water Catchment Model*. Internal Report, Technology and Development Division, Thames Water, UK.

Gupta, V.K. and Sarooshian, S. (1983) Uniqueness and observability of conceptual rainfall-runoff model parameters: The Percolation process examined, *Water Resources Research*, 19(1), 269-276.

Han, D. (1991) *Weather radar information processing and real-time flood forecasting*. PhD Thesis, Water Resources Research Group, Department of Civil Engineering, University of Salford, 277pp.

Hardy, R.L. (1971) Multiquadric equations of topography and other irregular surfaces. *J. Geophys. Res.*, 76(8), 1905-1915.

Horton, R.E. (1938) The interpretation and application of runoff plot experiments with reference to soil erosion problems. *Soil Sci. Soc. Am., Proc.*, 3, 340-349.

Horton, R.E. (1945) Erosional development of streams and their drainage basins: hydrophysical approach to quantitative morphology, *Bull. Geol. Soc. America*, 56, 275-370.

Institute of Hydrology (1992) *PDM: A generalized rainfall-runoff model for real-time use, Developers' Training Course*, National Rivers Authority River Flow Forecasting System, Version 1.0, March 1992, 26pp.

Institute of Hydrology (1996) *A guide to the PDM*. Version 1.0, January 1996, 45pp.

Jakeman, A.J., Littlewood, I.G. and Whitehead, P.G. (1990) Computation of the instantaneous unit hydrograph and identifiable component flows with application to two small upland catchments, *J. Hydrology*, 117, 275-300.

Jazwinski, A.H. (1970) *Stochastic processes and filtering theory*, Academic Press, 376 pp.

Jones, D.A. and Moore, R.J. (1980) A simple channel flow routing model for real-time use. Hydrological Forecasting, Proc. Oxford Symp., *IAHS-AISH Publ. No. 129*, 397-408.

Karlsson, M. and Yakowitz, S. (1987) Nearest-neighbour methods for nonparametric rainfall-runoff forecasting. *Water Resources Research*, 23(7), 1300-1308.

Lambert, A.O. (1972) Catchment models based on ISO-functions. *J. Instn. of Water Engineers*, 26, 413-422.

Lees, M., Young, P.C. and Ferguson, S. (1993) Flood Warning, Adaptive. In: P.C. Young (ed.), *Concise Encyclopaedia of Environmental Systems*, Pergamon.

Mandeville, A.N. (1975) *Non-linear conceptual catchment modelling of isolated storm event*, PhD thesis, University of Lancaster.

Moore, R.J. (1980) *Real-time forecasting of flood events using transfer function noise models: Part 2*; Contract report to Water Research Centre, 115pp, Institute of Hydrology.

Moore, R.J. (1982) Transfer functions, noise predictors and the forecasting of flood events in real-time. In: Singh, V.P. (ed.), *Statistical analysis of rainfall and runoff*, Water Resources Publ., 229-250.

Moore, R.J. (1982) Advances in real-time flood forecasting practice, Invited paper, *Symposium on Flood Warning Systems*, Winter Meeting of the River Engineering Section, The Institution of Water Engineers and Scientists, 23pp.

Moore, R.J. (1983) *Flood forecasting techniques*, WMO/UNDP Regional Training Seminar on Flood Forecasting, Bangkok, Thailand, 37 pp.

Moore, R.J. (1985) The probability-distributed principle and runoff production at point and basin scales. *Hydrological Sciences Journal*, 30(2), 273-297.

Moore, R.J. (1986) Advances in real-time flood forecasting practice. *Symposium on Flood Warning Systems*, Winter meeting of the River Engineering Section, Inst. Water Engineers and Scientists, 23 pp.

Moore, R.J. (1989) Two TF(1,1,1) models in parallel, the equivalent TF(2,2,1) model, and the relation with two linear reservoirs in parallel. Lecture notes on "Hydrological Models", International Course for Hydrologists, International Institute for Hydraulic and Environmental Engineering, Delft, The Netherlands, 3pp.

Moore, R.J. (1992) Grid-square rainfall-runoff modelling for the Wyre catchment in North-West England. *Proceedings of the CEC Workshop: Urban/rural application of weather radar for flow forecasting*, 3-4 December 1990, Dept. of Hydrology, Soil Physics and Hydraulics, University of Wageningen, The Netherlands, 4pp.

Moore, R.J. (1999) Real-time flood forecasting systems: Perspectives and prospects. In: R. Casale and C. Margottini (eds), *Floods and landslides: Integrated Risk Assessment*, Chapter 11, 147-189, Springer.

Moore, R.J., Austin, R.M., Carrington, D.S. (1993) *Evaluation of FRONTIERS and Local Radar Rainfall Forecasts for use in Flood Forecasting Models*. R&D Note 225, Research Contractor: Institute of Hydrology, National Rivers Authority, 156pp.

Moore, R.J., Austin, R.M. and Carrington, D.S. (1995) *Evaluation of Frontiers and Local Radar Rainfall forecasts for use in Flood Forecasting Models: Operational Guidance Note*, NRA R&D Note 387, Research contractors: Institute of Hydrology, National Rivers Authority, 39pp.

Moore, R.J. and Bell, V. (1994) A grid square runoff model for use with weather radar data. In: M.E. Almeida-Teixeira, R. Fantechi, R. Moore and V.M. Silva (eds), *Advances in Radar Hydrology*, Proc. Int. Workshop, Lisbon, Portugal, 11-13 November 1991, European Commission, Report EUR 14334 EN, 303-311.

Moore, R.J. and Bell, V.A. (1996) A grid-based flood forecasting model using weather radar, digital terrain and Landsat data, *Quaderni Di Idronomia Montana*, 16, (Special Issue, Proc. Workshop on “Integrating Radar Estimates of Rainfall in Real-Time Flood Forecasting”), 97-105.

Moore, R.J., Bell, V.A., Roberts, G.A. and Morris, D.G. (1994) *Development of distributed flood forecasting models using weather radar and digital terrain data*. R&D Note 252, Research Contractor: Institute of Hydrology, National Rivers Authority, 144pp

Moore, R.J., Harding, R.J., Austin, R.M., Bell, V.A. and Lewis, D.R. (1996) *Development of improved methods for snowmelt forecasting*. R & D Note 402, Research Contractor: Institute of Hydrology, National Rivers Authority, 192pp.

Moore, R.J., Hotchkiss, D.S., Jones, D.A. and Black, K.B. (1991) *London Weather Radar Local Rainfall Forecasting Study: Final Report*. Contract Report to the National Rivers Authority Thames Region, Institute of Hydrology, September 1991, 124 pp.

Moore, R.J. and Jones, D.A. (1978) An adaptive finite-difference approach to real-time channel flow routing. In G.C. Vansteenkiste (ed.), *Modelling and Control in Environmental Systems*, North Holland.

Moore, R.J., Jones, D.A. (1991) A river flow forecasting system for region-wide application, Invited paper, *MAFF conference of River and Coastal Engineers 1991*, 8-10 July 1991, Loughborough University, 12pp.

Moore, R.J., Watson, B.C. Jones, D.A. and Black, K.B. (1989) *London Weather Radar Local Calibration Study: Final Report*. Contract report prepared for the National Rivers Authority Thames Region, 85pp, September 1989, Institute of Hydrology.

Moore, R.J. and Weiss, G. (1980a) Recursive parameter estimation of a non-linear flow forecasting model using the extended Kalman filter, in O’Connell, P.E. (ed.), *Real-time hydrological forecasting and control*, Proc. 1st Int. Workshop, July 1977, pp 264, Institute of Hydrology.

Moore, R.J. and Weiss, G. (1980b) Real-time parameter estimation of a nonlinear catchment model using extended Kalman filters. In: Wood, E.G. & Szollosi-Nagy, A. (eds.), *Real-time forecasting/control of water resource systems*, 83-92, Pergamon Press.

Natural Environment Research Council (1975) *Flood Studies Report*, Vol. 1, Chap 7, 513-531.

Nelder, J.A. and Mead, R. (1965) A simplex method for function minimisation, *Computer Journal*, 7, 308-313.

O'Connor, K.M. (1982) Derivation of discretely coincident forms of continuous linear time-invariant models using the transfer function approach, *J. of Hydrology*, 59, 1-48.

Page, C. (1991) *Flow Forecasting System User Guide*, NRA Anglian Region, 13pp.

Penman, H.L. (1949) The dependence of transpiration on weather and soil conditions, *J. Soil Sci.*, 1, 74-89.

Pollard, O. (undated) *Development of a flow forecasting model for the Leigh Barrier Scheme, River Medway*. Technical Report submission for IWEM Membership, 11pp plus figures.

Shamseldin, A.Y. and O'Connor, K. M. (1996) A nearest neighbour linear perturbation model for river flow forecasting. *J. of Hydrology*, 179, 353-375.

Smith, J.M. (1977) *Mathematical Modelling and Digital Simulation for Engineers and Scientists*, J. Wiley, 332 pp.

Szollosi-Nagy, A. (1976) *Introductory remarks on the state space modelling of water resource systems*, Int. Inst. for Applied Systems Analysis, RM-76-73, 81 pp.

Todini, E. (1996) The ARNO rainfall-runoff model. *J. of Hydrology*, 175, 339-382.

Wallingford Water (1994) *A flood forecasting and warning system for the River Soar: Stage 2 Report*, contract report to the National Rivers Authority Severn Trent Region, November 1994, 91 pp plus Appendices, Wallingford Water, Wallingford, UK.

Wedgwood, O. (1993) *A knowledge based approach to modelling fast response catchments*. PhD thesis, Water Resources Research Group, University of Salford, 318pp.

Werner, P.H. and Sundquist, K.J. (1951) On the groundwater recession curve for large watersheds, Proc. AIHS General Assembly, Brussels, Vol. II, *IAHS Publ. No. 33*, 202-212.

World Meteorological Organisation (1975) *Intercomparison of conceptual models used in operational hydrological forecasting*, Operational Hydrology Report No. 7, WMO No. 429, 172pp.

World Meteorological Organisation (1992) *Simulated real-time intercomparison of hydrological models*, Operational Hydrology Report No. 38, WMO-No. 779, 241 pp.

Young, P.C. (1992) Parallel processes in hydrology and water quality: objective inference from hydrological data. In: Falconer, R.A. (ed.), *Water Quality Modelling*, Ashgate, Vermont, 10-52.

Zhao, R.J. and Zhuang, Y. (1963) *Regionalisation of the rainfall-runoff relations* (in Chinese). Proc. East China College of Hydraulic Engineering.

Zhao, R.J., Zhuang, Y., Fang, L.R., Lin, X.R. and Zhang, Q.S. (1980) The Xinanjiang model. In: Hydrological Forecasting (Proc. Oxford Symp., April 1980), *IAHS Publ. no. 129*, 351-356.

Zhu, M.-L. and Fujita, M. (1994) Comparisons between fuzzy reasoning and neural network methods to forecast runoff discharge. *J. Hydrosience and Hydraulic Engineering*, 12(2), 131-141.

APPENDIX A: NONLINEAR STORAGE MODELS

A.1 General

Nonlinear storage models commonly occur as one or more elements in many conceptual models of the rainfall-runoff process. They are reviewed here to provide part of the theoretical background necessary to understand the various models considered in this report.

The outflow from a conceptual model store, $q \equiv q(t)$, is considered to be proportional to some power of the volume of water held in the storage, $S \equiv S(t)$, so that

$$q = k S^m, \quad k > 0, m > 0. \quad (\text{A.1})$$

The storage, for example, could be a soil column or aquifer storage at the catchment scale. Combining the power equation (I.1) with the equation of continuity

$$\frac{dS}{dt} = u - q, \quad (\text{A.2})$$

where $u \equiv u(t)$ is the input to the store (e.g. effective rainfall), gives

$$\frac{dq}{dt} = a(u - q)q^b, \quad q > 0, -\infty < b < 1, \quad (\text{A.3})$$

where $a = mk^{1/m}$ and $b = (m-1)/m$ are two parameters. This ordinary differential equation has become known as the Horton-Izzard model (Dooge, 1973) and can be solved exactly for any rational value of n (Gill, 1976, 1977).

Horton (1945) considered nonlinear storage models as descriptors of the overland flow process. Considering turbulent sheet flow from a slope of unit width, Manning-Strickler gives the velocity as

$$v = n^{-1} R^{2/3} \sqrt{s_o}, \quad (\text{A.4})$$

where n is Manning's roughness, s_o is the slope, and R is the hydraulic radius which for sheet flow is the depth of water storage, S . Therefore the discharge is given by

$$q = vS = k S^{5/3} \quad (\text{A.5})$$

where $k = \sqrt{s_o}/n$, and consequently the exponent m for fully turbulent flow is $m = 5/3$. For fully laminar flow the exponent of the power relation can be shown to be 3. This allowed Horton to define an "index of turbulence":

$$I = \frac{3}{4} (3 - m) \quad (\text{A.6})$$

ranging from $I=1$ for turbulent flow ($m=5/3$) to $I=0$ for laminar flow ($m=3$). A solution in terms of tanh (the hyperbolic tangent) is obtained for the Horton-Izzard equation for $m=2$ ($b=1/3$) in Horton (1938). The exponent $m=2$ corresponds to $I=.75$ and therefore was referred to as the “75% turbulent flow” case. Horton remarked in his 1938 paper about the insensitivity to the value of the exponent m , provided k could be adjusted to compensate; subsequent workers have therefore tended to choose an appropriate value of m and optimised k in some manner to avoid the problem of interdependence between k and m . Horton found that $m=2$ was a reasonable choice for overland flow on most naturally occurring surfaces. Although Horton considered overland flow, and S to be the depth of overland flow, it is reasonable to extend the idea to any input-storage-output system, so S could, for example, be the average depth of water stored over a basin, possibly in the form of soil moisture and/or as channel storage. The Horton-Izzard equation may then be regarded as a lumped conceptual model of the rainfall-runoff process at the basin scale.

A.2 Linear Storage Model

For $m=1$ ($b=0$) the Horton-Izzard equation reduces to the linear reservoir model with the recursive solution in terms of $q(t)$ given by

$$q_{t+T} = e^{-Tk} q_t + (1 - e^{-Tk})u. \quad (\text{A.7})$$

This is used in the Thames Catchment Model (Greenfield, 1984) to represent unsaturated soil storage.

A.3 Quadratic Storage Model

When $m=2$, the resulting storage function, $q=kS^2$, is that for 75% overland flow (Horton, 1945); it is also termed an “unconfined or non-artesian” storage element by Ding (1967) following Werner and Sundquist’s (1951) solution for the recession curve (i.e. $u=0$) of a deep unconfined aquifer. This storage function was used by Mandeville (1975) as the basis of the Isolated Event Model (IEM) used in the UK Flood Study (NERC, 1975). Here it was developed for deriving design flood hydrographs, in part on account of its efficient parameterisation (the one parameter, k) and sensible response shape offering the prospect of successful regionalisation of the model to obtain design hydrographs for ungauged catchments. Mandeville found that its recession behaviour was too steep for larger, lowland basins, although it performed well on smaller, upland catchments.

To obtain a solution for the Horton-Izzard equation for $m=2$, consider first the solution of the general equation for all permissible values of m . Direct integration of (A.3) for a positive input, u , which is constant in the interval $(t, t+T)$, and noting that

$$\frac{dS}{dt} = \frac{dS}{dq^{1/m}}, \quad \frac{dq^{1/m}}{dt} = \frac{1}{k^{1/m}}, \quad \frac{dq^{1/m}}{dt} = u - q,$$

gives

$$\int_{q_t}^{q_{t+T}} \frac{1}{u-q} dq^{1/m} = k^{1/m} \int_t^{t+T} dt,$$

$$\frac{1}{u} \int_{q_t}^{q_{t+T}} \frac{1}{1-q/u} dq^{1/m} = k^{1/m} T.$$

Making the substitution $v=(q/u)^{1/m}$, and since $dq^{1/m}/dv=u^{1/m}$, then

$$\frac{1}{u} \int_{v_0}^{v_1} \frac{u^{1/m}}{1-v^m} dv = k^{1/m} T$$

$$\int_{v_0}^{v_1} \frac{1}{1-v^m} dv = u^{1/m} k^{1/m} T$$
(A.8)

where $v_1=(q_{t+T}/u)^{1/m}$, $v_0=(q_t/u)^{1/m}$; the integral on the left hand side is known as the varied flow function (Chow, 1959). For $m=2$ the varied flow function has the analytical solution

$$I_2 = \int \frac{1}{1-v^2} dv = \tanh^{-1} v + c$$

$$= \frac{1}{2} \log_e \left(\frac{1+v}{1-v} \right) + c,$$
(A.9)

where c is a constant of integration. Using this result it is readily shown that the solution of (A.3) for $m=2$ is

$$q_{t+T} = u_t \left[\frac{z-1}{1+z} \right]^2$$
(A.10a)

$$\text{where } z = \exp \left(a T u^{1/2} \right) \left[\frac{1 + (q_t/u)^{1/2}}{1 - (q_t/u)^{1/2}} \right],$$

or alternatively

$$q_{t+T} = u \left[\frac{(q_t/u)^{1/2} + \tanh \left\{ (uk)^{1/2} T \right\}}{1 + (q_t/u)^{1/2} \tanh \left\{ (uk)^{1/2} T \right\}} \right]^2.$$
(A.10b)

Note that the hyperbolic function relation, $\tanh (A+B)=(\tanh A+\tanh B)/(1+\tanh A \tanh B)$, is used in deriving (A.10b). This predictive equation forms the basis of the Isolated Event Model (NERC, 1975). Whilst originally developed for design application it has been used in modified form for real-time flow forecasting as part of a microprocessor based flood warning system at Haddington in Scotland (Brunsdon and Sargent, 1982); this system continues to be used operationally. The solution provided by equation (A.10b) is also used in the Thames Catchment Model to represent release from groundwater storage (Greenfield, 1984).

A.4 Exponential Storage Model

When $b=1$ in the nonlinear storage model (A.3) then Moore (1983) shows that the model derives from the storage equation

$$\log q = \gamma + aS \text{ or } q = \exp(\gamma + aS) \quad (\text{A.11})$$

where a is the same parameter as appears in (A.3), and γ is an intercept parameter. Integrating the nonlinear storage model

$$\frac{dq}{dt} = a(u - q)q,$$

directly so

$$\int_{q_t}^{q_{t+T}} \frac{1}{(u - q)q} dq = a \int_t^{t+T} dt$$

yields, after rearrangement, the result

$$\begin{aligned} q_{t+T} &= \frac{q_t}{(q_t/u) + (1 - q_t/u)\exp(-aTu)} \\ &= \frac{q_t}{\exp(-aTu) + (q_t/u)(1 - \exp(-aTu))}. \end{aligned} \quad (\text{A.12})$$

This is the “log-storage” model, or more properly the exponential storage model, derived by Lambert (1972), and which is in current use for flood forecasting on the River Dee (Central Water Planning Unit, 1977).

A.5 Cubic Storage Model

When $m = 3$, so the relation $q = k S^3$ holds, then a solution may be sought through the varied flow function type equation A.8. In this case the relevant function has the solution

$$F(x) = \int \frac{1}{1-x^3} dx = \frac{1}{6} \log \left(\frac{1+x+x^2}{(1-x)^2} \right) + \frac{1}{\sqrt{3}} \tan^{-1} \left(\frac{2x+1}{\sqrt{3}} \right). \quad (\text{A.13})$$

However, no simple recursive solution can be obtained.

The approach preferred here has been to develop an approximate recursive solution based on the piecewise linear difference equation solution suggested by Smith (1977, p213) for solving the general nonlinear differential equation

$$\frac{dx}{dt} = f(x, t). \quad (\text{A.14})$$

The solution, for a constant input over an interval (t,t+T) of duration T, is

$$x_{t+T} = x_t + J_t^{-1}(\exp(J_t T) - 1)f_t \quad (\text{A.15})$$

where $J_t = \partial f / \partial x \mid x_t$.

For the case considered here where the nonlinear differential equation is

$$\frac{dS}{dt} = u - q = u - kS^3, \quad (\text{A.16})$$

then $J_t = -3kS_t^2$, and therefore

$$S_{t+T} = S_t - \frac{1}{3kS_t^2} (\exp(-3kS_t^2 T) - 1)(u - kS_t^3). \quad (\text{A.17})$$

The forecast of flow at time t+T is obtained simply as

$$q_{t+T} = kS_{t+T}^3. \quad (\text{A.18})$$

A.6 General Storage Model in Recession

For the recession case when the input, $u=0$, then the Horton-Izzard equation can be solved for all permissible values of m and k by direct integration as follows:

$$\int_{q_t}^{q_{t+T}} \frac{1}{q^{b+1}} dq = - \int_t^{t+T} a d\tau$$

$$\left[-\frac{q^{-b}}{b} \right]_{q_t}^{q_{t+T}} = -aT$$

$$q_t^{-b} - q_{t+T}^{-b} = -abT$$

so

$$q_{t+T} = (q_t^{-b} + abT)^{-1/b} \quad b \neq 0; \quad (\text{A.19})$$

also for the linear reservoirs case (m=1, b=0), then for $u=0$

$$q_{t+T} = \exp(-kT)q_t. \quad (\text{A.20})$$

A.7 Groundwater Abstraction, Negative Storage and Ephemeral Flows

When the input, u , to the nonlinear storage is allowed to be negative and the storage is allowed to develop negative values, with no outflow, then additional theory is required. Such a case might arise when the nonlinear storage is used to represent a groundwater catchment with input, u , given by natural recharge less pumped abstractions with the possibility of ephemeral flows. Two additional expressions are needed to cater for the transition from the normal nonlinear storage with positive outflow to the case of zero outflow and a simple water balance calculation of negative storage values. If $(t, t+\Delta t)$ is the time interval containing the transition then two quantities are required: the time to flow cessation T' (at time $t+T'$) and the initial negative storage, $S(t+\Delta t)$. Expressions for these are given below for each type of nonlinear storage.

Linear store:

$$T' = -\frac{1}{k} \ln \left(\frac{u}{u - q_t} \right) \quad (\text{A.21})$$

$$S_{t+T'} = u \left(T' + \frac{1}{k} \ln \left(\frac{u}{u - q_t} \right) \right). \quad (\text{A.22})$$

Quadratic store:

$$T' = -\left(\frac{1}{-ku} \right)^{1/2} \tan^{-1} \left(\frac{q_t}{-u} \right)^{1/2} \quad (\text{A.23})$$

$$S_{t+T'} = uT' \left(1 - \frac{2}{aT'(-u)^{1/2}} \tan^{-1} \left(\frac{q_t}{-u} \right)^{1/2} \right). \quad (\text{A.24})$$

Exponential store:

This storage is inappropriate for ephemeral flows since positivity of flow is required.

Cubic store:

$$T' = -\frac{1}{3kS(t)^2} \ln \left\{ 1 + \frac{3kS(t)^3}{u - kS(t)^3} \right\} \quad (\text{A.25})$$

$$S(t + \Delta t) = u\Delta t \left\{ 1 + \frac{1}{a\Delta t q(t)^{2/3}} \ln \left\{ 1 + \frac{3q(t)}{u - q(t)} \right\} \right\}. \quad (\text{A.26})$$

APPENDIX B: PARALLEL TF MODELS AND EQUIVALENT SINGLE TF AND PARALLEL LINEAR STORAGE MODELS

This Appendix, by way of illustration, demonstrates the links between two TF(1,1,1) models in parallel, the equivalent TF(2,2,1) model, and the relation with two linear reservoirs in parallel. It derives from lecture notes presented at the International Institute for Hydraulic and Environmental Engineering (Moore, 1989).

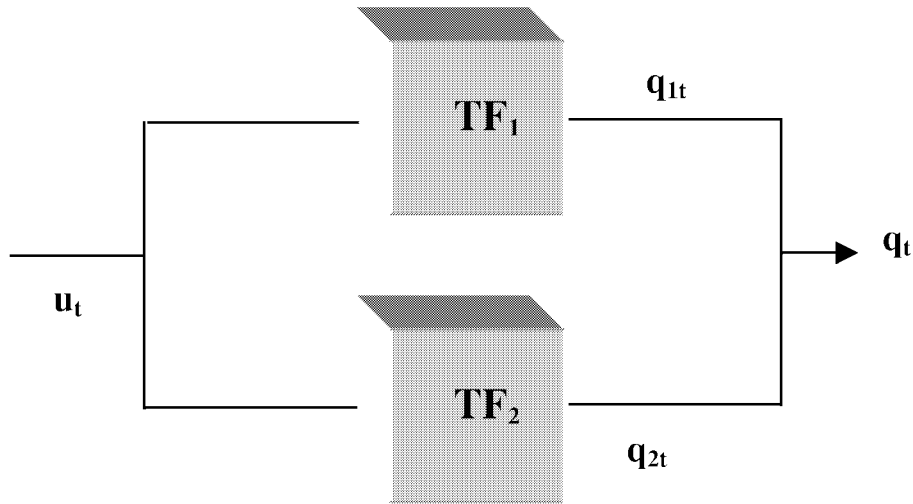


Figure B.1 Parallel configuration of TF models.

Figure B.1 shows two Transfer Function models arranged in a parallel configuration. In a rainfall-runoff modelling context they may be conceptualised as representing the partitioning and translation of an (effective) rainfall input, u_t , via fast and slow pathways to the basin outlet. Denoting the fast and slow response runoffs as q_{1t} and q_{2t} , the total basin flow at time t is given by

$$q_t = q_{1t} + q_{2t} \quad (\text{B.1})$$

Suppose both Transfer Functions have a TF (1,1,1) model structure such that

$$q_{1t} = \frac{\omega_{10}}{1 + \delta_{11}B} u_{t-1} \quad (\text{B.2a})$$

$$q_{2t} = \frac{\omega_{20}}{1 + \delta_{21}B} u_{t-1} \quad (\text{B.2b})$$

It follows that the total flow is given by

$$q_t = \left(\frac{\omega_{10}}{1 + \delta_{11}B} + \frac{\omega_{20}}{1 + \delta_{21}B} \right) u_{t-1} . \quad (\text{B.3})$$

Cross-multiplying gives

$$\left((1 + (\delta_{21} + \delta_{11})B + \delta_{11}\delta_{21}B^2) \right) q_t = (\omega_{10} + \omega_{20} + (\omega_{10}\delta_{21} + \omega_{20}\delta_{11})B) u_{t-1}$$

or

$$\left(1 + \delta_1^* B + \delta_2^* B^2 \right) q_t = \left(\omega_0^* + \omega_1^* B \right) u_{t-1} . \quad (\text{B.4})$$

This is the equivalent TF (2,2,1) model with $\delta_1^* = \delta_{21} + \delta_{11}$, $\delta_2^* = \delta_{11}\delta_{21}$, $\omega_0^* = \omega_{10} + \omega_{20}$ and $\omega_1^* = \omega_{10}\delta_{21} + \omega_{20}\delta_{11}$.

The model gains of the two TF models in parallel are

$$\alpha = g_1 = \frac{\omega_{10}}{1 + \delta_{11}} \quad ; \quad \beta = g_2 = \frac{\omega_{20}}{1 + \delta_{21}} . \quad (\text{B.5})$$

The model gains α and β serve to partition (effective) rainfall via fast (“surface runoff”) and slow (“baseflow”) pathways, and for total rainfall as input, $(\alpha + \beta)$ has the conceptual interpretation of the runoff coefficient of the basin.

Now consider two linear reservoir in parallel with storage coefficients k_1 and k_2 as depicted in Figure B.2.

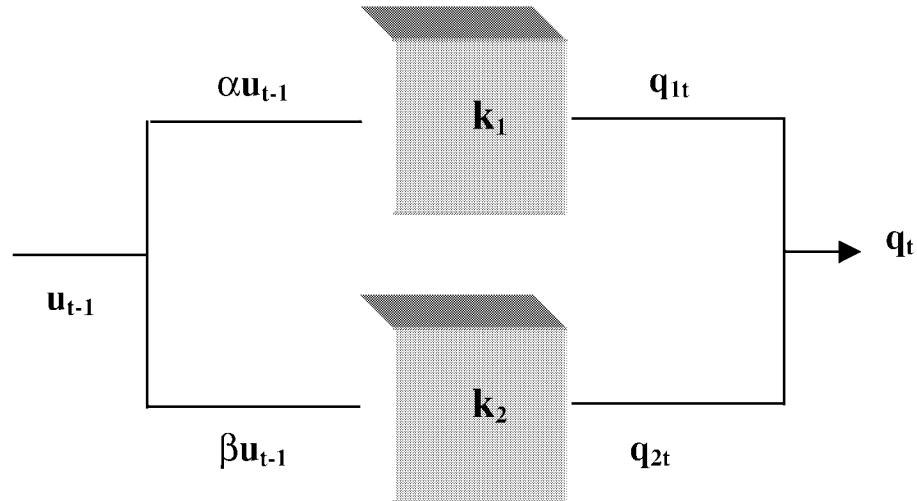


Figure B.2 Two linear reservoirs in parallel.

Their storage and continuity equations are given by

$$\begin{aligned} q_{1t} &= k_1 S_t^{(1)} & \frac{dS^{(1)}}{dt} &= \alpha u_{t-1} - q_{1t} \\ q_{2t} &= k_2 S_t^{(2)} & \frac{dS^{(2)}}{dt} &= \beta u_{t-1} - q_{2t}. \end{aligned} \quad (\text{B.6})$$

Appendix A shows that the Horton-Izzard equation (A.3) for a linear storage is $\frac{dq}{dt} = k(u - q)$ and for a constant input u over the interval of integration, $(t-\Delta t, t)$, it has the discrete time solution

$$q_t = \exp(-k\Delta t)q_{t-1} + (1 - \exp(-k\Delta t))u = -\delta_1 q_{t-1} + (1 + \delta_1)u.$$

For a delayed input $u=u_{t-1}$ we have for the parallel system of linear reservoirs

$$q_{1t} = -\delta_{11} q_{1,t-1} + (1 + \delta_{11})\alpha u_{t-1} \quad (\text{B.7a})$$

$$q_{2t} = -\delta_{12} q_{2,t-1} + (1 + \delta_{12})\beta u_{t-1}. \quad (\text{B.7b})$$

This yields

$$q_{1t} = \frac{\alpha(1 + \delta_{11})}{1 + \delta_{11}B} u_{t-1} \quad (\text{B.8a})$$

$$q_{2t} = \frac{\beta(1 + \delta_{12})}{1 + \delta_{12}B} u_{t-1}. \quad (\text{B.8b})$$

We can establish equivalence with the TF representation (B.2a) and (B.2b) via the following reparameterisation:

$$\omega_{10} = \alpha(1 + \delta_{11}), \omega_{20} = \beta(1 + \delta_{12}), \delta_{11} = -\exp(-k_1 \Delta t), \delta_{12} = \exp(-k_2 \Delta t). \quad (\text{B.9})$$

Therefore we can work with a conceptual parameterisation in terms of α , β , k_1 and k_2 but perform the *calculation* in terms of the TF (2,2,1) model equation (B.4) parameterised in terms of δ_1^* , δ_2^* , ω_0^* , ω_1^* given by

$$\delta_1^* = \delta_{11} + \delta_{21}, \delta_2^* = \delta_{11}\delta_{21}, \omega_0^* = \omega_{10} + \omega_{20}, \omega_1^* = \omega_{10}\delta_{21} + \omega_{20}\delta_{11}. \quad (\text{B.10})$$

Here the TF model parameters ω_{10} , ω_{20} , δ_{11} and δ_{12} are related to the model gains α and β and the storage coefficients k_1 and k_2 through equation set (B.9).

This theory provides a conceptual interpretation of TF models, a reparameterisation in terms of conceptually meaningful parameters (runoff and storage coefficients) and a means to derive TF model parameter values for a different model time-step Δt .